Rowe, R. K. (2005). *Géotechnique* **55**, No. 9, 631–678

Long-term performance of contaminant barrier systems

R. K. ROWE*

This lecture describes the latest findings with respect to the long-term performance of modern municipal solid waste (MSW) landfill barrier systems. Field data relating to the clogging of leachate collection systems and the latest techniques for predicting their performance are examined. It is indicated that the primary leachate collection systems may have service lives that range from less than a decade to more than a century, depending on the design details, waste characteristics and mode of operation. Recent data indicate that landfill liner temperatures can be expected to reach at least 30–40°C for normal landfill operations. With recirculation of leachate the liner temperature increases faster than under normal operating conditions, and may be expected to exceed 40°C. Temperatures (up to 40–60°C) may occur at the base of landfills where there is a significant leachate mound. Temperature is shown to have a significant impact on both contaminant migration and the service life of the liner system. Field measurements and theoretical calculations show that composite liners are substantially better than single liners in terms of controlling leakage from landfills. Also, the leakage rates with a composite liner are very small, and diffusion will dominate as a transport mechanism for contaminants that can readily diffuse through a geomembrane (GM). Composite liners involving a GM over a geosynthetic clay liner (GCL) gave rise to substantially less leakage than those involving a compacted clay liner (CCL). The observed leakage through composite liners can be explained by the holes in, or adjacent to, wrinkles/waves in the GM, and this leakage can be calculated using simple equations. High-density polyethylene (HDPE) GMs provide an excellent diffusive barrier to ions. However, some organic compounds readily diffuse through HDPE GMs, and a combination of GM and an adequate thickness of liner and attenuation layer are required to control impact to negligible levels. The long-term performance of HDPE GMs is discussed. Based on the currently available data, the service life for HDPE GM in MSW landfill is estimated to be about 160 years for a primary liner at 35°C and greater than 600 years for a secondary GM provided it is at a temperature of less than 20°C. Clay liners are susceptible to both shrinkage and cracking during construction (due to heating by solar radiation or freezing) and after placement of the waste (due to temperature gradients generated by the waste). The former can be controlled by quickly covering the liner with a suitable protection layer. The latter can be controlled by appropriate design. The use of numerical models for predicting the service lives of engineered systems and long-term contaminant transport is demonstrated.

KEYWORDS: case history; environmental engineering; geosynthetics; industrial waste; laboratory tests; landfills; numerical modelling & analysis; pollution migration/control; temperature effects; time dependence

Cet exposé donne les dernières conclusions sur la performance à long terme des systèmes de barrage modernes dans les décharges municipales de déchets solides (MSW). Nous examinons les données de terrain relatives à l'engorgement des systèmes de collecte au leachate ainsi que les dernières techniques pour prévoir leur performance. Nous savons que les systèmes primaires de collection au leachate peuvent avoir des vies utiles allant d'à peine dix ans à plus d'un siècle, selon leur conception, les caractéristiques des déchets et les modes d'exploitation. Des données récentes indiquent que les températures des doublures peuvent atteindre entre 30 et 40°C pour les sites normaux. Avec la recirculation du leachate, la température de la doublure augmente plus vite qu'en conditions d'exploitation normales et elle peut même dépasser les 40°C. Les températures peuvent atteindre jusqu'à 40–60°C à la base des décharges là où se trouve une accumulation significative de leachate. Nous montrons que la température a un impact significatif sur la migration des contaminants et sur la durée de vie utile du système de doublure. Des mesures prises sur le terrain et des calculs théoriques montrent que les doublures composites sont substantiellement meilleures que les doublures simples pour ce qui est du contrôle des fuites. De plus, le nombre de fuites avec une doublure composite est très faible et la diffusion va dominer comme mécanisme de transport des contaminants qui peuvent facilement passer à travers une géomembrane (GM). Les doublures composites constituées d'une GM sur une doublure en argile géosynthétique (GCL) donnent lieu à beaucoup moins de fuites que celles ayant une doublure d'argile compactée (CCL). Les fuites observées à travers la doublure composite peuvent s'expliquer par la présence de trous ou de plissement/vagues dans et à côté de la GM et ces fuites peuvent être calculées en utilisant des équations simples. Des GM en polyéthylène à haute densité (HDPE) sont une excellente barrière diffusive aux ions. Cependant, certains composés organiques se diffusent facilement à travers les GM en HDPE et une combinaison de GM, d'épaisseur adéquate de doublure et de couche d'atténuation est nécessaire pour maintenir l'impact à des niveaux négligeables. Nous étudions la performance à long terme des GM en HDPE. D'après les données disponibles actuellement, la durée de vie utile des GM en HDPE dans les décharges MSW est évaluée à environ 160 ans pour une doublure primaire à 35°C et à plus de 600 ans pour une GM secondaire du moment que sa température reste inférieure à 20°C. Les doublures en argile sont sujettes au rétrécissement et aux cassures pendant la construction (en raison de la chaleur solaire ou du gel) et après mise en place des déchets (en raison des montées de température produites par les déchets). Le premier problème peut être solutionné en couvrant rapidement la doublure d'une couche protectrice appropriée. Le second problème peut être résolu par une conception mieux adaptée. Nous montrons comment utiliser des modèles numériques pour prédire les durées de vie utile des systèmes industriels et du transport des contaminants à long terme.

Manuscript received 19 July 2005; revised manuscript accepted 9 September 2005.
Discussion on this paper closes on 2 May 2006, for further details see p. ii.
* GeoEngineering Centre at Queen's-RMC, Department of Civil Engineering, Queen's University, Kingston, Ontario, Canada.

INTRODUCTION

President Carter's declaration of a State of Emergency at Love Canal, NY, in 1978, and the associated evacuation of 236 families from homes around the landfill, highlighted for the public the potential risks associated with waste disposal. Following recognition of the problems of past waste disposal activities, waste disposal has changed very significantly since the 1970s. Today most developed countries have regulations controlling the location, design and operation of landfills. This typically involves limiting the type of waste that can be disposed in the landfill (e.g. not permitting landfill disposal of the liquid hazardous wastes that caused the most serious past problems) and requiring a barrier system to separate the waste and the associated leachate from the groundwater system. In some cases this is hoped (without any quantification) to provide environmental protection. In other cases the barrier system is explicitly (and quantitatively) designed to control contaminant impact to negligible levels. When such systems are well designed and constructed, there is now a wealth of data (mostly in unpublished monitoring reports, but a good publicly available example is given in the data collected by Bonaparte *et al.*, 2002) to suggest that they are performing well. However, most modern landfills with engineered liners have been in operation for less than 20 years. Thus the question arises as to what some of the key factors are that will influence the long-term performance of these systems. This paper addresses this critical question.

Amongst many possible applications, barrier systems can be used to contain possible future chemical spills (e.g. around tanks containing hydrocarbons), contain contaminated fluid in lagoons (e.g. leachate), collect solute from heap leach pads, minimise acid drainage from mine waste, and control contaminant migration from landfills. While there is material in this lecture applicable to this wide range of applications, the focus will be on barrier systems for municipal, industrial, hazardous and incinerator waste landfills (generically referred to as landfills), with particular emphasis on municipal solid waste (MSW) landfills. In the following discussion the term 'barrier system' should be interpreted as a landfill barrier system.

There is a wide variety of possible barrier systems (Rowe *et al.*, 2004), but most involve some combination of traditional soil materials (sand, gravel, clay) and geosynthetic materials. A barrier system typically involves many different components, including filtration/separation layers, drainage layers and protection layers, as well as one or more low-permeability liner. One possible barrier system is shown schematically in Fig. 1. An assessment of the long-term performance of these systems requires consideration of both the soil and geosynthetic components and their interactions, with the performance of one component typically impacting on that of another: this is the primary underlying theme of this lecture.

In many respects, the lecture logically follows from Mitchell's (1991) 31st Rankine Lecture on 'Conductivity phenomena', with the flow of fluids, chemicals and energy playing a key role in what will be discussed in the subsequent sections. Furthermore, these flows are generally coupled. Thus the second theme is the importance of coupled phenomena. Mitchell (1991) and more recently Rowe *et al.* (2004) and Mitchell & Soga (2005) have provided the fundamental framework for much of the discussion of conductivity phenomena to be presented herein.

Given the timescales involved, numerical analysis is a necessity if one wishes to predict the long-term performance of barrier systems. Of course that analysis must be rooted in reality, and it must be conducted by those who understand both the potential of the analysis for improving design and predictive monitoring, as well as its limitations and pitfalls.

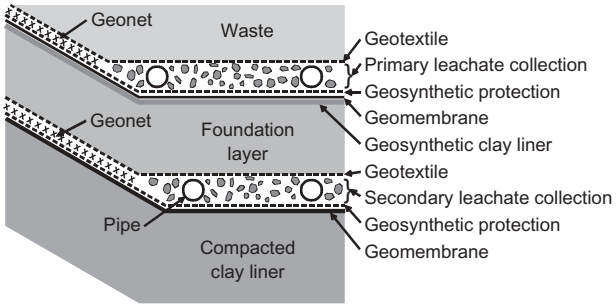

Fig. 1. Schematic showing one possible double composite liner system including, from top down: waste; primary leachate collection system (on the base comprising a geotextile separator/filter between the waste and underlying coarse gravel drainage blanket with perforated leachate collection pipes at a regular spacing and, on the side slope, a geotextile and geonet) used to control the leachate head on the underlying primary liner; a geotextile protection layer (this is often augmented with a sand protection layer not shown here); a primary liner (comprising an HDPE geomembrane, a geosynthetic clay liner, and a foundation layer (omitted in many designs)); a secondary leachate collection/leak detection system (similar configuration to primary system described above) intended to control the head on the secondary liner and to detect and collect leachate leakage through the primary liner; a secondary protection layer; and a secondary liner (comprising an HDPE geomembrane and a compacted clay liner, which in many designs is replaced by a GCL over a suitable attenuation layer)

Laboratory studies are required to identify the key phenomena, to obtain parameters for analysis, and as a relatively controlled benchmark against which the numerical analysis can be tested. There is also a need to test the models against observed field performance where data are available. To the extent that space permits, this lecture seeks to address each of these aspects, and thus the third theme of the lecture is the role of analysis in the assessment of long-term performance of barrier systems. The three themes are each intertwined, and will be touched upon in each of the following sections.

Some basic concepts

In the context of the lecture, a barrier system is intended to control contaminant transport and ensure negligible long-term environmental impact. To do so it is necessary to have a facility that will control contaminant impact for the contaminating lifespan of the landfill. (The reader is referred to Table 1 for a definition of terms not common in geotechnical engineering usage, such as 'contaminating lifespan'.) An evaluation of the potential long-term impact must involve consideration of contaminant transport in the context of the service lives of the various engineered components of the system. It must take account of the fact that components of the system are likely to fail at different times, with the primary leachate collection system (LCS) and geomembrane (GM) liner being the most vulnerable because they are subjected to the severest chemical and biological conditions. Thus one should not expect that each component of the barrier system will function for the entire contaminating lifespan (which, for a large landfill, can be expected to be hundreds of years; Rowe *et al.*, 2004) but, rather, that the system as a whole will provide the long-term protection that is required.

The primary mechanisms for contaminant transport that typically need to be considered for modern facilities are advection and diffusion. Other mechanisms relevant to the clean-up of past problems with unlined disposal sites for

hazardous waste or brines, such as density-driven migration, are omitted because the disposal of these contaminants as liquids is generally not permitted in modern waste disposal facilities. Advection is a physical process whereby contaminants introduced into a groundwater flow system migrate in solution (as solutes) or in suspension (e.g. silt and fine sand particles, microbes) along with the movement of leachate or groundwater. It is governed by Darcy's Law, with the Darcy flux, v_a, given by

$$v_a = -ki \quad (1)$$

where k is the hydraulic conductivity (coefficient of permeability) and i is the hydraulic gradient, which is often controlled by the level of leachate mounding on the landfill liner. Diffusion involves the migration of molecules or ions in air, water or a solid (e.g. a GM, as will be discussed later), as a result of their own random movements, from a region of higher concentration to a region of lower concentration. Diffusion can occur in the absence of any bulk air or water movement. Diffusive transport is generally governed by Fick's law, with the diffusive flux f given by

$$f = -Di_c \quad (2)$$

where D is the diffusion coefficient and i_c is the concentration gradient. In addition to being important as a contaminant transport mechanism from a landfill, diffusion is also a critical transport mechanism between leachate and biofilms that develop on drainage media in the landfill, and is therefore an important factor influencing the rate of clogging of LCSs (to be discussed subsequently). Diffusion of water vapour is also an important consideration when modelling the potential desiccation of clay liners.

When dealing with contaminant transport through porous media, the apparent diffusion of a contaminant from a source of high concentration to a receptor of lower concentration is a complex process, which involves molecular diffusion due to the concentration gradient. However, as discussed in more detail by Rowe *et al.* (2004), it is also influenced by factors such as the complex tortuosity of the porous media, osmotic flow, electrical imbalance, and possible anion exclusion. Typically, diffusion parameters are inferred from laboratory tests conducted using the soil of

Table 1. Definition of some terminology used in landfill design (based on Rowe *et al.*, 2004)

Term	Definition
Antioxidant	An additive in polymer formulation intended to halt oxidative reactions during manufacture and over the polymer's service life.
Attenuation	The process whereby the concentrations of chemical species in groundwater or leachate are reduced as contaminants move throughout the barrier system and subsurface.
BOD: biochemical oxygen demand	The amount of oxygen used in the biochemical oxidation of organic matter in water over a specified time under specified conditions. BOD_5 is the BOD measured in a 5-day test. It is a standard test used in assessing wastewater strength.
Biodegradation	The transformation (through metabolic or enzymatic action) of organic substances to smaller molecules via oxidation and reduction mechanisms induced by the metabolic activity of microorganisms.
BTEX	The group of volatile aromatic hydrocarbons: benzene, toluene, ethylbenzene and xylenes.
COD: chemical oxygen demand	A measure of the amount of organic substances in water. Includes non-biodegradable and recalcitrant (slowly degrading) compounds that are not included in BOD_5.
Clogging	A build-up of biofilm, chemical precipitates and small (e.g. silt and sand) particles that are deposited in pipes, granular material (e.g. sand or gravel), and geotextiles that are used in drainage systems. This build-up progressively reduces the hydraulic conductivity of the system and hence its ability to drain fluids (e.g. leachate).
Composite liner	A barrier to contaminant migration composed of two or more liner materials. Typically a geomembrane and compacted clay liner (CCL) or a geomembrane and geosynthetic clay liner (GCL).
Conservative contaminant	An unreactive contaminant that does not degrade and the movement of which is not retarded. A typical example is chloride (Cl^-).
Contaminating lifespan	The period of time during which the landfill will produce contaminants at levels that could have unacceptable impact if they were discharged into the surrounding environment.
CQA	Construction quality assurance.
CQC	Construction quality control.
DCM: dichloromethane	A volatile chlorinated hydrocarbon used in paint removers and chemical processing. Also known as methylene chloride; CH_2Cl_2.
Diffusion	Migration of molecules or ions in air, water or a solid as a result of their own random movements from a region of higher concentration to a region of lower concentration. Diffusion can occur in the absence of any bulk air or water movement.
Geonet (GN)	A planar, polymeric structure consisting of a regular, dense network of integrally connected overlapping ribs.
Geotextile (GT)	A planar, polymeric textile material, which may be woven or nonwoven.
Geomembrane (GM)	A relatively impermeable, polymeric sheet.
Geosynthetic clay liner (GCL)	Factory-manufactured hydraulic barrier consisting of a layer of bentonite clay supported by geotextiles and/or geomembranes, and held together by needle-punching, stitching, or chemical adhesives.
Flux	Rate of movement of mass or heat through a unit cross-sectional area per unit time in response to a concentration, hydraulic, or thermal gradient.
FSS: inorganic (sometimes called fixed) suspended solids	FSS is made up of inert biomass, mineral precipitate, and soil particles. FSS = TSS-VSS.
Geosynthetic	A polymeric material used in geotechnical applications.
Interface transmissivity	The capacity of the space between a geomembrane and an underlying material to convey fluid. Depends on interface contact conditions, and is required to estimate leakage through holes in geomembranes that are part of composite liners.

(*continued*)

Table 1. (*continued*)

Term	Definition
Leachate	A liquid produced from a landfill that contains dissolved, suspended and/or microbial contaminants from the waste.
Leachate mound	The surface of gravity-controlled water (leachate) in a landfill. It generally corresponds to the top of the zone of saturation in the waste or leachate collection system. Generally represents the water pressure acting on the primary liner in a landfill.
Leak detection system (LDS)	Refers to geonet or gravel drainage layer used to monitor volume of fluid and chemical concentrations passing through a liner system.
Leakage	The movement of fluid through a hole in a geomembrane under a hydraulic gradient. Typically expressed as litres per hectare per day (lphd).
Methanogenic conditions	Environment under which methane is formed by obligate anaerobes.
OIT: oxidative induction time	A relative measure of a material's resistance to oxidative decomposition as determined by the thermoanalytical measurement of the time interval to onset of exothermic oxidation of a material at a specified temperature in an oxygen atmosphere.
Service life	The period of time for which an engineered component of a barrier system performs in accordance with the design assumptions.
Stress cracking	An external or internal rupture in a plastic caused by a tensile stress less than its short-term mechanical strength.
TSS: total suspended solids	TSS comprises volatile suspended solids (VSS) and inorganic suspended solids (FSS), and is obtained using a gravimetric measurement of the residue retained on a 0·45 μm glass fibre filter dried at 105°C.
Transition metals	Metals that have a partially filled *d* shell. Examples include Cr, Mn, Fe, Co, Ni, Cu, Zn, Pd, Cd.
VOC	Volatile organic compound.
VFA: volatile fatty acid	Fatty acids contain only the elements of carbon, hydrogen and oxygen, and consist of an alkyl radical attached to a carboxyl group. The lower molecular weight, volatile, fatty acids are liquids that are soluble in water, volatile in steam, and have a notable odour. Examples commonly found in leachate include ethanoic (acetic) acid [CH_3COOH], propanoic (propionic) acid [CH_3CH_2COOH] and butanoic (butyric) acid [CH_3CH_2 CH_2COOH]. VFAs represent the primary component of COD, and their concentration is often expressed in terms of COD.
Volatile suspended solids (VSS)	VSS comprises active biomass (typically about 70%), including acetate, butyrate, and propionate degraders, and 'inactive' biomass (about 30%), which includes dead bacteria. VSS is obtained using a gravimetric measurement of the residue retained on a 0·45 μm glass fibre filter dried at 550°C.
Wrinkles (waves)	Unevenness of a geomembrane when placed on a flat surface. Often occurs as a result of thermal expansion (after placement) arising from solar radiation.

interest and a leachate similar to that anticipated in the field application, without explicitly considering the role of all these factors, and hence the corresponding effective diffusion coefficient reflects multiple factors (in addition to molecular diffusion).

For many practical situations (Rowe *et al.*, 2004), contaminant transport modelling through the soil component of barrier systems involves solving the equation for one-dimensional contaminant transport of a single reactive solute through a porous medium:

$$n\frac{\partial c}{\partial t} = nD_e\frac{\partial^2 c}{\partial z^2} - \rho_d K_d\frac{\partial c}{\partial t} \quad (3)$$

subject to appropriate boundary and initial conditions, where c is the concentration at depth z and time t, n is the effective porosity, D_e is the effective diffusion coefficient, ρ_d is the dry density, and K_d is the partitioning coefficient.

Landfills generate heat from the biodegradation of organic wastes and the hydration of certain inorganic wastes (e.g. incinerator ash). The consequent heat flow can influence liner temperatures and consequently contaminant transport (as both k and D are temperature dependent) as well as the service life of both the geomembrane and clay liners (as will be subsequently discussed). Heat flow is governed by Fourier's law, with the heat flux q_T given by

$$q_T = -\lambda' i_T \quad (4)$$

where λ' is the thermal conductivity and i_T is the thermal gradient.

Structure

This lecture will focus on seven key issues relevant to the assessment of the likely long-term performance of barrier systems. It begins with a discussion of the factors associated with the clogging of the LCS and the modelling of the bio-geochemical clogging processes that can ultimately reduce the porosity and hydraulic conductivity to the point where the leachate head on the liner can no longer be controlled to the design level (this is the point where the service life of the LCS has been reached). Based on field data, the temperature of landfill liners will then be reviewed, as this will impact on all subsequent issues. Leakage (advective flow) through composite liners is examined based on both field observations and theoretical calculations. Diffusive transport through natural clayey deposits, compacted clay liners (CCLs), geosynthetic clay liners (GCLs) and geomembranes (GMs) is examined, with emphasis on the potential for contaminant diffusion through a solid GM during the period that it is a very effective barrier to fluid flow (i.e. while there is very low leakage). The service life of primary and secondary high-density polyethylene (HDPE) GMs is then discussed, with particular attention being paid to the effect of liner temperature and the interaction between the liner and leachate on the service life of the GM. The potential for desiccation of clay liners due to thermal gradients induced by the waste is then examined with respect to both experimental evidence and coupled modelling of heat and moisture transfer as well as stress and deformations for the liner. Finally, the lecture considers the long-term performance of barrier systems, in terms both of some field experience and of long-term contaminant transport modelling (taking account of issues such as the service lives of components of the barrier system). One could give a lecture on each of these issues but, given space limitations, only a few key aspects of each issue will be discussed.

This lecture focuses on the geoenvironmental aspects of controlling contaminant migration. While important, this is

but one aspect of landfill design. To ensure a safe landfill, attention must also be paid to environmental geotechnics (especially issues of stability) and landfill operations: these issues are beyond the scope of this lecture.

LONG-TERM PERFORMANCE OF LEACHATE COLLECTION SYSTEMS

Overview

Leachate is the contaminated water predominantly generated from the percolation of precipitation through waste and by the biodegradation of the waste. It contains dissolved, suspended and microbial contaminants. Although modern MSW leachate typically has low concentrations of toxic compounds compared with the levels encountered when there is co-disposal of hazardous waste (as was once common practice), there is still a need to control their migration and prevent groundwater contamination.

The LCS represents a critical component of barrier systems for landfills. The primary function of the LCS is to control the leachate head acting on the underlying liner. The secondary function is to remove leachate for either recirculation or treatment and disposal. Clogging of LCSs involves a reduction in hydraulic conductivity of the drainage material and/or filter to the point where it results in the development of a leachate mound acting on the base of the landfill. As the mound increases in height, the advective transport of contaminants through the liner system increases, increasing the potential for groundwater contamination.

The design of LCSs has evolved considerably over time, and there are many misconceptions about appropriate design and operation procedures. The earliest form of LCS involved a toe drain and/or perimeter drain. These systems minimised surface water contamination by controlling leachate seeps through the landfill cover, but they were ineffective at controlling the height of the leachate mound within the waste and the consequent contaminant escape into the underlying soil and groundwater. The next generation of leachate removal systems involved the inclusion of granular material (French drains) in conjunction with perforated drainage pipes, typically located every 50–200 m along the landfill base. These systems provided greater control of the leachate mound than toe drains or perimeter drains, but the confluence of flow through a limited surface area made the drains particularly prone to clogging (especially when they were wrapped in a geotextile). As discussed below, clogging of either a granular material or a geotextile filter impairs the ability for leachate to enter the leachate collection pipe, causing a build-up of a leachate mound between the drains. This mound induces some flow towards the pipes, but also increases outward flow through the bottom of the landfill.

Modern LCSs typically comprise a continuous blanket of granular material covering the landfill base liner and a regular pattern of leachate collection pipes. Some systems use sand for the drainage blanket; however, it has been shown that sand can readily clog (e.g. Reades *et al.*, 1989). The replacement of sand by gravel has improved the performance of these systems, but clogging will still occur. This raises two questions: (a) how does one design a system to maximise the long-term performance and hence its service life; and (b) what is the service life of the system? This section will:

(*a*) examine the mechanisms governing the clogging of leachate collection systems
(*b*) discuss the insights gained from both field and laboratory studies
(*c*) examine techniques for modelling the performance of these systems.

Keele Valley Landfill (KVL)

The Keele Valley Landfill (KVL), located north of Toronto in Maple, Canada, covers 99 ha and is divided into four quadrants, referred to as Stages 1 to 4. The barrier system consists of a CCL, typically 1·5 m thick, overlain by a 0·3 m thick sand protection layer and an LCS as discussed below. Stage 1 (north-east portion) was constructed between 1983 and 1985. Stage 2 (north-west portion) was constructed between 1986 and 1988. Construction of Stages 3 and 4 was started in 1988 and 1990 respectively and completed in 1994. The LCS in Stages 1 and 2 consists of a series of French drains (50 mm washed, crushed gravel mounds 0·5 m high and spaced 65 m apart) draining into four main 150 mm diameter perforated collection pipes (8 mm diameter perforations) encapsulated in 40 mm washed crushed gravel mounds 0·5 m high and 200 m apart. In Stages 3 (south-east) and 4 (south-west), the LCS consists of a granular drainage blanket (0·3 m thick, 50 mm washed, crushed gravel) draining into the four main leachate collection pipes. The four primary pipes run predominantly north-west to south-east the full length of the landfill, are approximately 900 m, 950 m, 1200 m and 1200 m long, and drain to a common holding tank. In addition, a fifth 300 m long collection pipe drains the southeast corner of Stage 4.

The landfill capacity is approximately 33 million m^3, and the maximum depth of waste at closure was about 65 m. Between the first acceptance of waste in 1984 and landfill closure in December 2002, it received 28 million tonnes of MSW from the Greater Toronto Area. As will be discussed in several sections of this lecture, the KVL has been extensively monitored and studied.

Trends in KVL leachate data

As subsequent sections will discuss both field and laboratory studies related to the KVL leachate, it is useful to look at the changes in the concentration of key components of the leachate collected at the main holding tank at the KVL over the past 21 years. Armstrong & Rowe (1999) found a strong correlation between the variability of the KVL leachate characteristics and both precipitation and the sequence of waste placement. Periods of heavy precipitation tended to result in lower-strength leachate, especially after new sections of the LCS had been constructed. The data also suggested that when fresh waste lifts were placed over older waste, the older waste acted as a bioreactor that treated the leachate generated by the newer waste (much like what was observed in test cells by Ham & Bookter, 1982). These results suggest that planned waste placement can play a role in the treatment of leachate before collection and removal. However, as will be illustrated in the following sections, the waste is not the only place where leachate ‘treatment’ occurs.

Despite the variability in leachate characteristics, trends can be identified in plots of 2-month rolling average of key characteristics with time (Fig. 2). Chloride represents the ‘stable’ inorganic constituents, because its concentration is largely independent of biological and chemical interactions. The chloride concentration has increased over the past 21 years, although it may have levelled off over the past couple of years at an average concentration of about 4000 mg/l (Fig. 2). In contrast, the calcium concentration reached a peak annual average value of 1580 mg/l in 1991. The average calcium concentration over the first decade (1984–1993) was about 1200 mg/l. The end-of-pipe concentration of calcium has subsequently decreased to quite low values (average 45 mg/l since closure).

The level of organic contaminants in the leachate can be represented in terms of the chemical oxygen demand

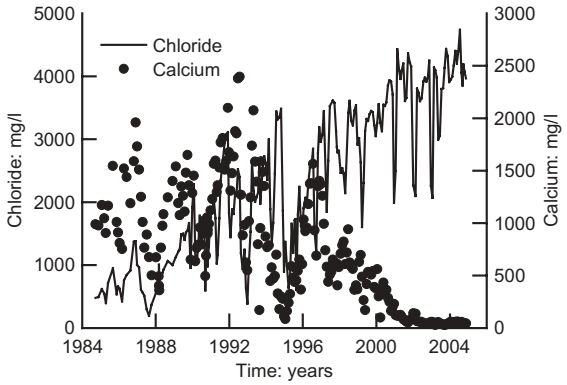

Fig. 2. Variation in end-of-pipe chloride and calcium concentrations with time for the period 1984–2004

(COD), which averaged about 12 200 mg/l over the first decade and has decreased to about 2300 mg/l over the last 2 years since closure. Over the first decade pH was relatively stable, with an average value of 6·3, which increased to an average of 7·4 over the next 9 years and to 7·7 since closure. Thus the leachate data suggest that there is a shift in the end-of-pipe leachate chemistry with the 'stable' inorganic load still increasing while the organic load (represented by COD) and 'unstable' inorganic load (represented by calcium) are decreasing. Of particular note is the strong correlation between the decrease in COD and calcium relative to chloride, as is evident from Fig. 3. This trend suggests that the decrease in calcium is related to the decrease in COD, as has been suggested, based on theoretical considerations, by Rittmann *et al.* (1996). COD has both a readily degradable component—the biochemical oxygen demand (BOD_5)—and a slowly degrading component. Thus the ratio of BOD_5 to COD provides an indication of the amount of COD that can be readily biodegraded. In the KVL leachate this ratio was relatively constant, with an average value of 0·65, typical of 'young' leachate, from 1984 until the end of 2000, after which it rapidly decreased to 0·11. Thus, prior to closure, the decrease in the concentrations of organic constituents (and consequently COD) at the end of the LCS does not appear to have been associated with an apparent 'ageing' of the waste. This is likely a consequence of end-of-pipe leachate reflecting the net effect of degradation of new waste (higher concentrations), treatment within the landfill, and degradation of old waste (lower concentrations).

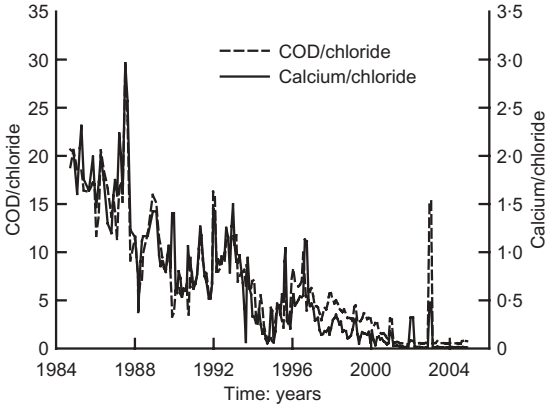

Fig. 3. Variation in end-of-pipe COD/chloride and calcium/chloride with time for the period 1984–2004

Thus 'ageing' or degradation of waste is occurring, but the overall net effect of new and old waste ageing at different rates is being observed. Although not conclusive, the change in the ratio of COD/Cl and in Ca/Cl (Fig. 3), combined with the fact that the average ratio of BOD_5/COD has remained at about 0·65 for almost the first 17 years, suggests that the leachate was being 'treated' as it passed through the LCS. If this is true, then one would expect to find a build-up of organic and inorganic material within the LCS. This will be shown to be the case in the following section.

Field examples of clogging

Clogging of LCSs has been observed in landfills that have involved a wide range of collection systems, ranging from French drains to continuous sand and gravel layers, and in systems both with and without geotextiles (Table 2). For example, field exhumations (Reades *et al.*, 1989; Barone *et al.*, 1993) found that the upper portion of the sand 'protection' layer over the liner at the KVL became clogged within the first four years, and did not contribute to the hydraulic performance of the collection system. In addition to visual evidence of clogging in the upper portion of the sand layer, the lack of flow in the sand layer was clearly evidenced by the development of a clear diffusion profile starting at the top of the sand layer (Fig. 4), which demonstrates that the sand layer was acting as part of the liner in terms of a 'diffusion barrier'. It is particularly notable that both the inorganic contaminant chloride and several organic contaminants (especially toluene) exhibit diffusion profiles through both the sand and the clay. One would not expect to find profiles such as this if there were any significant flow in the sand layer. Koerner & Koerner (1995b) have also reported clogging of a sand protection layer (Case 3, Table 2), where after 10 years the hydraulic conductivity dropped by three orders of magnitude, from 4×10^{-4} m/s to 2×10^{-7} m/s, and leachate was flowing through the waste rather than the sand.

Exhumation of portions of the continuous gravel drainage blanket in later stages of the KVL (Cases 1 and 2 in Table 2; Fleming *et al.*, 1999) indicated a three order of magnitude drop in the hydraulic conductivity of relatively uniform 50 mm gravel near the leachate collection pipe after 4 years (although the hydraulic conductivity was still sufficient to transmit leachate without the development of a leachate mound). Clogging was observed to be substantially less (Case 2 in Table 2) in areas where a geotextile filter was used between the waste and the gravel than where the waste was in direct contact with the gravel. Additional evidence of clogging at the KVL is provided by physical observations of clogging of the main header line leading to the main manhole. In the spring of 2001, the main header was so occluded with clog material that a pipe observation camera could not enter the pipe.

Koerner *et al.* (1994) and Koerner & Koerner (1995b) reported excessive clogging of a geotextile in two cases where the geotextile was wrapped either around the perforated pipe or around the gravel in a drainage trench (Cases 3 and 5 in Table 2) and some clogging in a third case (Case 4).

The field evidence cited above, and in Table 2, shows that there are deposits of both biofilm and inorganic precipitate on the surface of the granular material, which reduces the drainable porosity and hydraulic conductivity of the drainage material. Where clog compositions have been reported (e.g. Brune *et al.*, 1991; Fleming *et al.*, 1999), they comprised over 50% calcite ($CaCO_3$), 16–21% silica where there is no filter, and iron and manganese representing up to 8% and 5% respectively. Calcite was also the dominant mineral in clog scale obtained from a leachate collection pipe in a

Table 2. Summary of observations from exhumation of leachate collection systems (modified from Rowe, 1998a)

Case	Waste type*,† Age; leachate	Collection system design‡	Key observations
1.	MSW and LIW $\sim$4 years COD = 14 800 mg/l BOD_5 = 10 000 mg/l pH = 6·3 Performance: Adequate at time of exhumation	Blanket underdrain: waste over 50 mm relatively uniform gravel; 200 mm, SDR 11 HDPE pipe; 8 mm holes Pipe never cleaned No geotextile between waste and gravel	30–60% loss of void space in upper stone 50–100% loss of void space near pipe Permeability of gravel decreased from $\sim10^{-1}$ m/s to $\sim10^{-4}$ m/s All lower holes in pipe blocked; majority of upper holes blocked Large clog growth inside pipe
2.	MSW and LIW As for Case 1 above	Blanket underdrain: waste over geotextile over 50 mm gravel (rest as above) (GT: W; $M_A = 180$ g/m^2, AOS = 0·475 mm, $t_{GT} = 0{\cdot}6$ mm, $P = 0{\cdot}04$ s^{-1})	Substantially less clogging than observed in Case 1 above where there was no GT 0–20% loss of void space in upper gravel below geotextile
3.	MSW and LIW; LR $\sim$ 10 years COD = 31 000 mg/l BOD_5 = 27 000 mg/l pH $\sim$ 6·9 Performance: No flow in LCS; high leachate mound	Toe drain only Trench with 600 mm of crushed gravel (6–30 mm) around geotextile wrapped 100 mm SDR 41 perforated PVC pipe (GT:HBNW; $M_A = 150$ g/m^2, AOS = 0·15 mm; $t_{GT} = 0{\cdot}30$ mm, $P = 1{\cdot}1$ s^{-1})	Flow reduction noted after 1 year Pipe crushed (likely due to construction equipment) Substantial reduction in void space and cementing of gravel. k reduced from $2{\cdot}5 \times 10^{-1}$ m/s to $1{\cdot}2 \times 10^{-4}$ m/s Sand (SW; AASHTO #10) layer above GM was clogged and leachate drained on top (not through this layer). k reduced from 4×10^{-4} m/s to 2×10^{-7} m/s Excessive clogging of GT (k dropped from $4{\cdot}2 \times 10^{-4}$ m/s to $3{\cdot}1 \times 10^{-8}$ m/s)
4.	MSW and LIW; LR 6 years COD = 10 000 mg/l BOD_5 = 7500 mg/l pH $\sim$7·5 Performance: Drain functioning adequately	Perimeter drain to control leachate seeps Geotextile wrapped trench with 6–18 mm gravel and 100 mm SDR 30 HDPE perforated pipe (GT: W, $M_A = 170$ g/m^2; POA = 7%, AOS = 0·25 mm; $t_{GT} = 0{\cdot}41$ mm; $P = 0{\cdot}9$ s^{-1})	Only small reduction in k of gravel from $5{\cdot}3 \times 10^{-1}$ m/s to $2{\cdot}8 \times 10^{-1}$ m/s Marginal clogging of GT (k dropped from $3{\cdot}7 \times 10^{-4}$ m/s to $1{\cdot}4 \times 10^{-4}$ m/s)
5.	ISS (included slurried fines 70% finer than 150 μm) 0·5 years COD = 3000 mg/l BOD_5 = 1000 mg/l pH = 9·9 Performance: No flow in LCS	Blanket underdrain: Waste over protection sand (0·075–4 mm) over geotextile (AOS = 0·19 mm) over pea gravel (1–20 mm) drainage layer; 100 mm diameter geotextile wrapped HDPE perforated pipe; 12 mm dia. holes (GT: NPNW, $M_A = 220$ g/m^2, AOS = 0·19 mm; $t_{GT} = 2{\cdot}7$ mm, $P = 1{\cdot}8$ s^{-1})	High leachate mound Upper geotextile functioning (k dropped from $4{\cdot}9 \times 10^{-3}$ m/s to $8{\cdot}5 \times 10^{-5}$ m/s) Pea gravel relatively clean Geotextile wrapping around perforated pipe excessively clogged (k dropped from $4{\cdot}9 \times 10^{-3}$ m/s to $4{\cdot}4 \times 10^{-8}$ m/s) Once geotextile sock removed, leachate flowed freely Heavy geotextile sock clogging at location of perforations in pipe
6.	MSW, LIW, ISS 6 years COD = 24 000 mg/l BOD_5 = 11 000 mg/l pH = 6·1 Performance: No flow of methane into extraction wells	Injection wells – 100 mm perforated PVC pipes schedule 40 (GT: NPNW, $M_A = 176$ g/m^2, $t_{GT} = 2{\cdot}2$ mm, $P = 1{\cdot}1$ s^{-1}) LCS not exhumed	Geotextile filter wrapping around extraction wells excessively clogged $\sim$30% extraction wells stopped producing recoverable amounts of methane Geotextiles were black with organic material and caked with fine sediment Permeability reduction by as much as four orders of magnitude (k dropped from $2{\cdot}3 \times 10^{-3}$ m/s to $7{\cdot}5 \times 10^{-7}$ m/s).
7.	6 years Performance: Drain functioning adequately	Blanket underdrain: waste over 600 mm clean sand drainage material, HDPE collection pipes wrapped with geotextile, over HDPE geomembrane over 200 mm of clay, with saw tooth trench base configuration	Sections of manholes (consisting of flexible-walled PE segments) were collapsing and allowing drainage sand, cover soil, and waste into LCS. Sand layer permeability was reduced from $1{\cdot}85 \times 10^{-4}$ to $1{\cdot}23 \times 10^{-4}$ m/s (33% reduction) GT permittivity reduction was 48% but resulting increased head in the LCS was acceptable

(*continued*)

Table 2. (*continued*)

8.	ISS (also accepted salt slag) COD = 51 000 mg/l BOD_5 = 23 300 mg/l pH = 5·9 Ca = 3500 mg/l Performance: Drainage pipes functioning	No description of LCS	Rapid filling (10–20 m/yr) Clogging was particularly intensed despite pipes being flushed at least once a year Clog constituents – calcium (21%), carbonate (34%) Clogging occurred during the early acetogenic phase of decomposition
9.	4 years COD = 1000 mg/l BOD_5 = 40 mg/l pH = 7·0 Ca = 132 mg/l Performance: Drainage pipes functioning	No description of LCS	Slowly filled (~2 m/yr) Very little clogging exhibited between annual flushing events Encrustation consisted of both inorganic precipitate and bacterial slime Leachate phase: stable methanogenic
10.	MSW and ISS Performance: No flow in LCS	Toe drain only	Leachate mounding Leachate drains involving toe drains were clogged Toe drain was replaced
11.	MSW and ISS ~16 years COD = 2300–6500 mg/l BOD_5 = 3900–8300 mg/l pH = 7·0 Performance: Plugging of the leachate header	Blanket underdrain: Waste over LCS (pipe spacing ranging from 50 to 200 m with gravel (5–20 mm) drainage layer) over 100–150 mm thick sand bentonite liner	High leachate mound (20 m) Elevated leachate temperature caused by sludge Clogging occurred during the early acetogenic phase of decomposition Bypass system was installed to divert leachate around a plugged section of the perimeter drain
12.	MSW and incinerator ash 2·5 years Performance: Cell 6 – no flow in LCS	Class 1 – double-lined landfill	Layer of hard mineral substance that filled ~25–100% of the collection pipes Calcite was the only mineral detected
13.	MSW and LIW 12 years COD = 400–6500 mg/l BOD_5 = 15–3400 mg/l pH = 7·2–8·2 Performance: High leachate mound	Blanket underdrain: Waste over a 300 mm thick gravel layer (20–40 mm). Central 150 mm diameter perforated drainage pipe. One vertical leachate pumping well at the lowest point of the cell. LCS not exhumed	Clog deposits (analysed by SEM-EDS) consisted of calcite and ferrous sulphur Residual drainable porosity values ranged from 25% (around the pumping well) to 50%
14.	MSW and LIW 5 years COD = 1400–4000 mg/l pH = 7·6–7·9 Performance: Adequate at time of examination	Blanket underdrain: Waste over a 500 mm thick gravel layer (20–40 mm). Two 225 mm diameter perforated drainage pipes. One central 225 mm diameter HDPE leachate evacuation pipe (evacuation by gravity). High-pressure cleaning of the main pipe and analysis of the collected deposits. LCS not exhumed	Deposits (analysed by SEM-EDS) consisted of calcite, dolomite and ferrous sulphur. Residual drainable porosity values ranged from 10% (in the upper part of the drainage layer) to 50% Main evacuation pipe almost completely clogged (more than 80%)

* MSW: municipal solid waste; LIW: light industrial waste; ISS: industrial solids and sludge; LR: leachate recirculation.
† Cases 1 and 2 (Fleming *et al.*, 1999); Cases 3–6 (Koerner & Koerner, 1995b); Case 7 (Craven *et al.*, 1999); Cases 8–9 (Brune *et al.*, 1991); Case 10 (McBean *et al.*, 1993); Case 11 (Rowe, 1998b); Case 12 (Maliva *et al.*, 2000); Cases 13 and 14 (Bouchez *et al.*, 2003).
‡ GT: geotextile; W: woven; HBNW: heat-bonded non-woven; NPNW: needle-punched non-woven; SDR: standard dimension ratio; M_A, mass per unit area; AOS: apparent opening size; t_{GT}: geotextile thickness; P: permittivity.

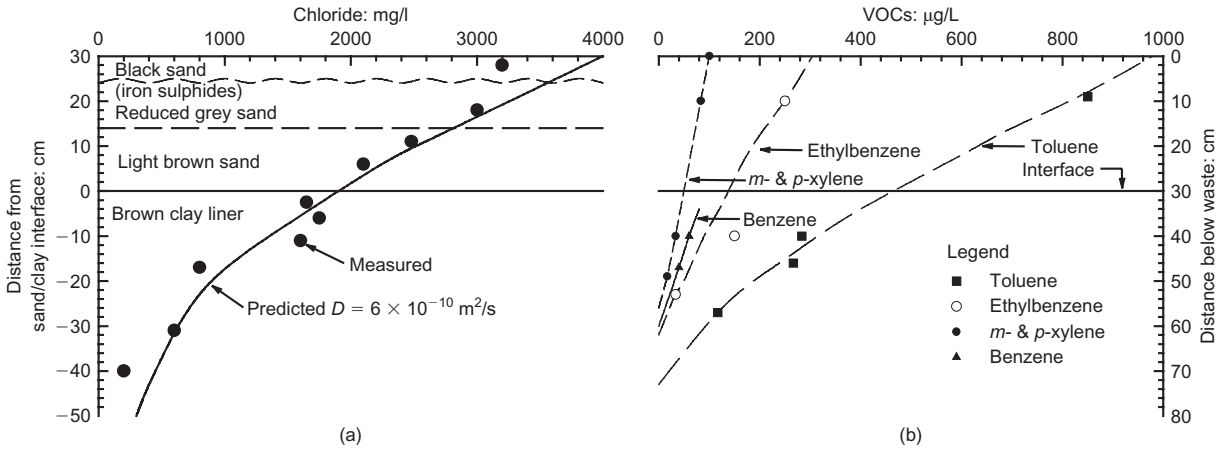

Fig. 4. Diffusion profile through a sand blanket and underlying compacted clay liner at the Keele Valley Landfill after 4·25 years: (a) chloride (modified from Reades *et al.*, 1989); (b) volatile organic compounds (modified from Barone *et al.*, 1993)

Florida landfill that received incinerator ash and MSW (Maliva *et al.*, 2000), and in clog scale obtained from a United Kingdom leachate collection pipe (Manning, 2000).

The leachate data for the KVL examined earlier (Figs 2 and 3) suggest that the clog material (both the organic and inorganic) is being formed by biologically induced processes that involve the removal of some of the organic leachate constituents (as implied by the reduction in COD) and precipitation of some inorganic leachate constituents (as implied by the reduction in calcium concentration). The following sections, which report the findings from laboratory mesocosm and column tests, provide clear evidence that this is indeed the case.

Laboratory mesocosm studies

To assess the performance of different LCS configurations, 18 flow cells (mesocosms) were set up (McIsaac *et al.*, 2000; Fleming & Rowe, 2004; Rowe & McIsaac, 2005) to simulate, at full scale and in real time, the last 0·5 m of a continuous granular blanket adjacent to a leachate collection pipe in a primary LCS. They involved waste material (a mix of waste and cover soil) overlying a 300 mm thick gravel drainage layer graded at 1·5% to a half section of PVC perforated pipe. Selected mesocosms also had a filter/separator layer between the waste material and drainage gravel. The various separator layers examined were a nonwoven needle-punched polypropylene geotextile, a woven slit-film geotextile, a graded granular filter consisting of 4 cm each of well-graded concrete sand and 6 mm nominal size pea gravel, and a 'sacrificial' layer of drainage gravel between the nonwoven geotextile and the waste material. Two sizes of gravel were examined (38 mm and 19 mm). KVL leachate was introduced vertically at a rate corresponding to an infiltration of 200 mm/yr and horizontally corresponding to the same infiltration over a catchment zone corresponding to 50 m spacing of the perforated drainage pipes. The mesocosm tests were conducted under anaerobic conditions at 27°C. Except for the fully saturated mesocosms, the bottom 100 mm of the gravel in each mesocosm remained saturated and the top 200 mm unsaturated during operation. Some of the mesocosms were placed in series, with the effluent from one mesocosm being the influent for another to demonstrate the effect of mass loading on clogging. Most of the mesocosms were terminated after 6 years of operation, although one was terminated after 11 years.

Designs without a separator/filter experienced increased amounts and rates of encrustation in the gravel drainage material and in the leachate collection pipes and perforations compared with those with a filtration/separation medium between the gravel and the waste material. The design with a woven geotextile separator prevented intrusion of the waste (and hence resulted in a void volume occupancy (VVO) of 25% over the full 300 mm of gravel, which was smaller than the VVO of 31% with no filter) but did not prevent migration of fines, because of its large filtration opening size (FOS) of 700 μm, and consequently there was more biological, physical and biochemical clogging within the gravel drainage layer than for mesocosms with either a nonwoven geotextile (VVO = 21%) or granular filter (VVO = 18%) separator/filter design.

The nonwoven geotextile (FOS of 110 μm) separator/filter resulted in increased biological and biochemical clog development in and above the nonwoven filter. The nonwoven geotextile effectively treated and filtered out fines from the vertically flowing leachate and resulted in less clog development within the drainage gravel than in the woven geotextile. Although some clogging of the nonwoven geotextile was observed, leachate still managed to percolate through the geotextile without any evidence of perching of leachate on the geotextile.

For designs with a graded granular filter, the sand layer readily clogged and reduced permeability was observed within the sand layer, which became cemented into clumps of sand and pea gravel. The granular filter was effective at filtering, straining and treating the leachate percolating through the waste layer, and resulted in the least clog mass in the underlying gravel of all the separator/filter designs. However, although no significant perched mounding was noted in the mesocosm, the clogging of the sand does have the potential to cause perched leachate mounding above the filter once the sand layer clogs.

Designs involving the placement of coarse gravel above and below a nonwoven geotextile developed a layer of gritty soft material on the top of the nonwoven geotextile owing to the retention of fines (washed through from the waste layer) and biofilm growth. Because of the large pore space of the gravel above the geotextile, the clog material in this layer was not sufficient to hinder its ability to transmit leachate.

Designs operated with the 300 mm gravel layer fully saturated exhibited an accumulation of soft clog throughout the full layer thickness and greater overall clogging (VVO = 45%) than for mesocosm where the saturated zone was only 100 mm (VVO = 31%). This difference in behav-

iour is attributed to longer leachate retention time and an environment more conducive to microbial growth in the fully saturated systems. Note that, for the saturated mesocosm, there was 51% VVO in the lower 100 mm of gravel after only 1·6 years—more than in most other mesocosms after 6 years.

Tests conducted with 19 mm and 38 mm gravel (no filter/separator) demonstrated a more uniform distribution of clog material through the layer thickness for the 19 mm gravel than for the 38 mm gravel (where the clog focused at the bottom of the layer). For 19 mm gravel there was less intrusion of the waste into the upper portion of the gravel than for 38 mm gravel, but there was substantially more accumulation of clog material within the gravel itself.

As might be anticipated, based on the column studies of Rowe *et al.* (2000a), reducing the mass loading reduces clogging. The lowest VVO was for the mesocosm fourth in series, where the leachate reaching this mesocosm by lateral flow had already passed through three other mesocosms and hence had been depleted in nutrients and inorganic elements (e.g. Ca^{2+}). In this mesocosm, most of the clogging was due to the vertically percolating fresh leachate. Examining the four mesocosms in series it was found that there was a clear progression of decreased VVO in the saturated 100 mm (58% > 29–32% > 16% > 12%) with reduced mass loading.

Clogging of geotextiles

The field and mesocosm studies discussed above have demonstrated that, although geotextiles can clog, when used appropriately they can also minimise the clogging of the underlying LCS. Laboratory tests reported by Koerner *et al.* (1994) showed that the hydraulic conductivity of a geotextile can drop by 4–5 orders of magnitude due to clogging (with the lowest values being $3–4 \times 10^{-8}$ m/s). Geotextile clogging follows a similar pattern to that for granular materials. The clogging process begins with bacteria adhering to the geotextile fibres and the development of a fixed biofilm, which grows in small micro communities (Mlynarek & Rollin, 1995). Needle-punched nonwoven geotextiles provide a particularly large surface area for biofilm development. The biomass utilises available nutrients from the surrounding environment for cell growth and secretion of extracellular polysaccharides (EPS). As the biofilms grow larger, they can combine with other neighbouring biofilms and engulf geotextile fibres, thereby creating a natural biological filter. The biofilm occupies voids within the geotextile, and acts to entrap additional bacteria, suspended solids and organic matter from the passing leachate. Kossendey *et al.* (1996) found that microorganisms could not gain significant nourishment from the carbon content of the polymers. However, the provision of nutrients by permeating geotextiles with leachate having a significant organic component resulted in microbial growth and clogging.

Numerous investigators have studied the clogging of geotextiles permeated by MSW leachate. The magnitude of the decrease in hydraulic conductivity k_n (and permittivity P) depends on the geotextile (e.g. openness of the pore structure), the flow rate, and the concentration of the leachate. Koerner & Koerner (1995b) observed a decrease in geotextile hydraulic conductivity of between about two and five orders of magnitude. The lowest hydraulic conductivity observed in the laboratory tests, for a heat-bonded nonwoven geotextile, was similar to the lowest value observed for the clogged geotextiles recovered from the field (4×10^{-8} m/s).

Laboratory column studies

Several investigators have performed laboratory column tests to assess the effect of different variables on the clogging of granular porous media. These studies, combined with the field and mesocosm studies described earlier and with theoretical considerations (Rittmann *et al.*, 1996), have shown that the clogging of granular media involves a combination of biological, chemical and physical processes. Microbes in the leachate attach to solid matter (e.g. granular material, geotextile fibres, and the walls of leachate collection pipes), and a biofilm grows as nutrients are supplied by the leachate. The methanogenesis and acetogenesis of volatile fatty acids in the leachate cause an increase in the pH of the leachate and production of carbonate, which results in precipitation of inert material (predominantly $CaCO_3$), which accumulates on available solid surfaces and, in some cases, also settles to the bottom of the drainage media. Finally there is an accumulation of inorganic particles originally suspended in the leachate.

Brune *et al.* (1991), Paksy *et al.* (1998) and Rowe *et al.* (2000b) demonstrated that particle size and grading have a significant impact on the rate and extent of clogging in a granular medium. Columns with large particle diameters give rise to bioreactors as efficient as smaller particle diameters (i.e. result in a similar reduction in organic and inorganic loading in a given time). However, for larger particles, the clogging is distributed over a large volume of the porous media, and consequently there is much less reduction in hydraulic conductivity and a longer time until the material can be said to be clogged than for smaller particles. This can be attributed to the fact that the larger the grain size and the more uniform the grading, the larger are the pores that must be occluded to cause clogging and the smaller the surface area per unit volume (the specific surface) available for the biofilm growth. Clogging caused a drop in hydraulic conductivity by up to five to eight orders of magnitude.

Leachate contaminant mass loading has a significant impact on the rate and extent of clogging (Rowe *et al.*, 2000a). This is primarily a result of the increased mass of nutrients and inorganic material available for biological activity and precipitation. Higher flow rates give rise to less efficient bioreactors (i.e. a smaller reduction in organic and inorganic loading per unit volume of leachate in a given time); however, this is more than compensated for by the increase in mass loading associated with the higher flow rates.

Temperature also has a significant effect on the rate of clogging because of the increased biological activity associated with increasing temperature (Armstrong, 1998). However, the clogging processes were similar at all temperatures, and the relationship between the hydraulic conductivity and drainable porosity did not appear to be temperature dependent.

The comparative study of the clogging of tyre shreds and gravel (Rowe & McIsaac, 2005) found that 38 mm gravel maintained a hydraulic conductivity greater than 10^{-5} m/s for about three times longer than a similar thickness of large (75 mm × 75 mm) tyre shreds compressed at 150 kPa.

The microbial consortia found within the columns consisted of methanogens, denitrifiers, sulphate-reducing and other facultative anaerobes. Methanogenic bacteria dominated in the most intensely clogged zones within the columns. There was no significant observable difference in the microbial consortia with particle size, flow rate or temperature (Armstrong, 1998; Rowe *et al.*, 2000a, 2000b; Fleming & Rowe, 2004).

Examination of the changes in leachate as it passed through porous media indicated that clogging was predominantly associated with the deposition of inorganic precipitates (mostly $CaCO_3$), but that the precipitation of $CaCO_3$ was linked to the biological processes and the reduction of COD. An empirical relationship between $CaCO_3$ precipita-

tion and COD reduction was found to be essentially independent of particle size and temperature, but did increase somewhat with increased flow rate, which may be due to biofilm shearing effects at higher flow rates. This shearing can increase the effluent COD (i.e. reduce the amount of COD removed, other things being equal) and hence increase the ratio of $CaCO_3$ removed to COD removed.

Summary of clogging mechanisms

Clogging is initiated by microorganisms suspended in leachate attaching to and colonising the porous media surfaces as a biofilm comprising a consortium of microbes. The microbes excrete extracellular polysaccharides, which contribute further to the reduction in pore space and hydraulic conductivity of the material. Leachate contains organic acids and other nutrients conducive to biofilm development. In particular, young leachate (characterised by a high BOD_5/COD ratio) contains a large proportion of short-chain carbon acids (e.g. volatile fatty acids such as acetate, propionate and butyrate), which can be biodegraded by suspended and attached biomass within the filter and drainage material. The development of the biofilm is a function of the growth rate of the microorganisms, the substrate concentration, the attachment of microorganisms from the leachate onto the surface of the porous medium, and the detachment of microorganisms from the biofilm into the passing leachate. Thus clogging involves:

(*a*) retention (from the passing leachate onto the medium) of biomass (VSS) and suspended solids (FSS)
(*b*) fermentation of volatile fatty acids (VFAs), primarily acetate, butyrate and propionate, by biomass attached to the medium and suspended biomass (VSS)
(*c*) precipitation of cations (predominantly as $CaCO_3$) with calcium representing 20–30% of the dry mass of clog material formed using real leachate.

For real leachate (which has high VSS and hence provides a continuous supply of acid-consuming biomass), butyrate degraded before acetate, and acetate degraded before propionate (VanGulck & Rowe, 2004b). For synthetic leachate (which has very low VSS), acetate was the first to degrade, followed by butyrate (VanGulck and Rowe, 2004a). There was little propionate degraded in tests over a 1 year period, because propionate degraders have a much slower growth rate than acetate and butyrate degraders. For leachate with significant concentrations of calcium (i.e. greater than 300 mg/l), the three distinct clogging mechanisms (biological, chemical and physical) resulted in a significant (typically greater than 60%) reduction in drainable porosity and a five to eight order of magnitude decrease in hydraulic conductivity.

The precipitation of Ca^{2+} as $CaCO_3$ is directly correlated with the biodegradation of organic acids (represented in the foregoing discussion in terms of a reduction in COD). When examined in more detail (VanGulck *et al.*, 2003), it is found that the amount of carbonate is related to the conversion of propionate to acetate, butyrate to acetate, and acetate to methane, and can be represented in terms of microbiologically catalysed reactions (Parkin & Owen, 1986), as summarised below.

Propionate is fermented to acetate, carbonic acid, and hydrogen:

$$CH_3CH_2COOH + 3H_2O \rightarrow CH_3COOH + H_2CO_3 + 3H_2 \quad (5)$$

and hydrogen gas is oxidised to reduce carbonic acid to methane:

$$3H_2 + \tfrac{3}{4}H_2CO_3 \rightarrow \tfrac{9}{4}H_2O + \tfrac{3}{4}CH_4 \quad (6)$$

As insignificant H_2 accumulates in a balanced anaerobic system, reactions (5) and (6) can be combined (Parkin & Owen, 1986):

$$CH_3CH_2COOH + \tfrac{3}{4}H_2O \rightarrow CH_3COOH + \tfrac{3}{4}CH_4 + \tfrac{1}{4}H_2CO_3 \quad (7)$$

Thus the fermentation of 1 mole of propionate produces 1 mole of acetate and 0·25 mole of H_2CO_3.

Butyrate is fermented to acetate and hydrogen:

$$CH_3CH_2CH_2COOH + 2H_2O \rightarrow 2CH_3COOH + 2H_2 \quad (8)$$

and hydrogen gas is oxidised to reduce carbonic acid to methane:

$$2H_2 + \tfrac{1}{2}H_2CO_3 \rightarrow \tfrac{3}{2}H_2O + \tfrac{1}{2}CH_4 \quad (9)$$

The combination of reactions (8) and (9) gives:

$$CH_3CH_2CH_2COOH + \tfrac{1}{2}H_2O + \tfrac{1}{2}H_2CO_3 \rightarrow 2CH_3COOH + \tfrac{1}{2}CH_4 \quad (10)$$

and so the fermentation of 1 mole of butyrate consumes 0·5 mole of H_2CO_3 and produces 2 moles of acetate.

Acetate is fermented to methane and carbonic acid:

$$CH_3COOH + H_2O \rightarrow CH_4 + H_2CO_3 \quad (11)$$

Thus the fermentation of 1 mole of acetate produces 1 mole of H_2CO_3. The CO_3^{2-} anion would not be expected to exist at the typical pH of leachate, and the details of the precise reaction mechanism causing precipitation of $CaCO_3$ have not been fully established. It may in part involve a reaction between Ca^{2+} and HCO_3^- in the leachate at typical leachate pH (6–8) and in part a possible reaction between Ca^{2+} and CO_3^{2-} adjacent to the biofilm, which has a higher pH. However, the net result is that $CaCO_3$(s) is precipitated, and although the actual mechanism may be more complicated than indicated above, for the purposes of this discussion it may be represented by

$$CO_3^{2-} + Ca^{2+} \rightarrow CaCO_3(s) \quad (12)$$

These reactions indicate that the fermentation of propionate replaces propionate with acetate, while fermentation of butyrate replaces butyrate with two acetate, thus increasing the acidity of the leachate. The bioconversion of a weak acid (acetic acid with $pK_a \sim 4{\cdot}7$) to a weaker acid (carbonic acid with $pK_a \sim 6{\cdot}3$) causes the pH of the leachate to increase. The increase in carbonic acid shifts the carbonic equilibrium to carbonate, which can combine with metals to precipitate carbonate-bearing minerals. As the fermentation of acetate generates four times more H_2CO_3 than propionate fermentation, and butyrate fermentation actually consumes H_2CO_3, it follows that the fermentation of acetate drives $CaCO_3$(s) precipitation.

Based on the foregoing it is convenient to relate the amount of Ca^{2+} removed from a leachate (by precipitation) to the amount of H_2CO_3 produced by reactions (7), (10), and (11) in terms of a carbonic acid yield coefficient Y_H (VanGulck *et al.*, 2003):

$$Y_H = \frac{Ca^{2+}\text{ removed}}{\text{net } H_2CO_3\text{ produced}} \quad (13)$$

It follows that the precipitation of $CaCO_3$ will be controlled by the availability of carbonate (and hence the biodegradation of VFAs and consequent reduction in COD) until Ca^{2+} is depleted in the leachate. As the inventory of

Ca^{2+} in the landfill is likely very large, the reduction of Ca^{2+} in the leachate may be due to a combination of geochemical changes in the waste that make calcium less soluble (e.g. an increase in pH) and hence reduce the concentration of Ca^{2+} in the leachate entering the LCS, and actual depletion from the leachate as it passes through the collection system and precipitates out of solution. The former can be dealt with in terms of the input function for Ca^{2+} ; the latter is dealt with in the modelling of clogging within the collection system. This then permits the development of numerical techniques that can be used to simulate clogging processes (Cooke *et al.*, 2005a) by modelling the biodegradation of VFAs, and a simple design method (Rowe & Fleming, 1998) based on the limit imposed by the availability of Ca^{2+} in the leachate, as discussed in subsequent subsections.

Practical implications

The various studies discussed above have demonstrated that development of a biofilm occurs relatively quickly, and then, with time, changes from a soft 'slime' to a slime with hard particles (sand-size solid material in a soft matrix), to a solid porous concretion of a coral-like 'biorock' structure (VanGulck & Rowe, 2004b). During the early phases of clog development the biofilm is relatively easy to clean from leachate collection pipes (e.g. by pressure jetting). However, once the biofilm becomes sufficiently established to cause significant precipitation of $CaCO_3$, the inorganic film becomes firmly attached to the adjacent media (e.g. perforation) and to the inside of pipes (Fleming *et al.*, 1999), and becomes very difficult to remove. This implies that leachate collection pipes in landfills should be regularly cleaned to remove the soft biofilm in its early stages of development. It has been found that the rate of clog development accelerates with time, and hence the rate of inspection/cleaning required in pipes may increase with time as biofilm develops and as the concentration of VFAs in the leachate (or COD) increases. Silica (sand and silt particles) can be controlled by the use of an appropriate filter. Although calcium and VFAs are ubiquitous in MSW, management practices such as the sequencing of the placement of waste will influence the concentrations of calcium and VFAs reaching the LCS, as discussed by Armstrong & Rowe (1999). For example, placing new waste over old waste where the biological processes are well established tends to increase the pH of the leachate as it migrates through the old waste, and hence tends to reduce the solubility of Ca^{2+} and thus its concentration in the leachate when it first enters the leachate collection system. Also, practices such as the recirculation of leachate serve to re-inject VFAs and calcium back into the waste, and this will have implications for the performance of the LCS.

Because of the level of 'treatment' that occurs in an LCS before the leachate reaches the collection point, end-of-pipe analyses of the leachate VFA and Ca^{2+} concentrations indicate only what it is like at the collection point, and provide little evidence regarding the nature of the leachate that enters the system.

The following observations led Rowe & Fleming (1998) to propose a simple method for estimating the rate of clogging of different collection system designs:

(*a*) The rate of clogging was related to mass loading.
(*b*) The dry densities of clog material, ρ_c, varied between 1·6 and 2·0 Mg/m^3.
(*c*) Clogging was a problem only for leachates with a significant concentration of Ca^{2+}, Mg^{2+} or Fe^{2+}, with $CaCO_3$ typically representing more than 50% of the clog material.
(*d*) The calcium fraction of total clog material (f_{Ca}) was typically 20–30% of the clog mass.
(*e*) Clogging was greatest near the leachate collection pipe, and decreased with distance from the pipe.

This approach uses calcium as a surrogate for other clog materials that may deposit within the drainage layer (i.e. magnesium, iron, silica). The methodology ignores the reaction kinetics of clogging and conservatively assumes that all calcium entering the drainage layer becomes deposited in the granular layer instantaneously. Thus the maximum possible volumetric yield, $Y(t)$, of clog per unit volume of leachate may be estimated to be

$$Y(t) = \frac{c_L(t)}{\rho_c f_{Ca}} \tag{14}$$

where $c_L(t)$ is the anticipated concentration of calcium in leachate, ρ_c is the dry density of the clog material, and f_{Ca} is the proportion of calcium in the total clog material. It then follows that the volume of pore space filled with clog material over a length of collection system x per unit width at some time t is given by

$$V(t) = \int_0^t \frac{c_L(t) q_0 x}{\rho_c f_{Ca}} \, d\tau \tag{15}$$

where q_0 is the rate of leachate percolation into the porous medium per unit area.

The time required to produce a particular level of clogging may be estimated from this relationship for any $c_L(t)$. For any particular degree of clogging a 'porosity reduction' v_f is defined such that:

$$n_b = n_0 - v_f \tag{16}$$

where n_b is the free porosity remaining at time t, n_0 is the initial porosity, and v_f is the porosity reduction (i.e. the porosity that is occupied by clog material at time t).

The foregoing relationships can be used to deduce clogging for a wide range of practical situations. However, for a blanket drain, the field observations at the KVL suggest that clogging will be greatest towards the collection pipes and least away from the pipes (Fleming *et al.*, 1999). Therefore it is assumed (Fig. 5) that the porosity reduction (v_f) and the portion of the overall thickness of drainage blanket subject to clogging (B') both vary linearly from essentially zero at the up-gradient edge of the drainage path (where lateral flow is zero) to a maximum value $v_f = v_f^*$ and $B' = B$ (where B is the thickness of the drainage layer) within a few metres of the collection pipe. Within a distance a of the pipe, the porosity reduction is assumed to remain constant at a peak value v_f^*, which is equated with a particular degree of performance impairment.

Therefore the volume of mineral clog corresponding to a permeability decrease represented by v_f is given by

$$V_{tot} = \int_0^L v_f(x) B'(x) dx \tag{17}$$

where

$$v_f = \begin{cases} v_f^* x/(L-a) & \text{for } x < L-a \\ v_f^* & \text{for } L-a < x < L \end{cases}$$

$$B'(x) = \begin{cases} Bx/(L-a) & \text{for } x < L-a \\ B & \text{for } L-a < x \end{cases}$$

and hence

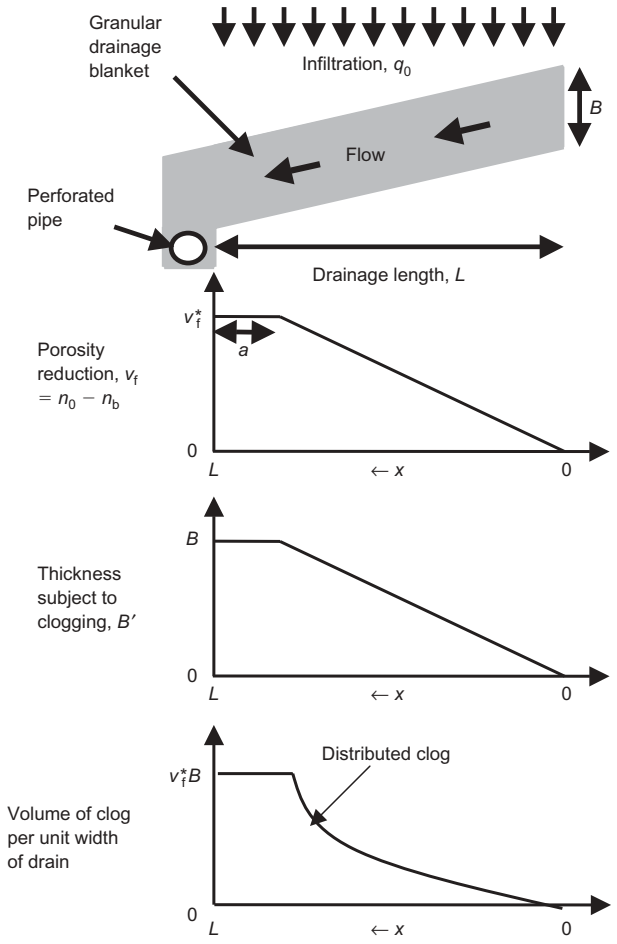

Fig. 5. Schematic of drainage layer configuration and clog development within the underdrain (modified from Rowe & Fleming, 1998)

$$V_{tot} = \frac{v_f^* BL(1 + 2a/L)}{3} \tag{18}$$

The time to reach the degree of clogging represented by V_{tot} is calculated by solving for the rate of mineral volume growth expressed above for constant or time-varying Ca concentration. For a constant Ca concentration c_L, the time to clog, t_c, is given (from equations (14) and (17)) by

$$t_c = \frac{(v_f^* BL/3 + 2v_f^* Ba/3)(\rho_c f_{Ca})}{(c_L q_0 L)} \tag{19}$$

For variable Ca concentration c, where $c = c_{L1}$ for $t < t_1$ and then linearly decreases with time to $c = c_{L2}$ at $t = t_2$, after which it remains constant at c_{L2}, then the total clog volume for $t > t_2$ is given by

$$V(t) = 0{\cdot}5\zeta(c_{L1} - c_{L2})(t_1 + t_2) + \zeta c_{L2} t \tag{20}$$

where $\zeta = q_0 L/(\rho_c f_{Ca})$.

Combining equations (18) and (20) for a time-varying Ca concentration, the time to clog t_c is given (for $t_c > t_2$) by

$$t_c = \frac{(1 + 2a/L)B\rho_c f_{Ca} v_f^*}{3q_0 c_{L2}} - \frac{(c_{L1} - c_{L2})(t_1 + t_2)}{2c_{L2}} \tag{21}$$

It follows from the foregoing that the time to clog decreases with increasing spacing between drains (L), increasing calcium concentrations (c_{L1} and c_{L2}) and increasing infiltration into the drainage blanket (q_0). This technique has been applied to predicting the clogging of old French drain systems, and gives relatively short service life predictions (a decade), consistent with observed field behaviour. When applied to well-designed modern systems with adequately spaced collection pipes and a suitable thickness of uniformly graded coarse gravel (e.g. $L = 25$ m, $B = 0{\cdot}5$ m), it gives predictions of service lives in excess of 100 years, assuming that the pipes are regularly cleaned (Rowe & Fleming, 1998).

The methodology described above has the advantage of simplicity; however, as with any simplified model it also has limitations. It assumes that the entire concentration $c_L(t)$ is used to cause clogging, and that the kinetic processes may be neglected. These assumptions are likely conservative, and would lead to an underestimate of the time required for clogging to occur. On the other hand, while the methodology is dependent on porosity, it does not distinguish the effects of different pore size for similar porosity. For example, one could have 5 mm and 50 mm particles with the same initial porosity, and the time predicted to get the same relative reduction in porosity would be the same. However, as indicated by the laboratory studies discussed earlier, particle size does have an effect because of the difference in the absolute size of the voids and the difference in specific surface (surface area per unit volume) that one has for larger-diameter particles. Thus the calculation method proposed above should be used with caution, and only for relatively uniformly graded granular material with a nominal size greater than 20 mm. A more sophisticated model that can address these issues is described in the next subsection.

Both the column and mesocosm studies discussed above have shown that clogging was greater in saturated systems than in unsaturated systems. Thus, to minimise clogging, LCS should be kept pumped and not allowed to remain in a saturated state for prolonged periods of time.

Studies comparing gravel with tyre shreds (Rowe & McIsaac, 2005) have indicated that an increased thickness of compressed tyre shred may be used to give a service life similar to that of a given thickness of gravel in non-critical zones. However, because of the greater variability in pore size, gravel should continue to be used in critical zones where there is a high leachate mass loading.

Giroud (1996) has discussed the issue of geotextile clogging as part of a broad review of filter design. He tentatively recommends that sand and nonwoven geotextile filters should not be used even if the waste has been stabilised to produce low-strength leachate by pre-treatment. Rather, he recommends the use of monofilament woven geotextiles with a minimum apparent opening size (AOS) of 0·5 mm and a minimum percentage open area (POA) of 15%, with a preference for a POA greater than 30%. The rationale for these recommendations arises from the following observations.

(*a*) The specific surface area for monofilament woven geotextile is much smaller than for nonwoven geotextiles, and this decreases the surface area for biofilm growth.
(*b*) The woven filter allows more effective and rapid movement of fine material (i.e. material not intended to be retained) and leachate through the filter.
(*c*) Because of their compressibility, the filtration characteristics of a nonwoven geotextile vary with applied pressure, and the critical filtration characteristics should be assessed under design pressures, which could be up to 500 kPa.

There is some evidence to suggest that geotextiles selected in accordance with Giroud's (1996) recommendations are likely to experience less clogging and reduction in hydraulic conductivity with time than needle-punched nonwoven or slit

film geotextiles normally used. Giroud's (1996) recommendations are based on the premise that one wishes to minimise clogging of the filter. This may indeed be the case for some design situations (e.g. if one insists on wrapping geotextile around pipe in LCS). However, although excessive clogging is undesirable, the processes that cause clogging also provide leachate treatment and, in so doing, (a) decrease the potential for clogging at more critical zones (e.g. near collection pipes) and (b) reduce the level of leachate treatment required after removal of leachate from the landfill. Based on the available evidence, as summarised earlier, it appears desirable to design the LCS to maximise leachate treatment while maintaining its design function. Under these circumstances, using a design such as the one shown in Fig. 6 with a sand and/or nonwoven geotextile filter between the waste and gravel may be desirable provided that perching of leachate on the filter does not have any negative effects (such as side seeps).

Based on published data (Koerner *et al.*, 1994; Rowe, 1998a), it is unlikely that the hydraulic conductivity of a typical nonwoven needle-punched geotextile would be below 4×10^{-8} m/s (1·3 m/yr) for normal conditions and more likely that it would be of the order of 1×10^{-7} m/s or higher. If the geotextile was used in a blanket drain (e.g. Fig. 6), one can quickly establish that there would be negligible perched leachate on the geotextile for typical rates of leachate generation (less than 3×10^{-8} m/s or 1 $m^3/(yr\,m^2)$). Thus, while recognising that geotextiles will clog, theoretical consideration, mesocosm studies and field observations all indicate that an appropriately selected geotextile used to protect gravel in a blanket drain will improve the performance and the service life of the drainage gravel and not cause excessive perched leachate mounding. There are two disadvantages to the use of the geotextile directly between the drainage gravel and the waste (Fig. 6(a)). First, unless considerable care is taken, the placement of the waste could cause tearing of the geotextile (creating holes). Second, if the geotextile is left exposed for any significant period of time before covering by waste, there will be degradation of the geotextile by exposure to ultraviolet rays, which will increase the tendency for it to tear. These problems can be avoided by placing a medium-to-coarse sand protection layer over the geotextile (Fig. 6(b)).

It has also been suggested (e.g. Brune *et al.*, 1991) that carbonate drainage gravel is unsuitable for use in the drainage layer because it could dissolve and contribute to subsequent calcite crystallisation on alkaline biofilms covering drainage gravel. However, there is now a considerable body of evidence (e.g. Rittmann *et al.*, 1996; Owen & Manning, 1997; Jefferis & Bath, 1999; Manning & Robinson, 1999; Bennett *et al.*, 2000) to suggest that calcium carbonate is supersaturated in landfill leachate very early in the life of the landfill, and that it is unlikely that dissolution would occur under these conditions. The evidence points to the Ca^{2+} being leached out of the waste and transported to the point of deposition by the leachate while the CO_3^{2-} arises predominantly from the mineralisation of organic carbon by methanogens (Brune *et al.*, 1991; Owen & Manning, 1997; Bennett *et al.*, 2000).

To address the concern that acetogenic leachate may cause dissolution of dolomitic limestone, Bennett *et al.* (2000) examined drainage gravel exhumed from the KVL (Case 2, Table 2) and looked for incipient dolomite dissolution, which is commonly characterised by the formation of small pits detected at high magnification on crystal surfaces. They were able to show that the surface of the dolomitic limestone exhumed from the KVL LCS was devoid of such pits. However, they did find significant fines (dolomite, quartz, feldspar), washed into the LCS as particulate material suspended in the leachate, which became part of the secondary calcite formed around the gravel. This, combined with the difference in observed clogging at the KVL where a geotextile filter was and was not used (Cases 1 and 2, Table 2), suggests that the clogging of the drainage gravel could be reduced by placing a geotextile filter between the waste and drainage gravel to limit the ingress of fines.

Numerical clogging model

The understanding of clogging derived from the studies summarised above has allowed the development of a numerical model, BioClog, to simulate clogging in both column experiments (Cooke *et al.*, 2005a) and 2D flow systems. A brief summary is presented here. Reactive chemical transport is modelled with consideration of biological growth, mineral precipitation, attachment and detachment of suspended

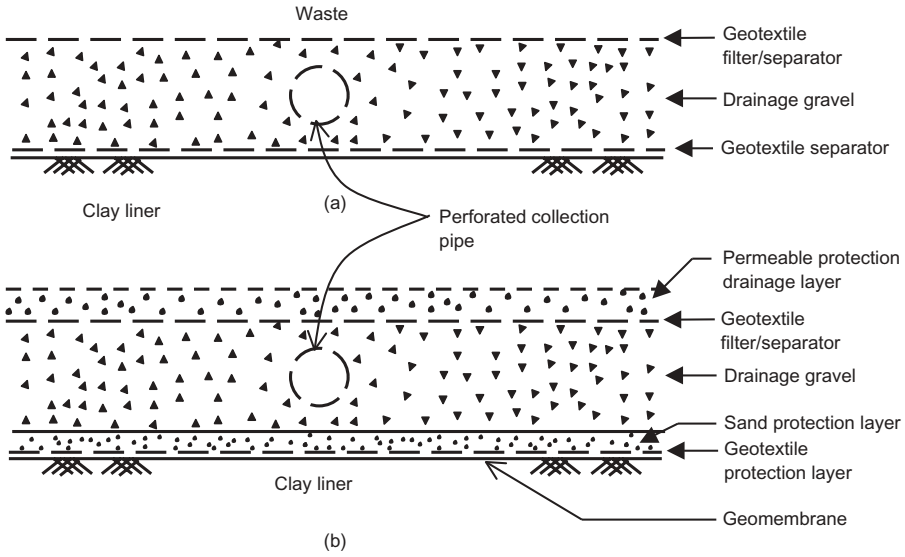

Fig. 6. Typical leachate collection drainage blankets: (a) geotextile alone; (b) geotextile and sand protection layers (note that upper permeable protection drainage layer would be medium to coarse sand or gravel (the latter preferred); the lower sand protection layer would be fine or medium sand)

solids. The porous medium is represented as a fixed-film reactor, and changes in porosity resulting from the development of biofilm and inorganic films can be calculated directly based on a geometric model. The corresponding changes in hydraulic conductivity are then deduced based on empirical relationships derived from laboratory tests. For 2D systems, a flow model is coupled with the transport model.

The transport and fate of three volatile fatty acids (VFAs), dissolved calcium, suspended inorganic solids and suspended biomass are modelled using the finite element method. Fig. 7 gives a schematic representation of species pathways and reactions modelled. Each species has a source/sink term representing the rate of loss or gain resulting from reaction of the species. The term may differ at each node, and is recalculated for each time step. The equations for the reaction terms for each species are given in Cooke *et al.* (2005a). The mechanisms modelled include the following.

(*a*) Acetogenesis of propionate and butyrate, and methanogenesis of acetate by the substrate degraders (both suspended microbes and in the biofilm on the porous media), together with the generation of acetate as a by-product of acetogenesis (equations (5) and (8)). Biofilm substrate utilisation accounts for diffusion of substrate into the biofilm. Once in the biofilm, the substrate consumption is modelled based on Monod kinetics.

(*b*) Detachment and attachment of suspended active biomass from/to the porous media and decay. The rate of detachment of biomass from the biofilm is computed using contributions from two different mechanisms: (i) detachment due to shear stress; and (ii) detachment due to growth rate. Monod kinetics is used to model growth and decay based on the cell decay rate for the species. Attachment is based on a first-order rate coefficient for attachment, which can be calculated using either a particle filtration method or a network method.

(*c*) The loss of suspended inert biomass (i.e. biomass such as dead bacteria, which do not consume substrate) from solution because of attachment to the porous medium, and the gain from detachment of inert biofilm and conversion of suspended active biomass to inert biomass through decay are modelled. The detachment and attachment rates are calculated using the same methodology as for the active suspended biomass. The production of suspended inert biomass is calculated based on the concentrations of suspended active biomass, the decay rate for the species, and the fraction that is refractory.

(*d*) The precipitation of calcium carbonate is based on the carbonic acid yield coefficient (equation (13)), and the net rate of production of carbonic acid calculated from the utilisation of the VFAs (equations (7), (10) and (11)).

(*e*) The increase in suspended inorganic solids due to detachment of inorganic solids is computed using the shear stress model; the attachment is based on the attachment rate, computed in a similar manner to that for the suspended active biomass.

The clog matter is modelled as comprising five separate films: a biofilm for each of the active degraders (acetate, propionate and butyrate degraders), an inert biofilm, and an inorganic solids film. Cooke *et al.* (2005a) provide equations for calculating film thickness based on the same processes as modelled for the reaction terms (Fig. 7):

(*f*) Active biofilms can grow by attachment of suspended active degraders and growth, and may shrink as a result of detachment and decay. Attachment and detachment are modelled as discussed in (*b*) above. Growth and decay are calculated according to the non-steady-state biofilm growth model.

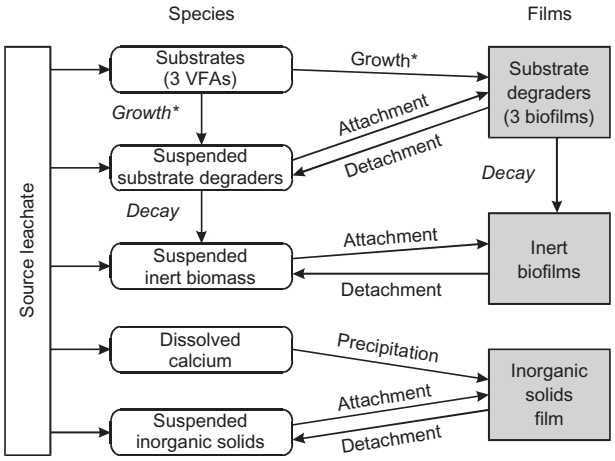

Fig. 7. Schematic of the species pathways and primary reactions incorporated in the BioClog model (after Cooke *et al.*, 2005a). *'Growth' represents growth of substrate degraders due to utilisation of substrate. Note: figure does not indicate production of acetate from degradation of other VFAs

(*g*) Inert biofilm thickness increases because of attachment of inert biomass and conversion of decayed active biomass, and decreases because of detachment.

(*h*) Inorganic solids film thickness increases because of attachment of suspended inorganic solids, precipitation of calcium carbonate, and production of 'other' inorganic solids, and decreases because of detachment. Attachment and detachment are as discussed previously. The mass of precipitate is computed from the mass of calcium removed from the leachate (see (*d*) above). The production of 'other' inorganic solids is calculated by applying a user-defined multiplier to the rate of calcium carbonate production, thereby allowing the model to represent additional precipitates, assuming they accumulate at a rate proportional to calcium carbonate. The contribution of 'other' precipitates is often small (Brune *et al.*, 1991; Fleming *et al.*, 1999; Manning & Robinson, 1999).

The active biofilm, inert biofilm and inorganic solids thicknesses are computed for each element in the finite element mesh. A geometric representation of the porous medium allows calculation of porosity and specific surface in each element based on the total thickness of the active and inactive films, as described by Cooke & Rowe (1999).

Two-dimensional modelling involves a 2D transport model that simulates the processes discussed above together with a 2D flow model. The flow model takes the porosity and corresponding hydraulic conductivity at each point in space, at a given time, from the transport model and calculates the leachate mound subject to these physical parameters and the infiltration from the waste into the collection system. This mound then provides input to the transport model for the next time step.

The model has been calibrated to well-controlled laboratory experiments permeated with synthetic (VanGulck, 2003) and KVL (VanGulck, 2003; Cooke *et al.*, 2005b) leachate. The results indicate that the processes simulated in the model are largely responsible for the biologically induced clogging of landfill LCSs. The application of the model can be briefly illustrated with respect to a laboratory column test involving 6 mm glass beads (VanGulck, 2003). The column was seeded with KVL leachate (to provide a source of

relevant bacteria for initial attachment to the beads), but for the bulk of the test the leachate was synthetic leachate with similar chemical characteristics to those of the KVL leachate but without volatile (e.g. microbes) and inorganic (i.e. particulate material) suspended solids. The leachate chemistry was monitored as it moved along the column from the influent to effluent end. Fig. 8 shows the observed variation in the concentration of calcium at the influent and effluent ends of the column. Also shown is the calcium concentration calculated using the BioClog model. Fig. 9 shows the calculated and observed changes in porosity along the column at 247, 295 and 427 days.

The data show three distinct stages that are captured by the model. For the first approximately 250 days (the lag or acclimation phase) the effluent concentration mirrors the influent, and there is no noticeable change in the calcium concentration (Fig. 8). However, Fig. 9 shows that there has been some decrease in porosity, which can be attributed to the development of a biofilm on the glass beads, which is occupying space but which, until the end of the lag phase, has not yet developed sufficiently to have a measurable effect on the calcium concentration. This situation changes in the transition phase, and the biological processes now result in an increasing production of carbonate (due predominantly to increased methanogenesis of acetate) and associated precipitation of calcium carbonate to the point where, in the steady phase, most of the calcium entering the column is precipitated and very little remains in the effluent. As a consequence there is increased clogging, and at test termination (427 days) the porosity at the influent end of the column is less than half the initial porosity, and the hydraulic conductivity has dropped to 10^{-6} m/s (i.e. by five orders of magnitude). Fig. 9(a) shows the glass beads in the first 15 cm of the column from the influent port at test termination; the clogging is visually evident.

It should also be noted that the general trend evident in Fig. 8 (a lag, a transition, and a steady phase) is also evident in the field data from the KVL (Fig. 2) when allowance is made for the operational effects on the leachate concentrations. Given the variability associated with biological processes and landfills in particular, the agreement between the BioClog calculations and the observed behaviour (Figs 8 and 9) is very encouraging (see references previously cited for more detailed comparisons).

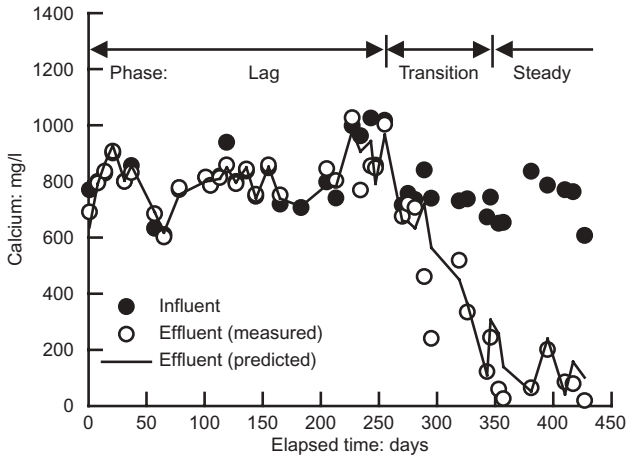

Fig. 8. Observed and calculated variation in effluent calcium concentration with time for a column test using 6 mm glass beads (data from VanGulck, 2003)

Rowe & VanGulck (2004) modelled a 1D flow column filled with 6 mm glass beads and permeated with KVL leachate. The primary difference between synthetic leachate and actual KVL leachate is the continuous supply of volatile and inorganic suspended solids in the influent leachate, which substantially accelerates the clogging process (all other things being equal). The next few paragraphs illustrate the complexities of the interactions being simulated by BioClog.

The change in porosity at 50-day intervals is shown in

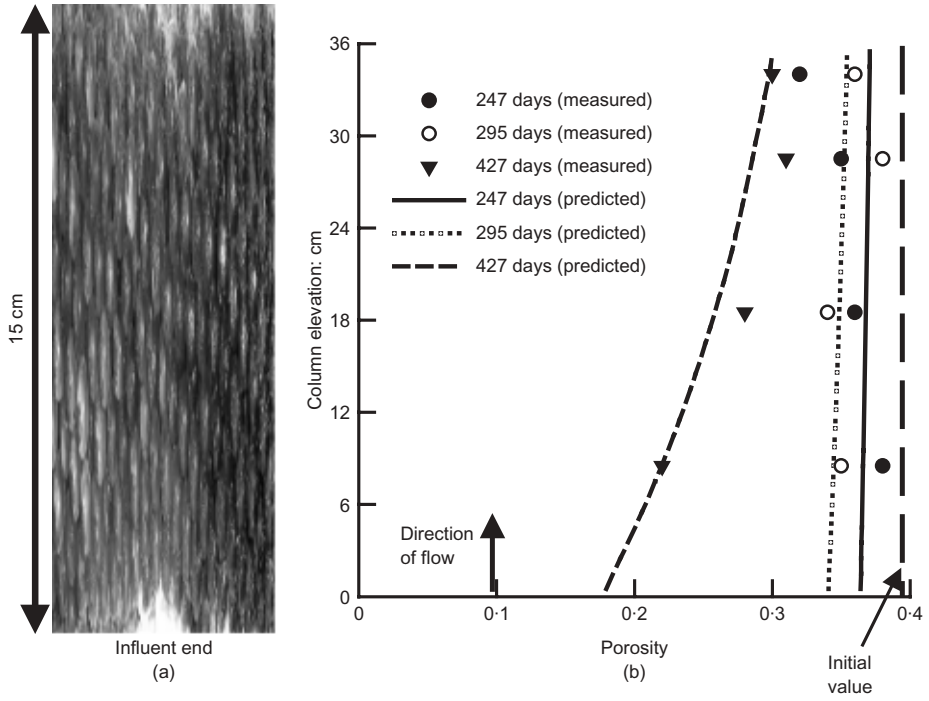

Fig. 9. Results from a column test using 6 mm glass beads: (a) glass beads at the end of a column test, showing greatest clogging at the bottom (influent end) and reduced clogging moving up the column; (b) observed and calculated variation in porosity with position at three times (data from VanGulck, 2003)

Fig. 10(a). This change is a consequence of an accumulation of inorganic (mostly $CaCO_3$, Fig. 10(b)) and volatile (biofilm, Fig. 10(c)) films on the glass beads. During the first 50 days, the reduction in porosity was small, with the volatile film being the primary contributor to the clogging that did occur. The volatile film was similar to, or thicker than, the inorganic film for the first 150–200 days. Subsequently, the inorganic film thickness exceeded the volatile film and the column became highly clogged (especially near the influent end). At 200–250 days there was a reduction in volatile film thickness due to biofilm detachment caused by the high seepage velocities (and hence fluid shear stresses) associated with low porosity and a fixed flow rate. In contrast, the inorganic film does not undergo detachment in this case. The column may be regarded as being completely clogged at locations where the porosity drops to about 5%.

The volatile film consists of active VFA-degrading bacteria (e.g. acetate, butyrate and propionate degraders) and non-active or non-substrate-consuming biomass (e.g. dead bacteria). Each degrader has a unique combination of Monod kinetic parameters, and its growth (and decay) is a function of these parameters, of the substrate concentration, and of the attachment and detachment of each degrader to and from the bead surface. As a consequence, the methanogenesis of acetate and fermentation of propionate and butyrate will occur at different rates. In addition, the concentration of acetate results from a combination of a decrease due to methanogenesis of acetate and an increase due to fermentation of propionate and butyrate, and hence is a function of the kinetics of all three primary degraders. This gives rise to results such as shown in Figs 10(d) and 10(e), where there was significant butyrate consumption but very little change in acetate concentration in the leachate within the first 50 days. There was also relatively little change in calcium concentration (Fig. 10(f)), as its precipitation is driven primarily by methanogenesis of acetate, as previously discussed. By 100 days the biofilm had developed sufficiently to cause significant acetate and butyrate removal, with a consequent large removal of calcium. Peak consumption occurred at 150–200 days. At later times, the low porosities resulted in shearing of the biofilm (Fig. 10(c)) and subsequently less consumption of VFAs and precipitation of calcium. Furthermore, the lower porosities imply higher seepage velocities and hence shorter retention times (during which biodegradation can occur) in the column. Propionate removal did not occur within the column owing to the slow net growth rate of propionate degraders compared with acetate and butyrate degraders and the limited (250 day) time frame examined.

The concentration of volatile suspended solids (VSS) in the leachate decreased along the length of the column during the first 150 days (Fig. 10(g)). Because of the high fluid shear stresses arising from clogging, the biofilm detachment in the first 10 cm resulted in the VSS concentration at an elevation of 10 cm being larger than in the influent at 200 days. The detached biomass subsequently reattached to beads further up the column. Detachment becomes even more significant with increased clogging, and hence by 250 days the effluent VSS concentration was slightly larger than the influent concentration.

The attachment of inorganic suspended solids (inert biomass, mineral precipitate, and soil particles, FSS) is a function of the pore throat size and seepage velocity. Clogging results in smaller pore throats and greater potential for attachment (straining); however, smaller pore throats also give rise to higher seepage velocities and lower potential for attachment. The net effect is being observed with time in the column for these particles, with the former dominating at earlier times but the latter dominating once the clogging becomes severe.

After a decade of development, the BioClog model is now reaching the point where it can go beyond column studies and be used to predict clogging in landfill drainage systems. Nevertheless, because of the highly coupled and complex nature of the model, which draws together microbiology, geochemistry, waste water engineering and geotechnical engineering, it is unlikely to be used in routine engineering practice. However, models such as this do provide insight that can both advance understanding of what is observed in laboratory tests and field monitoring, and aid in evaluating the likely difference in the performance of different types of LCS.

TEMPERATURE AT THE BASE OF A LANDFILL

Increases in landfill temperature arise from heat generated by biodegradation of waste or the heat of hydration of incinerated residues (ash). High temperatures (50–70°C) have been reported in many landfills (e.g. Collins, 1993; Yoshida *et al.*, 1996). For example, at the Tokyo Port Landfill in Japan, 35 m of MSW was placed directly on the surface of a natural clayey liner. This landfill has no effective LCS on the base, and a significant (20–25 m above the base of the landfill) leachate mound has developed. The temperatures at the base were up to 50°C 7–10 years after the beginning of landfilling and had reduced to 37–41°C after 20 years (Yoshida & Rowe, 2003). High temperature is not restricted to MSW landfills. At the Ingolstadt landfill in Germany (Klein *et al.*, 2001), MSW incinerator bottom ash was placed to a thickness of about 9 m over a composite (GM over clay) liner system. The temperature at the liner peaked at 46°C 17 months after the start of landfilling, and is subsequently decreasing at 0·6 deg C per month.

Typically the temperature has a maximum value in the main body of the waste and decreases towards the boundaries defined by the surface and the underlying liner (Collins, 1993). The rate of increase in temperature with time, both in the waste and at the liner, may vary depending on the waste management practice that is adopted. For example, the rate of waste placement can affect the rate at which the temperature increases at the liner, as illustrated by Brune *et al.* (1991), who reported temperatures ranging from 24°C to 38°C in a leachate drain beneath 4–6 year old waste at the Altwarmbüchen Landfill in Germany (waste placement rate 10–20 m/yr) but only 14–20°C after a similar period at the Venneberg Landfill (waste placement rate 2 m/yr). Similarly, the rates of percolation of moisture through the landfill cover can also affect temperature, as illustrated by Koerner & Koerner (2006), who monitored the temperature on the GM liner at two landfill cells for the same landfill (50 m of waste) north of Philadelphia, USA (mean annual temperature 12·6°C). Both cells had a similar low-permeability geosynthetic cover, but in one case (‘dry cell’) there was no additional moisture added whereas in the other case (‘wet cell’) moisture augmentation began after about 200 days at a rate of approximately 500 m^3 per month. The variation in temperature with time is shown in Fig. 11. The reported temperatures within the waste itself after 8 years and 2 years in the dry and wet cells were 32–43°C and 40–67°C (mean 55°C) respectively (Koerner *et al.*, 2003). For the dry cell, the average liner temperature was consistently about 20°C for 5·5 years. However, after 5·5 years the temperature quickly increased and after 10 years is averaging about 32°C. It may be hypothesised that the 5–6 year delay before the temperature increased reflected the time required for significant heat generation and conduction of that temperature downward to the liner; another similar example will be

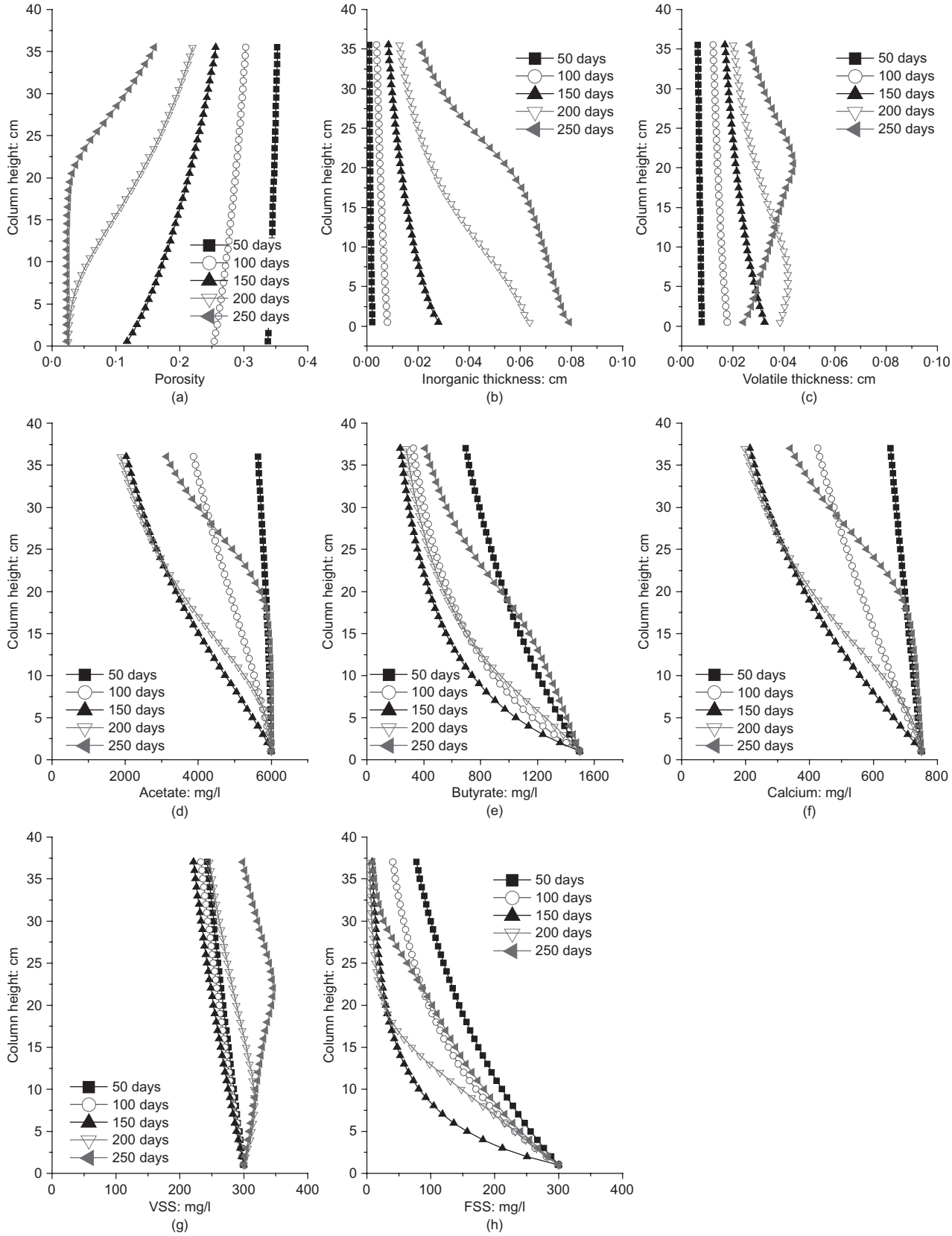

Fig. 10. Various aspects of clogging along a column of glass beads at 50-day intervals based on BioClog model results (after Rowe & VanGulck, 2004): (a) porosity; (b) inorganic film thickness; (c) volatile film thickness; (d) acetate concentration; (e) butyrate concentration; (f) calcium concentration; (g) VSS concentration; (h) FSS concentration

cited below. For the wet cell, the liner temperature was between 25°C and 28°C (i.e. 5–8°C higher than the dry cell) for the first year and then increased over the following 2 years to between 41°C and 46°C.

The KVL provides an example where liner temperature has been monitored above a CCL over a 21-year period. Barone *et al.* (2000) reported data at four locations in the landfill up to 1998. Fig. 12 provides updated data (up to December 2004) at those same four locations. As described in the previous section, Stages 1 and 2 have French drains

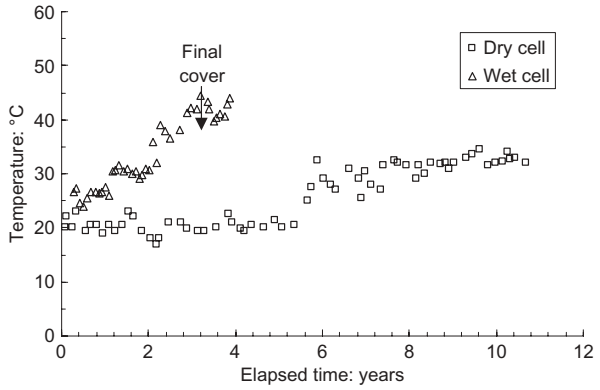

Fig. 11. Average geomembrane liner temperature for dry and wet cells (data replotted from Koerner & Koerner, 2006)

as the LCS. In Stage 1 the temperature increased slowly and remained low (average 12°C) for the first 6 years but then increased rapidly as the leachate mound increased from 1 m to 6·5 m. Subsequently, the temperature stabilised at about 37°C, although the leachate mound continued to increase to about 8·4 m (it has subsequently reduced slightly, probably as a result of the installation of final cover). In Stage 2, the temperature remained relatively constant and low (average 10°C) for the first 5 years but then increased rapidly to 24°C over the next 6 years, as the leachate mound increased from about 1 m to 5 m, and has continued to increase to 35°C (with no sign of it stabilising yet), even though the leachate mound has actually dropped to about 3 m (primarily because of the installation of final cover). In Stages 3 and 4 the blanket drain LCS continues to function well, but since 1998 the temperature has risen from 15°C to 31–32°C (in 2004) at the two monitors shown in Fig. 12, and appears still to be increasing. Fig. 13 shows the change in liner temperature with time at all monitors in the KVL where the leachate head is less than 0·3 m. In these cases it took 8–12 years for the temperature on the liner to reach 20°C but only another 3–4 years to reach 30°C. To the extent that temperatures appear to have levelled off, it is at about 40°C.

The data from the Philadelphia landfill suggest that the injection of fluid significantly accelerated the rate of increase in temperature at the liner. Likewise the build-up of a leachate mound at the KVL increased the rate at which the liner temperature increases. The current evidence suggests that the final maximum liner temperature is higher for landfills where there is a high waste moisture content due either to the addition of fluid (e.g. leachate recirculation) or to mounding of leachate, but it will be necessary to monitor landfill liners with no significant leachate mound for a longer period of time to confirm this, as it may be that, because of the slower rate of increase in temperature with time, these liners have not been monitored for long enough to know the maximum temperature that will be reached. With modest infiltration of leachate and a well-functioning LCS, the liner temperature exceeded 20°C after 5·5–11 years and exceeded 30°C after 7·5–14 years (Figs 11 and 12). These data suggest that estimates of service lives of liners should not be based on a temperature of 20°C but rather on a temperature at least of the order of 30–40°C. The length of time for which the temperature remains this high is unknown at present, but, based on available data, is likely to be at least a few decades for large landfills such as those where data is currently available (i.e. with 30 m of waste above the liner).

Temperature influences both hydraulic conductivity and diffusion coefficient (Collins, 1993). A groundwater temperature of around 10°C is typical of parts of the world where the local mean temperature is 8–10°C. Diffusive and

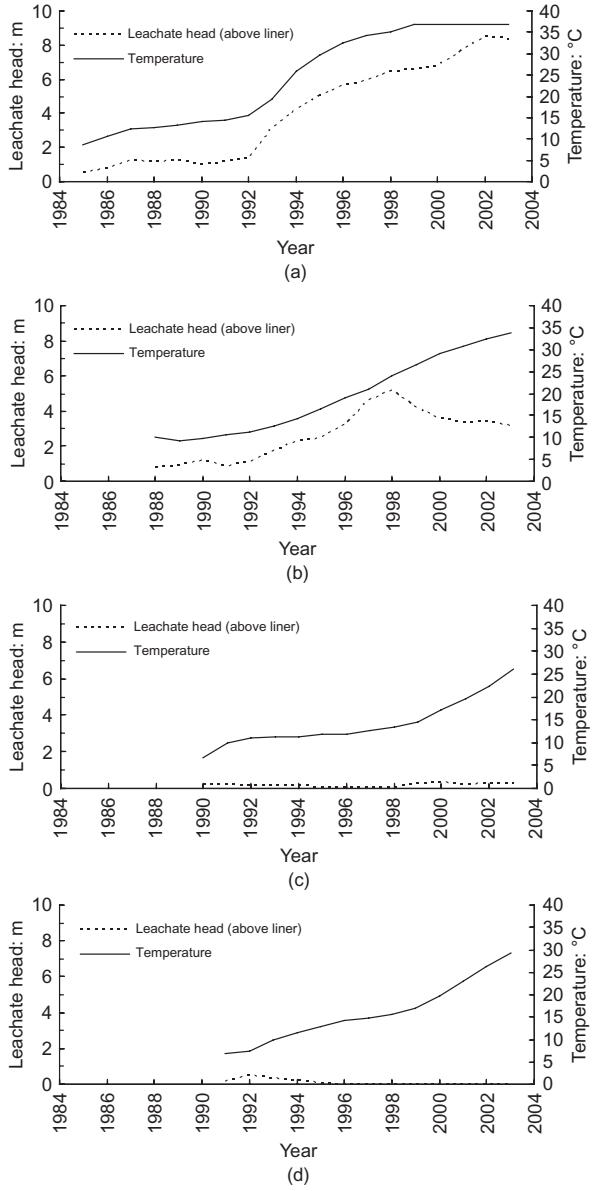

Fig. 12. Variation in leachate head and temperature at four locations in the Keele Valley Landfill (to December 2004): (a) Stage 1, Lysimeter 3; (b) Stage 2, Lysimeter 7; (c) Stage 3, Lysimeter 14B; (d) Stage 4, Lysimeter 16A

advective transport are, respectively, 40% and 30% higher at 20°C than at 10°C, and 100% and 80% higher at 35°C (Rowe *et al.*, 2004). Constant diffusion and hydraulic conductivity parameters may be used if the liner temperature remains relatively constant. However, if the temperature of the liner changes with time then the effect of the change in these parameters with temperature on contaminant impact should be considered. Rowe & Booker (1995, 2005) proposed an approach that readily models the effect of changes in diffusion coefficient and hydraulic conductivity with time. As will be discussed later, temperature also has a significant impact on service lives of geomembranes and clay liners, and on the transmissivity of geonet drainage layers.

LEAKAGE THROUGH LINERS

Change in hydraulic conductivity with time and leakage at the KVL

Leakage through liners is usually interpreted in terms of the actual advective flow through the liner. In the case of

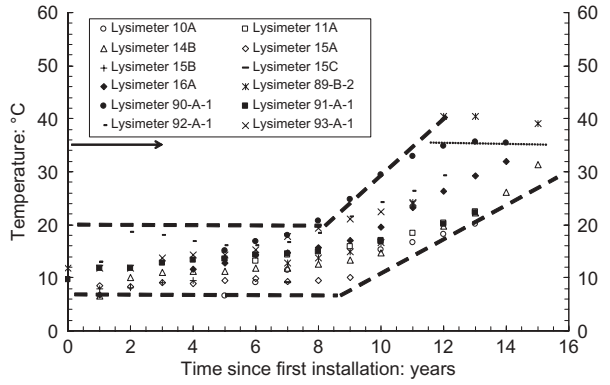

Fig. 13. Variation in liner temperature with time for monitors in parts of the KVL where the leachate head is less than 0·3 m for period to December 2004 (data courtesy of City of Toronto). Arrow and dotted horizontal line indicates 35°C

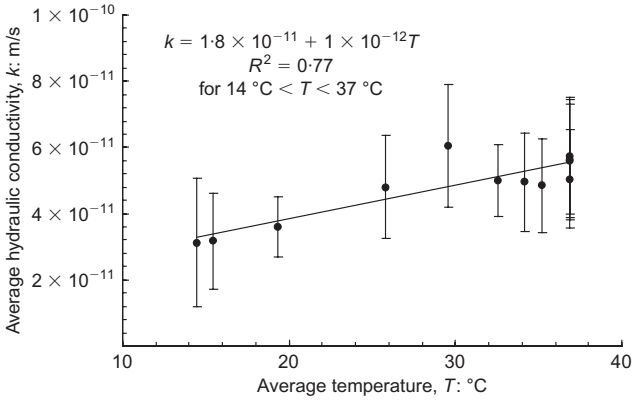

Fig. 15. Variation in annual average hydraulic conductivity with annual average liner temperature for compacted clay liner at Keele Valley Landfill, Lysimeter 3 (data courtesy of City of Toronto)

clay liners this will be given by Darcy's law (equation (1)) and will depend on the hydraulic conductivity k of the clay liner and the hydraulic gradient (i.e. the leachate mound above the liner and the head at the base of the liner). Both the gradient and hydraulic conductivity may vary with time. The latter is discussed below.

Both the inferred and actual hydraulic conductivity of a CCL may vary owing to liner consolidation as the waste thickness increases. For example, at the KVL (Lysimeter 3) the waste thickness increased from 1 m in November 1984 to 33 m in April 1987 and then remained relatively constant. As can be seen from Fig. 14, the annual average k dropped from 4×10^{-10} m/s in 1984 to $3{\cdot}1 \times 10^{-11}$ m/s in 1991. These values are deduced from the measured flow to the lysimeter located in the liner, and the heads above and below the liner, using Darcy's law. Two consolidation-related factors can affect the flow to the lysimeter during this period. First, expulsion of water from voids, due to consolidation, will lead to flow to the lysimeter, which is not explicitly considered in calculating k, and results in the inferred k value being higher than the actual value until consolidation is complete (the effect being greatest in the period 1984–1987 when the waste thickness increased). Second, the decrease in void ratio of the soil due to consolidation will result in an actual decrease in k with time. Both effects occur relatively quickly because, for KVL liner consolidation parameters, consolidation is fast (95% consolidation in less than a year for a given load increment). Based on the data shown in Fig. 14 it is evident that the effect of the decrease in void ratio dominates, because there was a significant decrease in inferred k (more than an order of magnitude) between 1984 and 1988.

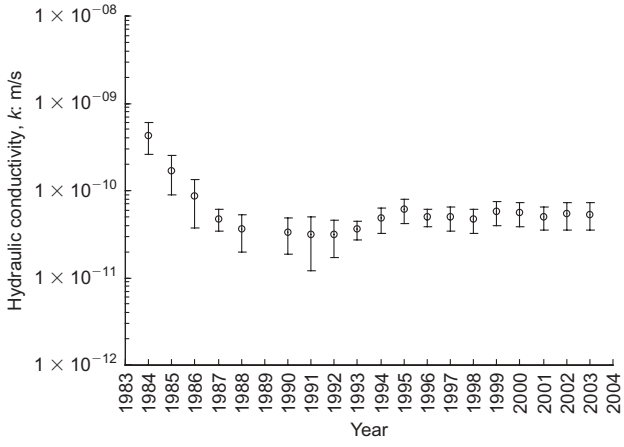

Fig. 14. Variation in annual average hydraulic conductivity with time for compacted clay liner at Keele Valley Landfill, Lysimeter 3 (data courtesy of City of Toronto)

Hydraulic conductivity can also be influenced by temperature, as discussed earlier. For example, inspection of the data in Fig. 14 shows an increase in annual average k with time between 1991 ($k = 3{\cdot}1 \times 10^{-11}$ m/s, $T_{ave} = 14{\cdot}4$°C) and 1995, after which it remained relatively constant at a value (1995–2003: $k_{ave} = 5{\cdot}3 \times 10^{-11}$ m/s, $T_{ave} = 34{\cdot}8$°C) still well below the specified k of 1×10^{-10} m/s. Inspection of Fig. 12 shows that during the period from 1991 to 1995 the temperature at the top of the liner rose from 14·4°C to 29·8°C and then had an average value of 34·8°C for 1995–2003. Fig. 15 shows the variation in annual average k with annual average temperature between 1991 and 2003. The increase closely corresponds to what one would expect from theoretical consideration of the effect of temperature on k. Since the temperature stabilised, so too has the hydraulic conductivity, suggesting no effect of clay–leachate interaction (Rowe *et al.*, 2004) over the period of time considered. This is consistent with unpublished laboratory studies by Quigley (pers. comm.) that showed no significant change in k due to interaction with MSW leachate after permeation with many pore volumes of leachate.

Based on the hydraulic conductivity of the liner (e.g. Fig. 14) and the leachate head (Fig. 12), the flow through the 1·5 m liner can be calculated. There is some uncertainty regarding the head at the base of the liner (there is unsaturated silty sand of variable thickness between the base of the liner and the water table), and the following leakage estimates are based on a typical 4 m distance between the base of liner and the water table. Thus in Stage 1 of KVL the leakage in 1991 (minimum k, $T \approx 14$°C, before the leachate mound began to rise significantly) was about 120 litres per hectare per day (lphd, the units commonly used for reporting leakage through landfill liners). By 2003 this had increased due to both an increase in k and, most significantly, an 8·4 m leachate mound, to about 430 lphd. In Stages 3 and 4 of the landfill, where the temperature has risen to over 30°C (e.g. Lysimeter 16A, Stage 4, Fig. 12) and the leachate mound is well within the drainage layer ($< 0{\cdot}3$ m), a hydraulic conductivity of 5×10^{-11} m/s gives an estimated leakage of 160 lphd. These numbers provide an indication of the magnitude of the expected leakage through a single CCL at KVL with (430 lphd) and without (160 lphd) a significant

leachate mound. They also provide a frame of reference for the discussion of leakage in the following subsection.

Observed leakage through liners involving a geomembrane

Double liner systems have a leak detection system (LDS) (which also serves as a secondary LCS, SLCS) that can be used to provide insight regarding the effectiveness of the primary liner. However, the interpretation of the data from LDS requires careful consideration of sources of fluid other than leakage from the landfill (Gross *et al.*, 1990). These include:

(*a*) water that infiltrated into the LDS layer during construction
(*b*) water arising from consolidation of the CCL
(*c*) groundwater from outside the landfill.

Bonaparte *et al.* (2002) examined data for 72 landfill cells containing one of: a single GM primary liner; a GM/GCL composite primary liner; a GM/CCL composite primary liner; or, in one case, a GM and GCL over a CCL (GM/GCL/CCL) composite primary liner. They identified three periods during which there may be very different flows to the LDS:

(*a*) the initial period of operation
(*b*) the active period of operation
(*c*) the post-closure period (after the final cover has been constructed).

Only the second and third periods are of interest here, because they provide a better indication of liner performance. The landfills examined had LDS composed of sand, gravel, or geonets (GN). All eventually provide useful information, but the gravel and GN systems are likely to provide the best data at early times because the response is faster than for sand systems, and they are unlikely to contain significant construction water or have significant storage for leakage water after the initial period of operation. Table 3 summarises the mean, standard deviations and maximum average monthly flows in the LDS for the three types of liner system discussed above and all types of LDS, and includes cells constructed with and without construction quality control (CQA). All data discussed below are from cells that were constructed with a formal CQA programme unless specifically noted otherwise.

For cells with a primary HDPE GM liner, formal CQA was adopted for 23 of the 25 cells. For these cells, the average monthly flow ranged from 0 to 790 lphd in the active period and from 2 to 100 lphd in the post-closure period (for cells without CQA the corresponding flows were up to 1600 lphd and 330 lphd). The peak flows were generally less than 500 lphd, but exceeded 1000 lphd for two cells. To put these numbers (and those in Table 3) into context, one can compare these leakage rates with those calculated for a 0·6 m CCL. A primary GM liner alone has leakage (Table 3) that often exceeds that for a primary CCL with $k = 5 \times 10^{-11}$ m/s (40–65 lphd) but is normally considerably less than that for a primary CCL with a typically specified $k = 1 \times 10^{-9}$ m/s (860–1300 lphd). However, there are cases where the leakage through a GM alone will exceed that of the CCL with $k = 1 \times 10^{-9}$ m/s.

The combination of a GM and GCL substantially reduces leakage (Table 3) relative to a GM alone. The average flow ranged from 0 to 11 lphd in the active period and from 0 to 2 lphd in the post-closure period. The maximum peak flow was 54 lphd.

The interpretation of leakage rates for GM/CCL systems is more complicated than for the cases discussed above, because part of the fluid collected is consolidation water from the overlying CCL. The leachate chemistry provides some support for the argument that there is consolidation water contributing to the collected fluid. In general, the chloride, COD and, where available, volatile organic compound (VOC) concentrations in the LDS were low compared with values in the leachate (Bonaparte *et al.*, 2002). Notwithstanding uncertainty regarding the proportion of collected fluid that is consolidation water, inspection of Table 3 indicates that the GM/CCL combination is significantly better than the GM

Table 3. Mean and standard deviations of flow in LDS for landfill cells with a primary liner and underlying LDS (in lphd). Numbers have been rounded (Based on data from Bonaparte *et al.*, 2002)

Liner/stage	No. of cells	Average monthly flows: lphd			Peak monthly flows: lphd		
		Mean*	SD†	Max‡	Mean*	SD†	Max‡
Single liner: GM alone							
Active	25	190	330	1600§ 790¶	360	610	3070§ 1830¶
Post-closure	6	130	120	330	330	30	1130
Composite GM/GCL liner							
Active	22	1·5	2·7	11¶	9	16	54¶
Post-closure	5	0·6	0·9	2	4	5	10
Composite GM/CCL or GM/GCL/CCL liner							
Active	11	90	90	370§ 260¶	250	370	1990§ 1240¶
Post-closure	3	50	50	220	60	90	250

*Mean and †standard deviation of reported average and peak average monthly flows: these were obtained for different cells over different periods, and include data obtained for systems with sand, gravel and GN LDS.
‡Maximum value reported.
§Largest value reported, but it is for sand LDS and so may reflect stored water in the LDS shortly after construction.
¶Largest value for liner system with GN LDS.

alone. Also, noting that the CCLs in Table 3 all had $k = 1 \times 10^{-9}$ m/s specified, the GM/CCL composite liner was typically significantly better than 860–1300 lphd calculated ($k = 1 \times 10^{-9}$ m/s, $i = 1$–$1{\cdot}5$) for a CCL alone.

Given the relatively fast primary consolidation typical of many CCLs, one would expect that the effect of consolidation water would be most significant in the active period and would quickly cease to be significant in the post-closure period, especially for landfills with a GN or gravel LDS that drains quickly. Table 4 summarises results for nine cells where the LDS was a GN or gravel. In several cases there are different cells at the same landfill, and so an assessment can be made of variability that occurs for nominally similar conditions.

Several observations arise from Table 4. First, there is considerable variability in leakage for a similar liner thickness (and maximum waste thickness), and this can be attributed to variability in the liner itself (rather than consolidation). For example, in the post-closure period there is a sixfold difference in average flow and more than a threefold difference in peak flow for two cells at landfill AQ. There is also an order of magnitude difference in the flows for landfills AM and AQ, which have a similar (450 mm) CCL and waste thicknesses.

Second, assuming that the water content and compaction are somewhat similar, if consolidation is an important factor, then one would expect about twice as much consolidation water for 900 mm thick CCLs as for 450 mm thick CCLs. However, during the active period (when consolidation water should be most significant), the flows at landfill AQ (450 mm) are similar to or larger than those for landfills AL and AO (900 mm). In the post-closure period the flows of the two cells at landfill AQ straddle that for landfill AD. More data are needed; however, the available data all lead to the conclusion that variability in the composite liners themselves is significant, and that the difference between the observed flows for the GM/GCL cases and the GM/CCL cases represents differences in leakage, and cannot be explained as the result of consolidation water. This suggests that, on the whole, GM/GCL composite liners can be constructed to give lower leakage than a GM/CCL composite. However, it appears that the flows for landfill AR, which had a GM/GCL/CCL (300 mm) system, are similar to some of those with both 900 mm and 450 mm CCL. While some of this flow is undoubtedly consolidation water, given the relatively small amount of waste (11 m) and thin CCL (300 mm) it appears that there are defects in the GM that are primarily responsible for the higher than otherwise expected leakage. A possible explanation for the differences in the observed flows for those landfills with a GM/GCL compared with those with a GM/CCL liner will be presented in a subsequent section.

It should be emphasised that all of the leakages reported for composite liners are small, and, correspondingly, the contaminant transport by advection will be very small.

Holes in geomembranes

As an intact GM is essentially impermeable to water, leakage through GMs such as those discussed in the previous section must arise from flaws in the GM. These flaws may:

(*a*) be in the GM following manufacturing
(*b*) arise from handling of the GM rolls during delivery to the site, on-site placement and seaming
(*c*) be caused by physical damage during the placement of material such as drainage gravel on top of the liner system
(*d*) arise from subsequent penetration or cracking of the GM during or following placement of the waste.

Holes due to sources (*a*)–(*c*) can be detected by an electrical leak detection survey. Compiling 205 results from four published leak detection surveys, Rowe *et al.* (2004) found that (a) no holes were detected for 30% of the cases, and (b) less than 5 holes/ha were detected for half of the surveys. Nosko & Touze-Foltz (2000) reported 3 holes/ha after installation and 12 holes/ha after placement of drainage layer. Giroud & Bonaparte (2001) suggested that, for GMs installed with strict construction quality assurance, 2·5–5 holes/ha can be used for design calculations of leakage. Colucci & Lavagnolo (1995) reported that 50% of holes had an area of less than 100 mm^2 ($r_0 < 5{\cdot}64$ mm). The number and size of holes will depend on the level of CQC/CQA. As the leak detection surveys are conducted shortly after construction of the liner system, it is uncertain how many holes may develop under combined overburden pressures, elevated temperatures and chemical exposure years after construction. These holes may arise from:

(*a*) indentations at gravel contacts following placement of the waste
(*b*) stress cracking at points of high tensile stress in wrinkles

Table 4. Weighted average flow rates and peak flow in LDS for landfills with composite liners involving GM and CCL and a GN or gravel LDS. All numbers have been rounded to nearest 10. (Based on data from Bonaparte *et al.*, 2002)

	Thickness of			Active operation		Post-closure	
Landfill	Waste: m	GM: mm	CCL: mm	Average:* lphd	Peak:† lphd	Average:* lphd	Peak† lphd
AL1	68	1·5	900	160	370		
AO1	23	1·5	900	120	350		
AO2	23	1·5	900	70	160		
AD7	24	1·5	900	60	390	80	170
AM1	27	2·0	450	10	60		
AM2	27	2·0	450	10	40		
AQ1	21	2·0	450	200	1240	120	250
AQ10	21	2·0	450	40	250	20	80
AR1	11	1·5	6/300‡	170	470		

*Time-weighted, based on the reported values for different time periods.
†Largest peak value reported for a monitoring period.
‡GCL/CCL.

(*c*) substandard seams subjected to tensile stresses.

Large-scale physical testing conducted by Tognon *et al.* (2000), discussed in more detail in a later section, indicated that the protection layer between the GM and the overlying drainage material has a critical effect on the tensile strains induced in the GM. For example, with a protection layer consisting of two layers of nonwoven geotextile having a total mass per unit area of 1200g/m^2, there were over 300 gravel indentations per square metre in the GM and a peak strain (13%) close to the yield strain. If only one out of every 10 000 indentations (i.e. 0·01%) eventually resulted in a defect, this would correspond to over 300 holes/ha. Consequently, if one is to design with 2·5 or even 5 holes/ha it is essential to have both a rigorous CQC/CQA programme and a protection layer that will limit the tensions that develop in the GM to a small value.

Wrinkles in geomembranes

Wrinkles in a GM arise both from construction practice and, in particular, from thermal expansion when the GM is heated by the sun after placement. These wrinkles do not disappear when the GM cools or when it is loaded (Stone, 1984; Soong & Koerner, 1998; Brachman & Gudina, 2002). Pelte *et al.* (1994) reported wrinkles 0·2–0·3 m wide, 0·05–0·1 m high at spacing of 4–5 m. Touze-Foltz *et al.* (2001a) reported wrinkles 0·1–0·8 m wide, 0·05–0·13 m high at spacing of 0·3–1·6 m. Rowe *et al.* (2004) reported a case where there were 1200 wrinkles/ha. Wrinkles are important because of the increased potential for contaminant migration through a hole in the GM at or near the wrinkle. There is also increased potential for development of future holes due to stress cracking at points of high tensile stress in the wrinkle. As wrinkles are often interconnected, the length of a wrinkle should be regarded as the total linear distance that fluid can migrate along a wrinkle and its interconnections.

Geomembrane–clay liner interface properties

Leakage through a defect in a composite liner (GM over clay) depends on the contact between the GM and the underlying soil (Brown *et al.*, 1987). Imperfect contact allows for a transmissive zone between the two liners, and hence, once fluid has migrated through the defect, it can then move laterally in the interface between the two liners before fully percolating through the clay liner. In addition to wrinkles, discussed above, there are three primary sources of this imperfect contact (Rowe, 1998a). First, even for a well-compacted soil, there may be protrusions related to particle size distribution in the liner material, and these protrusions will create some gap in which water may flow. Second, when compacting clay liners to obtain low hydraulic conductivity, it is usually desirable to compact at water contents 2–4% above the standard Proctor optimum value; however, this is often close to the plastic limit of the soil, and it is difficult to obtain a smooth surface because of rutting caused by construction equipment, either during construction of the liner or when the overlying GM and leachate collection layer is being placed. These undulations/ruts tend to provide linear zones where there will not be intimate contact between a GM and CCL (e.g. Cartaud *et al.*, 2005a). Third, the placement of a geotextile between the GM and clay liner either as a separate layer or as part of GCL may provide a continuous, potentially transmissive, layer. This is particularly true when there is a separate layer between the GM and a CCL, as is common in France (Cartaud & Touze-Foltz, 2004). To a lesser extent the presence of a geotextile component of a GCL in contact with a GM also provides for some transmissivity, although much less than for a geotextile over a CCL, because bentonite swelling into the geotextile substantially reduces the geotextile transmissivity (Touze-Foltz, pers. comm.).

Giroud & Bonaparte (1989) characterised two typical GM–CCL contacts: 'good' and 'poor'. Based on calculations for typical liner properties ($k = 10^{-9}$ m/s), these descriptors can be related to average transmissivities of the GM/CCL interface of $1{\cdot}6 \times 10^{-8}$ m^2/s and 1×10^{-7} m^2/s respectively (Rowe, 1998a). These values are useful for performing calculations; however, the actual interface conditions are far more complex. For a CCL with a hydraulic conductivity k of 1×10^{-9} m/s, 'good' and 'poor' contact correspond to an average 'gap' between the GM and the CCL of 27 μm and 50 μm respectively. Cartaud *et al.* (2005a, 2005b) used laser rugosimetry to study the topography of the interface between 2 mm thick HDPE GM and CCL, and found that, within a 1 m^2 area, the apertures could vary from direct contact up to 10 mm. Using numerical simulations for the aperture topography obtained at different pressures, they showed a three order of magnitude reduction in fluid velocities at the interface, and hence a substantial reduction in the transmissivity of the interface, as the applied pressure increased from 6 to 64 kPa.

When a GM is placed over a GCL, there is greater potential for obtaining good contact with a low-permeability layer than when placed over a CCL. This is because the GCL can be placed flat on a well-compacted, smooth and firm foundation (e.g. Giroud, 1997). Away from wrinkles, the factor controlling the leakage for GM over a GCL is the transmissivity of the interface between the GM and GCL. Harpur *et al.* (1993) reported tests for the transmissivities of these interfaces and reported values between 2×10^{-12} m^2/s (at a normal stress of 7 and 70 kPa) for bentonite in direct contact with the GM, and 2×10^{-10} m^2/s (7 kPa) and 1×10^{-12} m^1/s (70 kPa) for a GCL with a woven geotextile in contact with the GM. The highest of these transmissivities was two orders of magnitude below that for 'good' contact for a typical CCL discussed above ($1{\cdot}6 \times 10^{-8}$ m^2/s). This difference in interface transmissivity provides at least a partial explanation for why the leakage through composite liners with a GCL may be lower than that with a CCL.

Where there are wrinkles in a GM over a GCL, there is potential for the bentonite to 'extrude' laterally from the GCL in direct contact with the GM to the zone below the wrinkle. Provided that there is sufficient applied compressive stress (Giroud, 1997), and the wrinkle is small, this would reduce or eliminate the gap between the GM and GCL at that location and hence reduce the interface transmissivity by establishing closer contact between the GM and GCL. However, this also thins the GCL (Stark, 1998; Dickinson & Brachman, 2003). For large wrinkles there may be: (a) significant thinning of the GCL adjacent to the wrinkle, which could impact negatively on the GCL performance; and (b) failure to fill the gap between the GCL and GM.

Solutions for assessing leakage through composite liners—no significant wrinkles

Leakage through composite liners can be calculated using empirical equations or analytical equations, or from numerical analysis. Empirical equations are established by curve-fitting families of solutions from analytical equations (Giroud & Bonaparte, 1989; Giroud, 1997), and although they may be convenient to those without access to analytical solutions, they really do not provide any original information. Analytical equations involve either the assumption of perfect contact (Rowe & Booker, 2000) or lateral migration in a transmissive zone below the GM combined with 1D

flow into the underlying soil (Jayawickrama *et al.*, 1988; Rowe, 1998a; Touze-Foltz *et al.*, 1999, 2001b). Numerical methods allow modelling of the actual three-dimensional conditions near the hole (Foose *et al.*, 2001) or the complete variability of the interface topography if it is known (Cartaud *et al.*, 2005b). This raises three questions.

(*a*) Does the assumption of 1D flow in the subsoil have any practical effect on the accuracy of the analytical solutions?
(*b*) Does the additional flexibility afforded by numerical analysis imply that it should be used for calculating leakage in practical problems?
(*c*) Do these equations, which neglect the presence of significant wrinkles, give reasonable predictions of observed leakage through primary liners?

These three questions are addressed below.

Except for the case where a low-permeability soil is deposited as a slurry in contact with the GM and it consolidates with time under a large compressive stress, perfect contact between the GM and the subsoil (as assumed by Rowe & Booker, 2000) is likely to provide a lower bound to the leakage through holes in a GM that is placed above a CCL or GCL. Assuming that there is a uniform transmissive zone between the GM and clay liner, one can use Rowe's (1998a) direct contact analytical equation or Giroud's (1997) empirical charts to calculate leakage. However, the question regarding the significance of the assumption of 1D flow in the liner needs to be addressed. Foose *et al.* (2001) partly addressed this question and showed that, for a GM over a GCL, Rowe's (1998a) direct contact analytical solution provided very good agreement with the results of numerical analysis for the typical reported transmissivity values discussed above. Similarly the author has found excellent agreement (error of less than 4%) between the direct contact analytical solution and the axisymmetric numerical analysis for interface transmissivities within the practical range of interest for both the GM/GCL composite liner and the GM/CCL composite liner.

Both the numerical and analytical solutions discussed above assume a uniform transmissivity of the interface. Analytical solutions have also been developed for regular variations in the transmissivity of the interface (Touze-Foltz *et al.*, 2001b), and numerical methods are available to model more complex situations (Cartaud *et al.*, 2005b). These may be useful in interpreting laboratory tests where the actual interface topography is well defined, but in practical situations the interface topography will vary significantly (e.g. as is evident from the work of Cartaud *et al.*, 2005a, 2005b), but is unknown at the location of the (assumed) holes used in design calculations. Thus for practical purposes, the more simplified approaches used in conjunction with a range of likely transmissivities will provide the information needed for design purposes, and the really critical question is whether these equations, which neglect the presence of significant wrinkles, give reasonable predictions of observed leakage through primary liners. To address this question, it is useful to calculate leakage for typical interface conditions and a range of numbers of holes and compare these results with leakage reported by Bonaparte *et al.* (2002).

The upper two curves in Fig. 16 show the calculated leakage through a composite liner (GM + CCL) for poor contact and good contact, together with the shaded zone defined by the mean value of the average monthly flows in the active (90 lphd) and post-closure (50 lphd) periods for the different landfill cells summarised in Table 3. With poor contact conditions 20–30 holes/ha would be required to explain the typical leakage. For good contact conditions more than 90 holes/ha would be required to explain the lower value for typical leakage, and in excess of 100 holes/ha would be required to explain the upper end of the range. A very large number of holes ($\gg$ 100 holes/ha) would be required to explain the maximum flow shown by an arrow at the right of the figure.

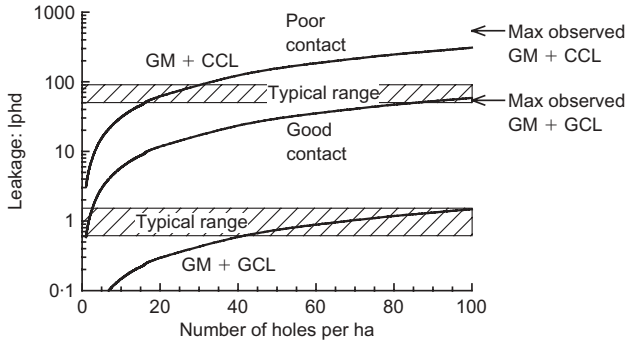

Fig. 16. Comparison with observed leakage and calculated leakage through composite liners, neglecting significant wrinkles. Upper solid curve for GM + 0·6 m CCL ($k = 1 \times 10^{-9}$ m/s) and poor contact ($\theta = 1 \times 10^{-7}$ m^2/s); centre solid curve for GM + 0·6 m CCL ($k = 1 \times 10^{-9}$ m/s) and good contact ($\theta = 1{\cdot}6 \times 10^{-8}$ m^2/s); and lower solid curve for GM + 10 mm GCL ($k = 2 \times 10^{-10}$ m/s; $\theta = 2 \times 10^{-10}$ m^2/s). In each case hole radius $r_0 = 10$ mm, depth of fluid above GM is 0·3 m. The upper shaded region shows typical field leakage rates for GM/CCL, with the upper and lower limits defined by the mean value of the average monthly flows in the active (90 lphd) and post-closure (50 lphd) periods for the different landfill cells summarised in Table 3. The lower shaded region shows typical field leakage rates (0·6–1·5 lphd) for GM/GCL leakage (again from Table 3 and based on data reported by Bonaparte *et al.*, 2002). Upper and lower arrows on right-hand side show maximum observed leakage for GM/CCL and GM/GCL based on data reported by Bonaparte *et al.* (2002)

The calculated leakage for a GM + GCL composite is shown by the lowest curve in Fig. 16, and the lower shaded zone shows the observed typical (0·6–1·5 lphd) leakage (again from Table 3). About 40 holes/ha would be required to explain the bottom end of the typical range and more than 100 holes/ha to explain the upper end of the typical range. The maximum observed leakage shown by the lower arrow on the right is more than an order of magnitude greater than the predictions with 100 holes/ha. Thus it would appear that the predications above, which assume no major wrinkles, are not consistent with the observed leakage and the likely number of holes/ha for either the GM/CCL or GM/GCL systems.

Solutions for assessing leakage through composite liners with wrinkles

Rowe (1998a) presented an analytical solution for the case where a hole coincides with a wrinkle in the GM of length L and width $2b$ (Fig. 17). The transmissivity beneath the wrinkle is much greater than the interface transmissivity, θ, where the GM is in contact with the underlying soil. It is also assumed that $L \gg b$ such that the effects of leakage at the ends of the wrinkle can be neglected. This solution assumes unobstructed lateral flow along the length L and across the width $2b$ of the wrinkle, and then lateral flow between the GM and the soil outside the wrinkle. One-dimensional, vertical flow is assumed from the transmissive layer through the underlying soil beneath the wetted distance from the wrinkle (this is an approximation). Rowe's solution allows consideration of interactions between adjacent similar wrinkles assumed to be spaced at a distance $2x$ apart, and the leakage Q is given by

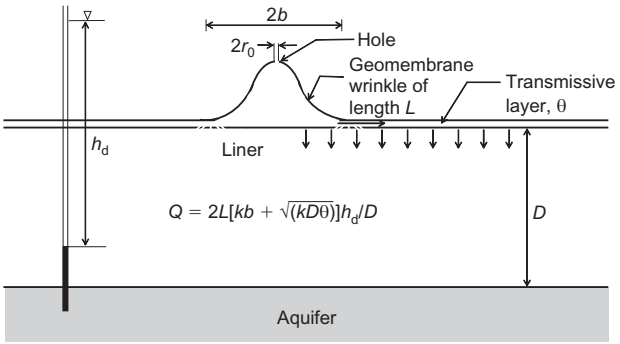

Fig. 17. Schematic defining leakage through a composite liner with a wrinkle. Assumes lateral migration at interface and vertical flow in clay liner

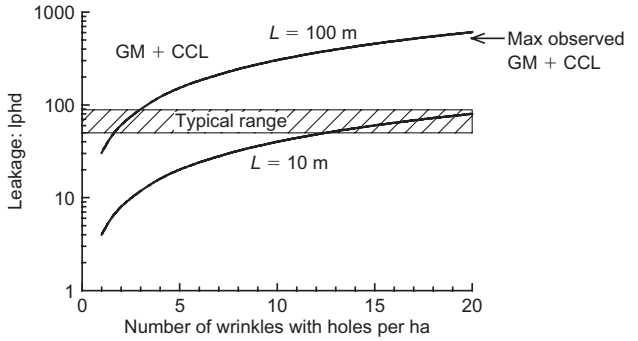

Fig. 18. Comparison with observed leakage and calculated leakage through composite liner accounting for significant wrinkles. Calculated curves for GM + 0·6 m CCL ($k = 1 \times 10^{-9}$ m/s; good contact $\theta = 1{\cdot}6 \times 10^{-8}$ m^2/s), wrinkle width, $2b = 0{\cdot}2$ m, and depth of fluid above GM, $h_w = 0{\cdot}3$ m; based on Rowe *et al.* (2004). Typical field leakage rates and maximum observed values from Table 3 and based on data reported by Bonaparte *et al.* (2002)

$$Q = 2Lk\left(b + \left\{1 - \exp\left[-\alpha(x-b)\right]\right\}/\alpha\right)\frac{h_d}{D} \tag{22}$$

where L is the length of the wrinkle; $2b$ is the width of the wrinkle; k is the hydraulic conductivity of the clay liner; θ is the transmissivity of the GM–clay liner interface; $\alpha = [k/(D\theta)]^{0{\cdot}5}$; h_d is the head loss across the composite liner; and D is the thickness of the clay liner. Assuming no interaction with an adjacent wrinkle, the leakage Q is given by

$$Q = 2L\left[kb + (kD\theta)^{0{\cdot}5}\right]\frac{h_d}{D} \tag{23}$$

The leakage calculated using this wrinkle analytical solution was compared with that from a 2D finite element analysis and found to be in excellent agreement (an error of 5% or less) for both the GM/GCL composite liner and the GM/CCL composite liner for the range of cases considered.

Figure 18 shows the calculated leakage (using equation (23)) through GM over a 0·6 m CCL for wrinkles of total length 10 m and 100 m together with the typical leakage range previously shown in Fig. 16 and summarised in Table 3. With 10 m long wrinkles, between 12–22 holed wrinkles/ha are required to explain the typical leakage, and for 100 m long wrinkles only 1–3 holed wrinkles/ha would be required to explain the typical leakage. A similar comparison for a GM over a GCL indicated that the typical range of leakage could be explained by 2–3·5 holed 10 m long winkles/ha, and the maximum leakage could be explained by about 5 holed 100 m long winkles/ha. Thus the typical observed leakage for composite liners with both CCLs and GCLs can be readily explained by holes in wrinkles for the typical number of holes/ha and reasonable combinations of other parameters.

Some factors that can influence leak detection

As noted in previous sections, leakage through composite liners (and hence the fluid collected in LDS) is controlled by the leachate head, the number and size of holes in the GM, wrinkles, the transmissivity of the GM/clay liner interface, and the hydraulic conductivity and thickness of the liner. However, there are a number of additional factors that can influence the amount of fluid that is collected. These include:

(*a*) the hydraulic characteristics of the material above the GM
(*b*) consolidation of the liner
(*c*) the initial degree of saturation of the soil and geosynthetics below the GM
(*d*) the potential for the GCL to significantly reduce the transmissivity of an underlying geonet drainage layer.

These will each be briefly discussed below.

The leakage through a hole in a GM cannot exceed (a) the flow from Bernoulli's equation if the permeability of the overlying layer is high enough, or (b) the capacity of the fluid to drain to the hole. Giroud *et al.* (1997b) considered both of these cases, and one can (iteratively) calculate the limiting flow Q through a hole from

$$h_w = \left\{\frac{r_0^2 q_0}{2k_{om}} + \frac{Q}{2k_{om}\pi}\left[\ln\left(\frac{Q}{\pi r_0^2 q_0}\right) - 1\right] + \frac{1}{4g^2}\left(\frac{Q}{1{\cdot}88r_0^2}\right)^4\right\}^{0{\cdot}5} \tag{24}$$

where q_0 is the liquid supply (e.g. permeation through the waste per unit area reaching the LCS), k_{om} is the hydraulic conductivity of the permeable leachate collection layer over the GM, r_0 is the radius of the hole in the GM, and g is the acceleration due to gravity. This expression reduces to the Bernoulli equation as k_{om} tends to infinity. For typical sizes of hole, equation (24) may limit leakage only for very long wrinkles.

Expulsion of water from voids due to consolidation will lead to flow to the LDS. It will also result in a reduction in hydraulic conductivity with time, as discussed earlier for the KVL. The significance of this mechanism will depend on the properties of the liner; however, for CCLs such as that at Keele Valley (discussed earlier) and Halton (Rowe *et al.*, 2000c) consolidation occurs quickly (95% consolidation in less than a year), and the rate of expulsion of fluid is controlled largely by the rate of loading due to increasing waste thickness above the liner. This may increase apparent leakage; however, as discussed earlier in the context of the Bonaparte *et al.* (2002) data, there is no evidence that this is significantly affecting the reported leakage rates.

Rowe & Iryo (2005) have examined the hydraulic performance of an LDS below a composite liner consisting of a GM over a GCL. The time for leakage to be detected was shown to be highly dependent on the initial degree of saturation of the material below the GM and the distance between the hole/wrinkle and the drainage point in the system. Under some circumstances this could result in leakage not being detected for a considerable period of time

(several years). The predicted leakage was shown to be of a similar magnitude to that reported in field monitoring and discussed earlier. The effect was at a minimum (although not necessarily negligible) for a GCL alone between the GM and the underlying LDS, and greatest when the GCL was on an unsaturated foundation layer located above the LDS. This raises the caution that it may take considerable time before the full steady-state leakage is established for situations where the soil and geosynthetics below the GM are not initially saturated.

Although geonets have a number of advantages in terms of the potential speed of leak detection, there is potential for a significant reduction in the flow capacity of the geonet due to intrusion of adjacent materials into the structure of the geonet. For example, Hwu *et al.* (1990) showed that the flow rate could be reduced by an order of magnitude as a result of geotextile intrusion into the apertures of geonets. The intrusion could be reduced by stiffening the geotextile by resin treating, burnishing, and scrim reinforcing, and there was a substantial benefit from using a composite fabric (a needle-punched nonwoven over a woven slit-film geotextile). Drainage layers can be designed with a three-layer system, and limited opening size adjacent to the geotextile, to minimise the effect of geotextile/soil intrusion.

Special care is needed when the geonet is overlain by a GCL (e.g. in an LDS below a composite liner) owing to the potential swelling of the bentonite into the geonet. Here the choice of the geosynthetic between the bentonite core and the geonet may be critical. Shaner & Menoff (1992) examined the effect of using a number of geotextiles placed between the GCL and the underlying geonet to limit the intrusion of the bentonite into the geonet. Legge & Davies (2002) also examined this issue. Fig. 19 shows the flow rate for a bi-planar geonet in a standard test between two steel plates. Also shown is the flow rate for a GCL in direct contact with the geonet, and finally for the case of a geogrid placed between the GCL and geonet. Legge & Davies (2002) reported that when the applied pressure of 400 kPa was maintained for 14 h for the GCL/geonet system the flow rate dropped to zero under a unit gradient (165 mm head difference). As this gradient greatly exceeds that typically encountered in landfills ($< 0{\cdot}05$ on the base and $< 0{\cdot}33$ on side slopes), it is apparent that a geonet should not be used as an LDS below a GCL unless a reinforcing layer sufficient to prevent intrusion of the bentonite into the geonet is placed between the GCL and geonet. There should also be a geosynthetic, either as part of the GCL or between the GCL and geonet, which will prevent potential internal erosion of the bentonite into the geonet (Rowe & Orsini, 2003). The details regarding what measures were taken to avoid bentonite intrusion in the landfills examined by Bonaparte *et al.* (2002) were not reported, and hence the effects of bentonite intrusion into geonets on the leakage detected are not known. However, this mechanism could serve to slow (and hence delay the reporting) of leachate to the sump and, if there is no reinforcing layer and sufficient pressure, could reduce or even cut off flow to the sump. Thus care is needed in the design and construction of these systems to ensure that the swelling of the GCL under vertical stress does not compromise the drainage function of any underlying geonet. It should also be noted that Davies & Legge (2003) have shown that this geonet transmissivity can also be substantially reduced by an increase in temperature.

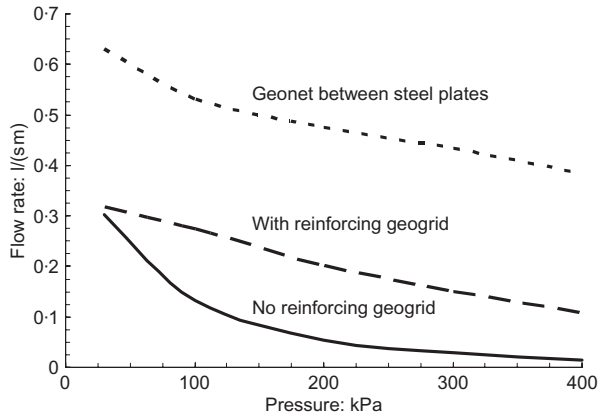

Fig. 19. Variation in flow rate with applied pressure for a transmissivity test at 165 mm head for: geonet between steel plates (standard test); GCL, geogrid and geonet; and GCL in direct contact with geonet. Note: GCL has polypropylene woven ($M_A = 270$ g/m^2) cover and composite nonwoven ($M_A = 270$ g/m^2)-woven slit film ($M_A = 110$ g/m^2) carrier geotextiles, and bentonite ($M_A = 3700$ g/m^2). Geonet was 3·3–4·4 mm thick at 2 kPa ($M_A = 700$ g/m^2). Woven biaxial geogrid had high-strength polyester yarns with polymeric coating and grid aperture 1 mm × 1·3 mm, tensile strength of 32·6 kN/m, and tensile stiffness of 200 kN/m at 2% strain. Partially adapted from Legge & Davies (2002), and with additional data from Legge & Davies (pers. comm.)

DIFFUSION THROUGH LINERS

Any assessment of long-term impact for a landfill requires contaminant transport modelling. Although this is a common practice in some parts of the world, there are still jurisdictions where advective transport (leakage as discussed in the last section) is the only consideration in assessing potential impact. However, as will be demonstrated below, diffusive transport may result in contaminant transport over even relatively small times.

Othman *et al.* (1996) reported significant levels of 1,1 DCA and DCM in the leak detection system for a landfill with a 1·5 mm thick HDPE GM and 6 mm thick GCL composite liner and a 5 mm thick geonet LDS. This same system had exhibited low leakage rates (average value of 3·6 lphd from 14 to 21 months, reducing to 0·7 lphd between 22 and 31 months), and the inorganic chemistry was not characteristic of leachate. This implies that any leakage through holes in the GM was very small. However, the concentrations of DCM and 1,1 DCA were significant over a period of between 6 and 28 months after commencement of waste placement. This suggests possible diffusion through the GM/GCL system. Workman (1993) also examined the chemistry of the fluid in the LDS of a number of cells and detected several VOCs including chloroethane, ethylbenzene and trichloroethene at low concentrations. Workman hypothesised that they migrated as gases from the primary to secondary system at the side slopes. Although this is possible, the alternative hypothesis of migration through the primary liner by diffusion warrants further consideration. In this section the diffusion through naturally deposited and compacted clays, GCL and GMs will be examined.

Diffusion through naturally deposited clay

Natural diffusion profiles through clays deposited at the end of the last glacial period in southern Ontario, Canada, have provided an ideal means of assessing long-term diffusion through thick (30–40 m) low-permeability deposits. These cases (Desaulniers *et al.*, 1981; Quigley *et al.*, 1983; Rowe & Sawicki, 1992) have demonstrated the migration by diffusion over a period of 10 000–12 000 years (against small downward advective flow in two of the cases). The corresponding diffusion coefficients (2×10^{-10}, 3×10^{-10}

and $4–6 \times 10^{-10}$ m^2/s) varied over only a relatively small range, which can be attributed, in part, to the different tortuosity of the three clayey soils and, in part, to the effect of the need to maintain an ion balance and hence the dependence of the rate of chloride migration on the rate of migration of associated cations.

Near the Sarnia site, dissolved gases originating from the underlying sedimentary bedrock have also been diffusing upwards in the groundwater. These gases come out of solution upon stress release, and have been observed venting in boreholes drilled into the till. These gases have contributed to two geotechnical problems (Rowe *et al.*, 2002) in the area. In one of these cases, excavation to a depth of 25 m for a new cell for a hazardous waste landfill resulted in venting of gas and water through the remaining 14–15 m of low-permeability till at three separate locations, and resulted in the abandonment of the cell. This case highlights the implication of the diffusion of gas and the importance of identifying the presence of dissolved gas and assessing its implications with respect to stability when considering excavations in areas underlain by gas.

Diffusion profiles have also been observed migrating downwards from landfills in the same till deposit. For example, an extensive study of the Confederation Road Landfill showed that, over the first 15 years, chloride migrated about 1 m. An effective diffusion coefficient of $6{\cdot}3 \times 10^{-10}$ m^2/s based on short-term (1 week) laboratory tests provided a good prediction of the observed profile (Quigley & Rowe, 1986). It should be noted that the temperature below waste is higher than the long-term groundwater temperature, and that this will increase the diffusion coefficient, other things being equal, as discussed earlier. Most cations moved much less than chloride, with potassium experiencing significant ion exchange and, as a result, migrating less than half the distance of chloride. Heavy metals (lead, copper, zinc, iron and manganese) migrated less than 0·2 m (likely only 0·1 m) in the same time period and were largely removed from solution by precipitation (Yanful *et al.*, 1988).

Diffusion through compacted clay at the Keele Valley Landfill

As discussed earlier, the 0·3 m thick sand blanket at the KVL clogged significantly in the upper few centimetres, and, as a consequence of negligible flow through the sand, a diffusion profile developed within both the sand blanket and the underlying CCL (Fig. 4). Over a period of 4·25 years, chloride diffused about 0·75 m, and the profile was well predicted using a diffusion coefficient of 6×10^{-10} m^2/s obtained from short-term diffusion tests (Fig. 4(a)). This is consistent with the diffusion coefficient obtained for the Confederation Landfill noted above. These two cases illustrate how diffusion gives rise to rapid contaminant migration over the first few years, but the rate of advance of the contaminant front decreases with time (Rowe *et al.*, 2004). At the Keele Valley Landfill, chloride migrated 0·7–0·75 m in 4·25 years, whereas at the Confederation Road landfill it had migrated only a little over 1 m in 15 years. The organic contaminants appear to have diffused almost 0·6 m in 4·25 years (especially toluene, Fig. 4(b)).

Diffusion through GCLs

Lake & Rowe (2000a) examined the diffusion of sodium chloride through GCLs and showed that the diffusion coefficient decreased linearly with decreasing final bulk GCL void ratio. The method of GCL manufacture did not significantly affect the diffusion coefficients at a given void ratio; however, the method of manufacture can influence swelling (Lake & Rowe, 2000b) and hence the diffusion coefficient, especially for samples hydrated at low stress. At low concentrations (3–5 g/l, 0·05–0·08M) the diffusion coefficient deduced at a given void ratio was independent of test method adopted. However, as the NaCl concentration increased to 0·6M or 2·0M there was an increase in the diffusion coefficients in tests conducted at constant void ratio. This increase was largely mitigated when a constant stress was applied to the sample throughout the testing. For the range of conditions examined, the chloride diffusion coefficient was between 1×10^{-10} m^2/s and 4×10^{-10} m^2/s. This is slightly smaller than, but of a similar order of magnitude to, that for diffusion from waste disposal sites through natural and compacted clay (6×10^{-10} m^2/s), as noted earlier.

Lake & Rowe (2004) examined diffusion of DCM, DCA, TCE, benzene and toluene through a GCL at room temperature. They concluded that the order of the rate of mass transport through the GCL was dichloromethane (DCM) $\approx$ 1,2 dichloroethane (DCA) > benzene > trichloroethylene (TCE) > toluene. The diffusion coefficients at room temperature (at confining pressures less than 10 kPa) ranged from approximately 2×10^{-10} m^2/s to 3×10^{-10} m^2/s. The difference in mass transport was attributed largely to varying degrees of sorption of the different compounds to the geotextile component of the GCL. Rowe *et al.* (2005) extended this work by examining the effect of temperature on the diffusion of benzene, toluene, ethylbenzene, *m*- and *p*-xylene and *o*-xylene (BTEX). They confirmed that the geotextile component of a GCL was the primary contributor to sorption of hydrocarbons by the GCL, with partitioning coefficients (K_d at 22°C and 7°C in ml/g) for the entire GCL following the order: *m*- and *p*-xylene (42, 25) > ethylbenzene (36, 22) > *o*-xylene (27, 14) > toluene (15, 8·7) > benzene (4·4, 2·6). The diffusion coefficients (at 22°C and 7°C in m^2/s) followed the order benzene ($3{\cdot}7 \times 10^{-10}$, $2{\cdot}2 \times 10^{-10}$) > toluene ($3{\cdot}1 \times 10^{-10}$, $1{\cdot}8 \times 10^{-10}$) > ethylbenzene ($2{\cdot}9 \times 10^{-10}$, $1{\cdot}7 \times 10^{-10}$) > *m*- and *p*-xylene ($2{\cdot}5 \times 10^{-10}$, $1{\cdot}5 \times 10^{-10}$) $\approx$ *o*-xylene ($2{\cdot}6 \times 10^{-10}$, $1{\cdot}5 \times 10^{-10}$). The reduction in both the diffusion and sorption coefficients with decreasing temperature had opposite effects on mass transport through the GCL. However, the decrease in transport due to a reduced diffusion coefficient is more significant than the increased transport due to smaller sorption, and the net effect was reduced mass transport at lower temperature.

As the typical sodium bentonite used in GCL provided relatively little sorption for volatile organic compounds (VOCs), Lake & Rowe (2005) examined the potential improvement in the sorption that could be achieved for several organoclays and bentonite-activated carbon mixtures. Batch tests performed for four different organoclays showed two to three orders of magnitude higher sorption to DCM, DCA, TCE, benzene, and toluene relative to typical bentonite currently used in GCLs. A mixture of 2% of powdered activated carbon with powdered bentonite (2% PAC/PB) gave much higher sorption than for the organoclays examined for TCE, benzene and toluene. DCM sorption to the 2% PAC/PB mixture was less than for the organoclays, whereas DCA sorption was similar between the 2% PAC/PB mixture and the organoclays. Contaminant transport modelling was used to assess the engineering relevance of the potential improvement in GCL sorption due to the use of these alternative materials. Because of the relatively thin nature of the GCL, it was found that, despite the large potential increases in GCL sorption, the replacement of standard bentonite with the alternative materials had only a slight effect on contaminant migration. Thus the increased costs associated with modifying GCLs likely outweigh the

benefit of such additives when considering the use of GCLs as part of the liner system for MSW landfills.

Given the fact that the diffusion coefficients and sorption capacity of the GCL are not substantially better than for a CCL, and yet the GCL is 50 to 100 times thinner than a typical CCL, it follows that in order to have equivalent performance as a diffusion barrier a GCL will need to be combined with a foundation soil such that the total thickness of the GCL and foundation soil (attenuation layer) is similar to the thickness of the CCL. This will be demonstrated in a subsequent section.

Diffusion through geomembranes and composite liners

Geomembranes are solids. Thus, putting aside leakage through holes as discussed earlier, there is no 'flow' through an intact GM. However, water and contaminants can potentially migrate through the GM by molecular diffusion. This migration is a molecule-activated process that can be envisaged as occurring by steps or jumps over a series of potential barriers, following the path of least resistance. For dilute aqueous solutions the process involves three key steps (Haxo & Lahey, 1988):

(*a*) partition of the contaminant between the medium containing the contaminant and the inner (i.e. contacting) surface of the GM (adsorption)
(*b*) diffusion of the permeant through the GM
(*c*) partition between the outer surface of the GM and the outer medium (desorption).

The diffusive movement of a contaminant (or water) through a GM involves a cooperative rearrangement of the penetrant molecule and the surrounding polymer chain segments. The process requires a localisation of energy to be available to allow a diffusive jump of the penetrant molecule in the polymer structure. The penetrant molecule and part of the polymer's molecular chain may share some common volume both before and after the jump. However, this jump will involve the breaking of some van der Waals forces or other interaction between the component molecules and polymer segments (Rogers, 1985). Thus, the diffusive motion depends on the energy availability and the relative mobilities of the penetrant molecules and polymer chains. This will depend on temperature, the size and shape of the penetrant, the nature of the polymer and, potentially, concentration.

The extent to which permeant molecules are sorbed in a polymer depends upon the activity of the permeant within the polymer at equilibrium (Müller *et al.*, 1998). When a GM is in contact with a fluid, there will be a relationship between the final equilibrium concentration in the GM, c_g, and the equilibrium concentration in the fluid, c_f. For the simplest case where the permeant does not interact with the polymer (e.g. as is the case for dilute solutions such as typical landfill leachates and HDPE), the relationship between the concentration in the fluid and the GM is given by (Henry's law)

$$c_g = S_{gf} c_f \tag{25}$$

where S_{gf} is called a partitioning coefficient and in principle is a constant for the given molecule, fluid, GM and temperature of interest.

At the second stage of the migration, diffusion of the sorbed penetrant within the material can be described by Fick's first law:

$$f = -D_g \frac{dc_g}{dz} \tag{26}$$

where f is the mass flux, D_g is the diffusion coefficient in the GM, c_g is the concentration of diffusing substance in the GM, and z is the direction parallel to the direction of diffusion. In transient state, the governing differential equation is (Fick's second law)

$$\frac{\partial c_g}{\partial t} = D_g \frac{\partial^2 c_g}{\partial z^2} \tag{27}$$

which must be solved for the appropriate boundary and initial conditions.

The last stage in the migration process is permeant desorption from the GM to the outer solution. This stage is similar to the first with an inverted process, and the contaminant concentration in the adjacent fluid can be expressed as

$$c'_g = S'_{gf} c_f \tag{28}$$

where S'_{gf} is the contaminant partitioning coefficient between the outside fluid and the GM. In the simplest case where the solutions on either side of the GM are aqueous, these two partitioning coefficients may be assumed to be the same ($S_{gf} = S'_{gf}$).

As the primary interest is in the concentrations of contaminant in water (not the GM), it is convenient to express the diffusion equations in terms of the concentration in adjacent solutions. Substituting equation (25) into equation (26), the flux from an aqueous solution on one side of the GM to an aqueous solution on the other side is given by

$$f = -D_g \frac{dc_g}{dz} = -S_{gf} D_g \frac{dc_f}{dz} = -P_g \frac{dc_f}{dz} \tag{29}$$

where the permeation coefficient (called the permeability in the polymer literature), P_g, is given by

$$P_g = S_{gf} D_g \tag{30}$$

and where P_g is a mass transfer coefficient that takes into account the partitioning and diffusion processes.

There are various methodologies that can be used (Rowe, 1998a) to deduce the partitioning, diffusion and permeation coefficients. The technique that best matches actual situations uses a two-compartment diffusion cell (insert to Fig. 20), where contaminant diffusion is monitored from the source to the receptor. When equilibrium is reached, the value of S_{gf} can be deduced from mass balance considerations. The diffusion coefficient can then be calculated knowing the value of S_{gf} by fitting the variation of the source and receptor concentration with time using computer software that models the boundary conditions, phase change and transport through the GM (e.g. Rowe & Booker, 2005).

The permeation coefficient P_g is highly dependent on the similarity of the penetrant and polymer. For example, Eloy-Giorni *et al.* (1996) indicated values of $S_{gf} = 8 \times 10^{-4}$ and $D_g = 2{\cdot}9 \times 10^{-13}$ m^2/s, giving a very low value of $P_g = 2{\cdot}3 \times 10^{-16}$ m^2/s for water and HDPE. Similarly, August & Tatzky (1984) found that strongly polar penetrant molecules have very low permeation coefficients through polyethylene (with the permeation coefficients being in the following order: alcohols < acids < nitroderivatives < aldehydes < ketones < esters < ethers < hydrocarbons). August *et al.* (1992) found that there was negligible diffusion of heavy metal salts (Zn^{2+}, Ni^{2+}, Mn^{2+}, Cu^{2+}, Cd^{2+}, Pb^{2+}) from a concentrated (0·5M) acid solution (pH = 1–2) through HDPE over a 4 year test period.

Chloride diffusion tests have now been running for about 12 years, and the results of this monitoring for one test are shown in Fig. 20. The receptor concentration remains below about 0·02% of the source concentration and lies within the range of analytical uncertainty for the chemical analysis. However, these data do allow an upper bound of 3×10^{-17} m^2/s to be placed on the permeation coefficient. In practical terms, this means negligible migration of chlor-

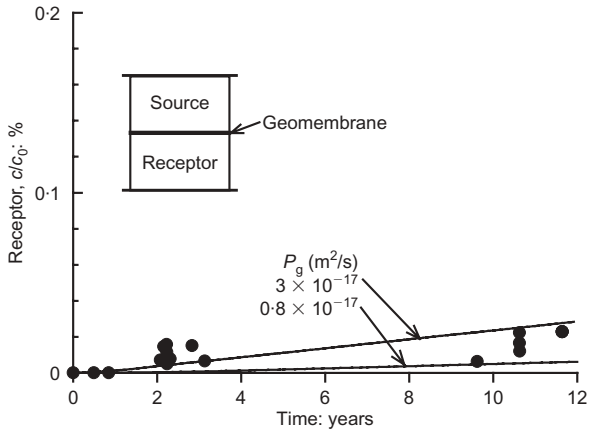

Fig. 20. Increase in chloride concentration in receptor as percentage of source concentration for a two-compartment diffusion test on 2 mm thick HDPE with an aqueous sodium chloride source solution ($c_0 = 2200$ mg/l)

ide (and likely other similar ions) through an HDPE GM for so long as it remains intact (i.e. for its service life, discussed later).

Figure 21 (▲) shows the increase in receptor concentration for diffusion of dichloromethane (DCM) through a 2 mm thick HDPE GM. In contrast to the case of chloride (Fig. 20), where after almost 12 years the receptor is less than 0·02% of the source concentration, for DCM the receptor reached 20% of the initial source concentration in only 70 days. This translates into a permeation coefficient $P_g = 4 \times 10^{-12}$ m²/s and demonstrates relatively rapid diffusion through HDPE. To put these results in context, Fig. 21 also shows the increase in receptor concentration for tests involving 30 mm of compacted clay (■) and a composite liner comprising the 2 mm GM and 30 mm of compacted clay (●). The mass transport through 30 mm of compacted clay was much faster (corresponding to a diffusion coefficient $D_g = 3{\cdot}5 \times 10^{-12}$ m²/s) than for the 2 mm thick GM, indicating that although the GM does not prevent diffusion, it does slow it compared with even a 15-fold thicker clay plug. The composite liner, not surprisingly, proves to be a better barrier than either the GM or clay alone. It will be shown later that the impact on an underlying aquifer can be controlled by the use of a GM in association with suitable thickness of compacted clay and attenuation layer. Given the rapid diffusion through the GM it may also be anticipated (as will be later demonstrated) that the impact of contaminant migration of VOCs such as DCM will occur during the service life of the GM (in contrast to chloride, discussed above, where the GM is likely to control impact for its service life provided that it does not have too many holes initially).

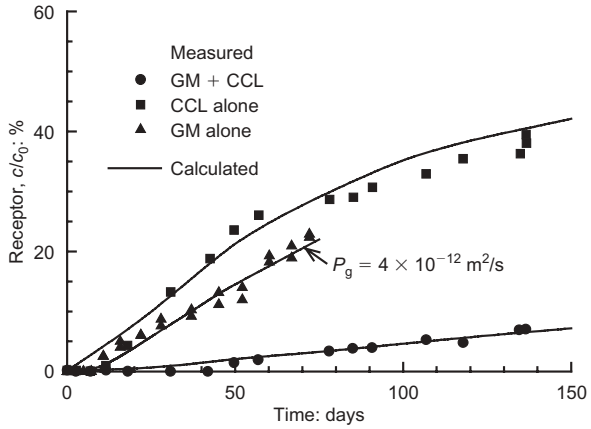

Fig. 21. Increase in DCM concentration in receptor chamber as percentage of source concentration for a two-compartment diffusion test examining: 2 mm thick HDPE (GM alone); 30 mm of compacted clay; and 2 mm thick HDPE GM over 30 mm of compacted clay. All cases involve an aqueous DCM source solution with $c_0 = 5$ mg/l. Data based on Sangam & Rowe (2001a, 2001b)

Published values for the partitioning coefficient S_{gf} and diffusion coefficient D_g have been summarised by Rowe *et al.* (2004) together with effective diffusion coefficient (D_e) and sorption (K_d) values for CCLs and GCLs. These values should be used with caution, because they are dependent on temperature and, in some cases, the chemical composition and concentrations in the contaminant source. The values may also vary because of polymer crystallinity, additives etc., and hence published values should be used only as an initial guide; they do not replace experimentally determined values for the GM of interest for projects where uncertainty regarding the diffusion coefficient or sorption could have a significant impact.

SERVICE LIFE OF GEOMEMBRANE LINERS

Primary and secondary GMs have different exposure conditions and hence may be expected to have different service lives. The primary GM is subject to direct contact with leachate and temperatures higher than normal groundwater temperatures. For double composite lined landfills, leachate that passes through a primary clay liner can be expected to have lower concentrations of important constituents such as transition metals and organic compounds (due to cation exchange, precipitation and biodegradation as it migrates through the clay) than the leachate in contact with the primary GM. The secondary GM is also further from the waste and hence is likely to be at a lower temperature than the primary liner if there is adequate thermal insulation between the primary and secondary GM (e.g. as may be provided by a CCL and granular LDS); however, it does have greater exposure to oxygen. In most other respects they are similar, and so the factors affecting the service life of both primary and secondary GMs will be discussed in this section.

Potential failure mechanisms

Given appropriate engineering design and CQC/CQA during the manufacture and installation, experience (e.g. Bonaparte *et al.*, 2002) has shown that GM liners may be expected to perform satisfactorily in the short term. However, the service life (i.e. long-term performance) of the GM is still uncertain, because it is influenced primarily by the synergistic effects of chemical and physical stresses over an extended period of time. Of particular relevance to this service life are the tensile strains (which can be induced by the overlying drainage material and wrinkles in the GM), the GM stress crack resistance, crystallinity, oxidative induction time (as a measure of the antioxidants in the GM), the exposure to chemicals in the leachate, and temperature.

Geomembrane protection

Typically GMs are designed from consideration of short-term puncture resistance. For example, Badu-Tweneboah *et al.* (1998) proposed a technique for assessing the effectiveness of protection layers for HDPE GM liners. Reddy *et al.* (1996) reported on a field trial of construction damage

which concluded that 'a geotextile as light as 270 g/m^2... completely protects the GM from construction loading.' Narejo *et al.* (1996) showed that there is a linear increase in protection resistance with increasing thickness (mass per unit area) of the protection layer, and proposed a methodology for selection of geotextile protection layers that will provide short-term protection against puncture under the loads applied by the overlying waste. However, there are some who believe that protection against short-term puncture, although necessary, is not sufficient to ensure adequate long-term performance, and so the German approach (Bishop, 1996; Seeger & Müller, 1996) focuses on minimising the contribution of indentation (and subsequent potential stress cracking), due to stresses induced by the collection gravel under long-term loading conditions, to a very low strain level (~0·25%).

Tognon *et al.* (2000) developed a method for estimating the local strain in a GM due to the indentation of gravel particles. This approach, which was calibrated against direct strain measurements, considers the combined membrane and bending strains. It provides a better representation of the distribution of strain than techniques previously used (e.g. arch elongation), and enhances the evaluation of the peak strains in the GM caused by local indentations. Tognon *et al.* (2000) reported results from a series of large-scale tests conducted using different protection layers. It was found that the best protection for the underlying GM was provided by a sand filled geocushion ($M_A = 2130$ g/m^2) or a special rubber geomat with a polyester scrim ($M_A = 6000$ g/m^2), which limited strains induced by coarse (40–50 mm) angular gravel to 0·9% at 900 kPa and 1·2% at 600 kPa respectively and the number of indentations/m^2 to 78 and 38 respectively. The largest GM strains were observed when the nonwoven geotextiles were used with a maximum strain of 8% and 350 indentations/m^2 being obtained with a 435 g/m^2 geotextile at 250 kPa and a maximum strain of 13% and 338 indentations/m^2 with 1200 g/m^2 of geotextile at 900 kPa. In each case there was adequate protection to avoid holes in the GM in the short term; however, the short-term strain of 13% is very close to yield, and it is not clear what the long-term performance would be with these large, locally induced strains.

The large difference in maximum strains (7·5% and 1·2% respectively at a pressure of 600 kPa) observed for the two rubber geomats suggests that the tensile stiffness provided by the polyester grid in the second geomat played a significant role in reducing lateral deformation of the rubber and hence reducing indentation and strains in the GM. This suggests that the tensile stiffness of the protection layers may be a critical factor in minimising strains in GMs. Although consistent with previous findings, in that a combination of increased cushioning and tensile strength (both of which increase with increasing mass per unit area for needle-punched geotextiles) can be expected to be beneficial in providing GM protection, this does imply that additional benefits may be gained from the use of composite materials (such as the scrim-reinforced rubber mat) as an alternative to simply increasing the mass of nonwoven geotextiles in an attempt to improve GM protection.

The geomembrane strains reported by Tognon *et al.* (2000) were obtained from relatively short-term tests (200–720 min) and at room temperature (24 ± 1°C). Time dependence of the strains resulting from the local incursion of the gravel particles will be based on the deformation/relaxation characteristics of the polyethylene, protection layer, and the time-dependent behaviour of the underlying clay. Thus the peak short-term strain may not represent the maximum localised strain that could develop in longer-term tests, and further research is needed to clarify the time-dependent effects on the local strains caused by the gravel particles. Nevertheless, it is clear that the sand cushion and the scrim-reinforced rubber mat provided far superior protection and are likely to give smaller short- and long-term strains than the nonwoven geotextile layers examined. From a practical perspective, this suggests the desirability of a protection layer involving a sand protection layer (potentially in conjunction with a geotextile).

Wrinkles (waves)

Wrinkles were previously discussed in the context of their impact on increased leakage due to the easy distribution of fluid passing though any hole in the wrinkle. They may also contribute to the formation of holes because of the increased potential for stress cracking related to the tensile strains induced by the wrinkle and its interaction with any adjacent gravel. Brachman & Gudina (2002) have examined the interaction between the granular material and the wrinkle using specially designed apparatus. They found, when the wrinkle was in gravel, there was both pinching and flattening at the top of the GM, which gave rise to increased tensions in the GM. This reinforces the desirability of having a sand protection layer, which is of sufficient thickness to cover the wrinkles, between the gravel drainage layer and the underlying GM (e.g. a design as shown in Fig. 6(b)).

Service life of geomembranes

Given the relatively short history of GM use in waste containment applications, there are relatively few field data relating to the long-term performance of GMs. Brady *et al.* (1994) observed relatively little change in samples over a 30-year period, although the impact resistance changed after 15·5 years and had reduced by about 50% after 30 years. Rollin *et al.* (1994) found that HDPE GM used in a contaminated soil containment facility for 7 years exhibited lower tensile force and elongation at rupture than the original material. Hsuan *et al.* (1991) examined HDPE GM samples from a 7-year-old leachate lagoon and concluded that over the 7-year period there was no substantial change in the internal structure of the GM or its engineering/hydraulic containment properties. In contrast, Rowe *et al.* (1998, 2003) found that an exposed GM exhumed from a leachate lagoon liner after 14 years of operation had very low standard oxidative induction (OIT) values as well as low tensile break properties. The results of the Melt Index test suggest that the degradation was induced by a chain scission reaction in the polymers. The GM was severely cracked (a large portion of this cracking was due to improper maintenance activities on the lagoon), and was found to be highly susceptible to stress cracking (this case will be examined further in a later section). Geomembrane from the bottom of the same lagoon (i.e. that had been covered by leachate rather than being exposed to the elements) experienced slower depletion of antioxidant and appeared to have been sufficiently protected by the antioxidant package to prevent significant oxidation degradation over the 14-year period.

These observations are useful in that they indicate that reasonable GM performance might be expected for buried GMs for at least 15 years, if adequately protected from damage, but they are not sufficient to provide an estimate of long-term GM performance or the service life of HDPE GMs. Consequently, accelerated ageing tests have been developed in an effort to simulate long-term exposure of HDPE. Rowe & Sangam (2002) have provided a relatively recent review and discussion of basic concepts and mechanisms influencing the durability of HDPE and the service life of GM liners. This will not be repeated here other than to

highlight the basic concepts needed to present the most recent results relating to service life of HDPE GMs.

HDPE GMs typically comprise 96–97·5% of polyethylene resin, 2–3% of carbon black and 0·5–1·0% of other additives such as antioxidants and stabilisers (Hsuan & Koerner, 1998). Two key properties are the stress crack resistance (a function of the resin used) and the oxidative induction time (OIT: a measure of the amount and characteristics of the antioxidant package used in the GM). Common GM specifications (e.g. GRI-GM13) require both a minimum stress crack resistance and antioxidant package (OIT). Based on GRI-GM13, GMs used as liners should not fail in 300 h in a single-point notched constant-load test (SP-NCLT; ASTM D5397 (ASTM, 2005)) at 30% of the yield stress. They should also have a minimum OIT value of 100 min for the standard test (ASTM D3895 (ASTM, 2004a)) or 400 min in the high-pressure test (ASTM D5885 (ASTM, 2004b)). After oven-ageing at 85°C for 90 days (ASTM D5721 (ASTM, 2002)), the GM should retain 55% of the standard Std-OIT or 80% of the HP-OIT value. The assessment of service lives presented in this section assumes that the GM meets these criteria, and in fact the calculated service lives are based on test data for a GM with an initial OIT of about 135 min (ASTM D3895).

In a GM, the polyethylene chains may be neatly folded and tightly packed as crystal lamellae or in looser amorphous layers where the chains or chain segments are disordered (Apse, 1989). The lamellae are linked via tie molecules that start and end in adjacent lamellae and influence some of the polyethylene properties. Thus changes in the packing structure or molecules may affect the durability and long-term performance of the GM.

As discussed by Hsuan & Koerner (1998), physical and chemical ageing may take place simultaneously. With physical ageing, the polymer attempts to establish equilibrium from its as-manufactured non-equilibrium state. There is an increase in the crystallinity of the material but, by definition, there is no breaking of covalent bonds (Petermann *et al.*, 1976). Physical ageing may change crystallinity-dependent properties such as the diffusion coefficient, which gets lower (better) with higher crystallinity (Rowe *et al.*, 2003). With chemical ageing there will be bond scission in the backbone of the macromolecules, intermolecular cross-linking and/or chemical reactions in the side-chains (Schnabel, 1981) that will eventually lead to a decrease in mechanical properties and eventually to failure. Hence chemical ageing is of greatest interest with respect to long-term performance.

Chemical ageing is commonly envisaged as having three distinct stages (Viebke *et al.*, 1994; Hsuan & Koerner, 1998):

(*a*) depletion time of antioxidants
(*b*) induction time to the onset of polymer degradation
(*c*) degradation of the polymer to decrease some property (or properties) to an arbitrary level (e.g. to 50% of the original value).

Hsuan & Koerner (1998) note that the oxidation reaction of polyethylene can be increased in the presence of transition metals (e.g. Co, Mn, Cu, Pd and Fe). As these are all potentially present in leachate, it may be expected that GMs will age faster in leachate than in water (even in an anaerobic environment commonly associated with leachate).

It is not feasible to measure the length of these stages for actual field conditions because of the long time required to obtain useful results. Consequently, tests are conducted at elevated temperatures to accelerate ageing, and the results are extrapolated to temperatures expected at the base of a landfill (discussed earlier). This is believed to be reasonable provided that the fundamental mechanisms being evaluated (e.g. oxidation) are not altered by the elevated exposure.

Antioxidant depletion rates (Stage 1) have been examined by Hsuan & Koerner (1998) for a GM with water-saturated sand above, dry sand below, and subject to a stress of 260 kPa at temperatures of 55–85°C for up to 2 years. Mueller & Jacob (2003) reported results for air ageing and water bath ageing of HDPE GMs, and concluded that the service life 'is essentially determined by the slow loss of stabilisers due to migration.' Their paper reports tests involving nine (2·5 mm thick) HDPE geomembranes over a period of 13 years. They reported two-stage depletion of antioxidants, with the second stage being considerably slower and being noted only after two or three years. As they did tests at only one temperature (80°C), they could not produce an Arrhenius plot to establish the activation energy. However, they claim that the activation energy values for antioxidant depletion estimated by Hsuan & Koerner (1998) are too low and should be much higher.

Sangam & Rowe (2002) investigated the antioxidant depletion rates for unstressed specimens immersed in air, water and synthetic leachate (at 22–85°C). After different periods of immersion, samples were removed, tested to obtain the OIT, and then the ln(OIT) was plotted against the period of incubation (Fig. 22). The linear plot implies a first-order relationship between OIT and time, and hence the OIT (an indicator of the total amount of antioxidants) remaining at time t can be given by

$$\mathrm{OIT}(t) = \mathrm{OIT}_0 \mathrm{e}^{-st} \tag{31}$$

where OIT_0 is the initial OIT value (typically in minutes) and s is the rate of antioxidant depletion (typically in month^{-1}). The antioxidant depletion rate s in leachate was 2·3 times faster than in water and 4 times faster than in air. The synthetic leachate (pH = 6) was highly reduced ($E_\mathrm{h} \approx -328$ mV). The loss of antioxidants can in part be attributed to diffusion out of the GM into the fluid (extraction). However, as the same mechanism was also possible for water, this does not represent the complete explanation. The higher rate observed for leachate-immersed samples (relative to water-immersed samples) may be attributed to the transition metals and other inorganic compounds present in the leachate. Osawa & Saito (1978) and Wisse *et al.* (1990) have indicated that reaction with transition metals increases the consumption of antioxidant even in a relatively anoxic

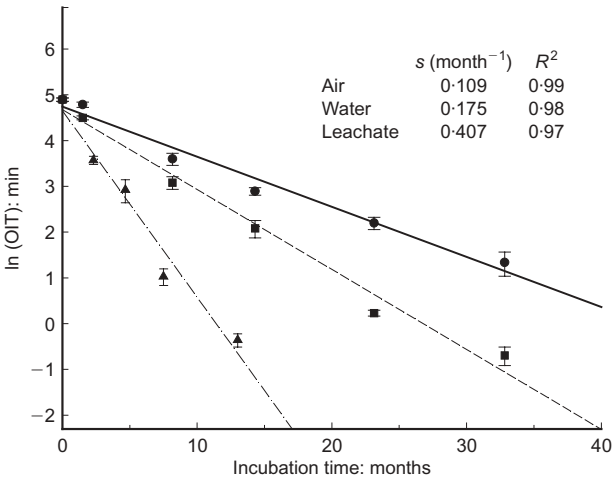

Fig. 22. Plot of ln(OIT) with incubation time at 85°C for different exposure conditions. The slope of the regression curves gives depletion rate s for a given exposure condition and temperature (modified from Sangam & Rowe, 2002)

environment. Because of the low diffusion coefficient for metals in HDPE (August *et al.*, 1992), the reaction with the antioxidant may be expected to occur predominantly at the surface of the GM.

Assuming that diffusion, ageing and degradation are activated processes in which the activation energy E_a remains relatively constant, the time required to deplete the antioxidants at any given temperature (for the same exposure conditions) can be inferred using a time–temperature shift (Arrhenius modelling) based on the relationship (Hsuan & Koerner, 1998)

$$s = A \exp\left(\frac{-E_a}{RT}\right) \tag{32}$$

where s represents antioxidant depletion rate; T is the absolute temperature (K); A is a constant (often called the collisional factor), and is material-exposure system dependent; E_a is the activation energy (J/mol); and R is the universal gas constant (8·314 J/(mol K)).

The activation energy can be deduced from the antioxidant depletion rates obtained at different temperatures by plotting ln(s) against $1/T$ (Fig. 23) and then inferring parameters from a regression curve through the data (Fig. 23). Based on this information the antioxidant depletion time at any temperature of interest can be deduced by first establishing the depletion rate s from equation (32) and then calculating the time to deplete the antioxidant from the initial OIT value ($OIT_0 = 133$ min for this case) to the final (residual) value (taken to be 0·5 min when all antioxidant is depleted) from equation (31). The depletion times at temperatures between 10°C (potentially applicable to a secondary GM) and 60°C (upper end of likely range for a primary liner) so deduced are given in Table 5. As discussed earlier, primary liners are most likely to reach temperatures of 30–40°C, and 35°C is taken as a typical median temperature.

The results shown in Table 5 indicate a very large range of times required to deplete the antioxidants depending on the exposure condition, ranging between 50 and 510 years at 10°C and 10 to 80 years at 35°C. At 60°C, all depletion times are short (3–15 years). These results clearly demonstrate the critical importance of liner temperature on the service life of HDPE GMs. In addition they show that leachate exposure has a significant impact on antioxidant depletion times compared with both water and air immersion, and hence that it is essential to consider chemical exposure. However, they also show a need to realistically simulate the chemical exposure conditions (i.e. leachate on only one side of liner), because simple immersion of the GM in a chemical solution produces conditions too severe to characterise its lifetime in a landfill.

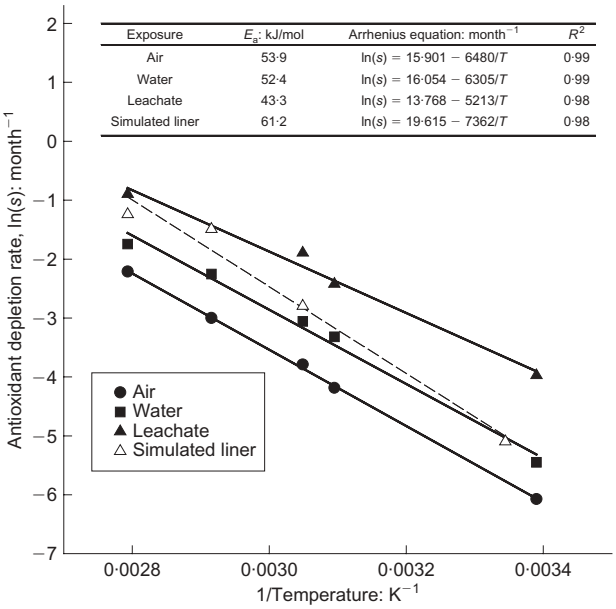

Fig. 23. Arrhenius plot of antioxidant depletion rate for different exposure conditions. Simulated liner with geotextile above and GCL and unsaturated sand below the geomembrane. E_a = activation energy (data for air, water and leachate from Sangam & Rowe, 2002)

Sangam & Rowe (2002) noted that a GM used in a primary composite liner for a landfill will perpetually have leachate on its top surface and soil (e.g. CCL or GCL) in contact with the bottom surface. They suggested that, in the absence of other data, the depletion time could be estimated based on leachate exposure on one side of the GM but considering the response to the contact with the underlining clay as being represented as an average of the exposure to air and water conditions. Based on this assumption the inferred liner depletion time t_{il} was calculated from the depletion times in air, t_{air}, water, t_{water}, and leachate, $t_{leachate}$, as follows:

$$t_{il} = 0{\cdot}25(t_{air} + t_{water}) + 0{\cdot}5\,t_{leachate} \tag{33}$$

and the resulting times (Table 5) are 210 years at 10°C and 35 years at 35°C. These are considered a better estimate of the likely field depletion time than those for air, water or leachate alone. However, they are only an approximation.

Recognising the limitations of immersion tests, a series of tests was initiated to better simulate the ageing of GM liners. These tests involve cells where the configuration consists (from bottom up) of an unsaturated sand subgrade, GCL, 1·5 mm thick HDPE GM, geotextile protection layer, and gravel. The gravel is saturated with leachate (which is changed regularly). These 'simulated liner' cells were placed in baths and maintained at temperatures of 26, 55, 70 and 85°C. The test cells were periodically terminated and the GM tested. Based on the OIT results the activation energy and relationship between depletion time and temperature were deduced (Fig. 23). The depletion times for the temperatures of interest for this simulated liner were then calculated, and are given in Table 5.

Compared with the simulated liner results (Table 5), the inferred liner depletion times (deduced from equation (33)) are conservative at 10°C (280 compared with 210 years) but similar at 35°C (both 35 years) and 60°C (6 and 7 years). However, this agreement should be viewed with some caution. Although the GMs used in the simulated liner tests and the immersion tests (used to get the inferred liner results) had very similar initial OIT values (135 min and 133 min), they did have different crystallinity (49% and 44%) and thickness (1·5 mm and 2 mm). Of these, the most significant difference is the thickness.

One would expect the depletion time for the 2 mm thick GM to be greater than that for 1·5 mm (assuming that depletion is predominantly diffusion controlled): thus the fact that the inferred results obtained for the 2 mm GM are less than those for the 1·5 mm simulated liner suggests that this approach is likely more conservative than appears from a direct comparison of the numbers in Table 5. This is consistent with the suggestion by Sangam & Rowe (2002) that the approach given by equation (33) is conservative. There are several reasons for conservatism. First, for a predominantly diffusion-controlled process, averaging of times for immersed condition to estimate times for different exposure conditions on each side is likely to underestimate the depletion time for the mixed condition. Second, in the

Table 5. Estimated antioxidant depletion time for an HDPE geomembrane

Temperature: °C	Air,* t_{air}: years	Water,* t_{water}: years	Leachate,* $t_{leachate}$: years	Inferred liner,† t_{il}: years	Simulated liner,‡ t_{sl}: years
10	510	235	50	210	280
20	235	110	25	100	115
30	110	55	15	50	50
35	80	40	10	35	35
40	55	30	8	25	25
50	30	15	5	15	10
60	15	8	3	7	6

All times greater than 10 have been rounded to nearest 5 years.
*2 mm HDPE, $OIT_0 = 133$ min (ASTM D3895 (ASTM, 2004a)), crystallinity = 44%; based on data from Sangam & Rowe (2002; Fig. 23).
†Inferred from immersion data, $t = 0{\cdot}25(t_{air} + t_{water}) + 0{\cdot}5t_{leachate}$.
‡1·5 mm HDPE, $OIT_0 = 135$ min (ASTM D3895 (ASTM, 2004a)), crystallinity = 49%.

immersion tests, the leachate strength was essentially constant because the leachate was regularly replaced, and so the exposure was essentially constant over the testing period. In the simulated liner tests (or field) the leachate above the GM is regularly changed, but the soil below is not changed, and hence one can expect a build-up of antioxidant in the soil at the interface, which would slow diffusion of antioxidant to this side of the GM.

The simulated liner results presented in Table 5 represent the best information on depletion time of antioxidants currently available for GM liners in landfills. However, as discussed earlier, this represents only the first stage of the service life, and although these numbers give a likely lower bound to the expected service life, a more realistic estimate should also consider Stages 2 and 3. At present there are very limited data for the other stages of ageing. Karlsson *et al.* (1992) and Gedde *et al.* (1994) have examined medium-density (934 kg/m^3) polyethylene gas pipe with a wall thickness comparable to that of a GM (2·2 mm). Their tests involved having stagnant water inside the pipe and circulating air around the outside for samples aged at a range of temperatures between 70°C and 105°C. Karlsson *et al.* (1992) found that there was a much greater loss of antioxidants near the wall exposed to water than near the wall exposed to air, and as a consequence identified an asymmetric antioxidant diffusion profile through the wall of the pipe. Failure of the pipes was generally initiated from oxidised zones on the inside (water side) of the pipe, and they suggested (based on limited data) that the chain scissions occur randomly in the amorphous phase. They found that oxidation was accompanied by an increase in mass crystallinity and a significant decrease (30%) in molar mass.

Viebke *et al.* (1994) published data relating to both the induction (Stage 2) and polymer degradation (Stage 3) stages of degradation for polyethylene gas pipe with minimal antioxidant and a wall thickness comparable to a GM thickness (2·1 mm). Their tests involved having stagnant deionised water inside the pipe and circulating air around the outside for samples aged at temperatures of 70, 80, 95 and 105°C. For the induction stage (Stage 2), an activation energy of 75 kJ/mol was deduced, and for the degradation stage (Stage 3) an activation energy of 80 kJ/mol was inferred. Based on these values, estimated times t_V for Stage 2 can be calculated for this air/water system (Table 6, column 3). Recognising that interaction with leachate may also influence degradation, a second estimate may be obtained by adjusting based on the difference in the effect observed in the test conducted by Sangam & Rowe (2002). It is considered that a lower-bound estimate could be obtained by:

(*a*) calculating an air/water time, $t_{a/w}$:

$$t_{a/w} = 0{\cdot}5(t_{air} + t_{water}) \quad (34)$$

from results given in Table 5
(*b*) calculating t_{il} for the inferred liner from equation (33)
(*c*) calculating the adjusted Stage 2 time t_{Va} from

$$t_{Va} = t_V \times t_{il}/t_{a/w} \quad (35)$$

and the corresponding value of t_{Va} is given in Table 6 (column 4). It should be noted that these times are relatively short, and less than the 25 years inferred by Bonaparte *et al.* (2002) based on a comparison of the properties of HDPE milk and water containers recovered from landfills after 25 years relative to new containers (assuming that they had the same polymer resin and manufacturing process). Although these containers were probably not immersed in leachate (as adjacent newspapers could still be read) they likely were at typical landfill temperature, and so suggest that the estimates in Table 6 (columns 3 and 4) may be conservative.

As noted earlier, Viebke *et al.* (1994) reported activation energy for Stage 3 of 80 kJ/mol (although they caution that this should be considered a 'rough estimate'). Using this and a half-life at 115°C of 90 days, as reported by Hsuan & Guan (1998) and Bonaparte *et al.* (2002), one can calculate Stage 3 half-lives at different temperatures t_B, as given in column 5 of Table 6. These may then be adjusted for the possible effect of leachate exactly as described above for Stage 2, and hence the adjusted values, t_{Ba}, are calculated from

$$t_{Ba} = t_B \times t_{il}/t_{a/w} \quad (36)$$

and are given in column 6 of Table 6. The service life estimates can then be obtained by summing the Stage 1, 2 and 3 contributions, and are given in column 7 (unadjusted) and 8 (adjusted) of Table 6.

A number of observations can be made based on the numbers presented in Table 6. First, the estimated service lives of secondary GMs at temperatures in the range 10–20°C are between 565 and 2775 years depending on the assumptions. This is a large range, but they are also large times, and suggest that secondary GM liners are likely to have a service life of 600 years or more if maintained at a temperature less than 20°C. Second, at a 'typical' primary liner temperature of 35°C the service life is of the order of 130–190 years (median 160 years). Finally, at temperatures of 50–60°C the service lives are very short (15–50 years). The foregoing assumes leachate on one side of the liner. In areas where there is a hole in the GM, and there is leachate both above and below the GM, the service life may be less than indicated in Table 6. Also, for secondary liners the

Table 6. Estimated times for three stages of degradation and resulting service lives for different methods of calculation for an HDPE geomembrane (All times greater than 10 have been rounded to nearest 5 years. Because of rounding, numbers may not add up exactly)

(1) Temp: °C	(2) Stage 1: years Simulated,* t_{siml}	(3) Stage 2: years Base,† t_V	(4) Stage 2: years Adjusted,‡ t_{Va}	(5) Stage 3: years Base,§ t_B	(6) Stage 3: years Adjusted,¶ t_{Ba}	(7) Service life: years Unadjusted,** t_{SL}	(8) Service life: years Adjusted,†† t_{SLa}
10	280	50	30	2445	1380	2775	1690
20	115	15	10	765	440	900	565
30	50	6	4	260	150	315	205
35	35	4	2	155	90	190	130
40	25	2	1	95	55	120	80
50	10	1	0·6	35	20	50	35
60	6	0·4	0·3	15	9	20	15

*Based on simulated liner antioxidant depletion tests (Table 5).
†Calculated using data from Viebke *et al.* (1994) for 2·1 mm wall thickness pipe with water inside and air outside.
‡As per previous note, but adjusted for possible effect of leachate using equation (35) and data from Table 5.
§Calculated using activation energy from Viebke *et al.* (1994) for 2·1 mm wall thickness pipe with water inside and air outside and half-life of 90 days at 115°C from Bonaparte *et al.* (2002).
¶As per previous note, but adjusted for possible effect of leachate using equation (36) and data from Table 5.
**$t_{SL} = t_{siml} + t_V + t_B$.
††$t_{SLa} = t_{siml} + t_{Va} + t_{Ba}$.

temperature will depend on the thermal insulation provided by the material between the primary and secondary GM liner. In the case of double composite liner systems involving just a GM and GCL as the primary liner (i.e. no foundation layer between the GCL and LDS), unpublished data indicate that the temperature of the secondary GM may be only about 3°C less than that of the primary GM (Legge, pers. comm.), and under these circumstances the service life of the secondary GM will be substantially less than the values discussed above and much closer to that of the primary GM.

The service lives presented in Table 6 are useful for obtaining a general idea of the order of magnitude of the GM service life, and for highlighting the importance of liner temperature. However, they should be used with considerable caution. Only the results for Stage 1 are based on actual tests on GM typically used in landfill application in a simulated liner configuration. The uncertainty regarding the Stage 2 and 3 components highlights the need for additional testing to examine their contributions to service life. This testing is under way, but is very time consuming.

The calculated antioxidant depletion times (Table 5) and service lives (Table 6) discussed above all assume a constant temperature. However, the temperature of the liner is likely to vary with time (e.g. Figs 11–13), and this will influence both the antioxidant depletion time and the service life. As the parameters for the antioxidant depletion times are the most reliable for a simulated liner (Table 5), the significance of variable temperature will be illustrated only with respect to the data obtained for this condition in Stage 1. Consider an idealised variation in temperature with time, with a lag period ($0 < t < t_1$) prior to temperature increase (e.g. see Fig. 11, 'Dry cell'), a period where the temperature increases linearly from T_0 to a maximum value T_p ($t_1 < t < t_2$: e.g. see Fig. 11, 'Dry cell'), a period where temperature remains constant at the maximum, T_p ($t_2 < t < t_3$: e.g. see Fig. 12(a)), a period when the temperature decreases linearly with time from T_p to T_0 ($t_3 < t < t_4$), and finally a period ($t_4 < t$) when the temperature is back to its original value, T_0. The variation in OIT with time can be modelled using equations (31) and (32), where temperature T is a function of time for different assumed values of the times t_1–t_4 and temperatures T_0 and T_p. The times t_1 and t_2 can be estimated from data such as those given in Figs 11–13. There is much more uncertainty regarding times t_3 and t_4. More data are needed to define the temperature history of landfills, and unfortunately this can only be realised in real time; however, numerical examples can provide some insight regarding the potential significance of the temperature history for the time at which the antioxidants are depleted. The results for several cases are summarised in Table 7.

For modelling the depletion that occurs during the period when the temperature is increasing, the average depletion rate s_{av} can be used, where it is given by

$$s_{av} = \frac{\int_{t_1}^{t_2} A \exp\left\{\frac{-E_a}{R\left[T_0 + \xi(t - t_1)\right]}\right\} dt}{t_2 - t_1} \quad (37)$$

where ξ is the rate of temperature increase with time ($\xi = (T_p - T_0)/(t_2 - t_1)$), T_0 and T_p are in K, and all other terms are as previously defined. Likewise, when temperature is decreasing it is given by

$$s_{av} = \frac{\int_{3}^{t_4} A \exp\left\{\frac{-E_a}{R\left[T_p + \xi(t - t_3)\right]}\right\} dt}{t_4 - t_3} \quad (38)$$

where ξ is the rate of temperature decrease with time ($\xi = (T_p - T_0)/(t_4 - t_3)$), and all other terms are as previously defined.

Referring to Table 7, Cases 1–4 all correspond to an initial increase in temperature from $T_0 = 10$°C to $T_p = 35$°C after 8 years but different times at the peak temperature and times for the decrease to occur. Assuming only a short, 12-year period at peak temperature and a decrease over a decade (Case 1), the antioxidant depletion time is 150 years. For otherwise similar conditions but a 30-year period over which the temperature decreases, the depletion time drops to 100 years (Case 2). However, longer periods of time at the peak concentration have a profound effect, with the depletion time dropping to about 40 years for Cases 3 and 4 where the liner is at 35°C for 32 years. Cases 5–10 similarly illustrate the significance of the time period at the peak concentration for the time to antioxidant depletion. Cases 11–13 illustrate the potential effects of leachate recirculation on the time to antioxidant depletion, and show a value of 25 years (Case 11) assuming the peak temperature is maintained for only 10 years and reduces to the baseline value over the following decade, and 20 years (Cases 12 and 13)

Table 7. Examination of the effect of liner temperature history on the time to antioxidant depletion. Geomembrane is assumed to have $OIT_0 = 135$ min and a depletion rate defined by parameters given for the simulated liner in Fig. 23. All times have been rounded to nearest 5 years

Case	t_1: years	t_2: years	t_3: years	t_4: years	T_0: °C	T_p: °C	Time to OIT depletion: years
1	0	8	20	30	10*	35*	150
2	0	8	20	50	10*	35*	100
3	0	8	40	50	10*	35*	40
4	0	8	40	70	10*	35*	40
5	8†	14†	20	50	10†	35†	145
6	8†	14†	40	70	10†	35†	45
7	6‡	10‡	20	50	20‡	35‡	60
8	6‡	10‡	40	70	20‡	35‡	40
9	3§	7§	20	50	15§	37§	50
10	3§	7§	40	70	15§	37§	35
11	0¶	4¶	14	24	20¶	45¶	25
12	0¶	4¶	20	30	20¶	45¶	20
13	0¶	4¶	30	40	20¶	45¶	20

* Idealised based on Lysimeter 7, Fig. 12.
† Idealised based on Fig. 13.
‡ Idealised based on dry cell, Fig. 11.
§ Idealised based on Lysimeter 3, Fig. 12.
¶ Idealised based on wet cell, Fig. 11.

when the temperature remains at peak for 16 years. The difference of only 6 years at the peak temperature reduces the time to antioxidant depletion from 25 years to less than 20 years (18 years), which is within the operating life of many landfills. These results highlight the importance of considering the mode of operation when developing a liner design. Thus if leachate recirculation is envisaged, then consideration should be given both to enhancing the LCSs design (as discussed earlier) and to having a double liner system where the secondary GM is thermally separated from the primary liner. The thermal separation is required to ensure that the secondary GM is at a much lower temperature than the primary GM so that it will have an adequate service life. This is particularly important for containing conservative contaminants that do not degrade as a result of the enhanced biological activity induced by recirculation of leachate, and for operating the landfill as a bioreactor.

SERVICE LIFE OF CLAY LINERS

The clay liner beneath a GM is intended to substantially decrease leakage through any holes in the GM, to act as a partial diffusion barrier, and to provide attenuation of certain (e.g. organic and metal) contaminants. To do so, the bulk hydraulic conductivity must remain less than or equal to the design value for the contaminating lifespan of the landfill.

Provided that a CCL has been properly designed and constructed, and provided that appropriate account has been taken of the potential for an increase in hydraulic conductivity due to clay–leachate interaction (Rowe *et al.*, 2004), the CCL can be expected to have a hydraulic conductivity below the specified design value for thousands of years provided that it is not allowed to desiccate after placement. Desiccation will be discussed in the following subsections.

A GCL used as part of a composite base liner system may also be expected to have a service life of thousands of years provided that (Rowe *et al.*, 2004):

(*a*) there is no significant loss or movement of bentonite from the GCL during placement. Loss into underlying drainage layers is of particular concern, and a filter may be required to avoid bentonite loss for some GCLs (e.g. Estornell & Daniel, 1992). Construction procedures should be selected to ensure a uniform distribution of the bentonite in the GCL after placement. The potential for bentonite movement may vary from one GCL product to another. GCLs are not all the same, and the construction specifications should recognise this fact.

(*b*) there is no significant lateral movement (thinning) of bentonite during and following hydration that would cause an uneven distribution of the bentonite in the GCL during the contaminating life of the landfill (e.g. Stark, 1998). Particular care is needed on side slopes (especially steep side slopes) to avoid bentonite migration downslope, in both the 'dry' and hydrated states.

(*c*) the choice of GCL and the design are such that there is no significant long-term loss of bentonite due to migration (internal erosion) through the GCL under the hydraulic gradients that may occur either during or after termination of the operation of the LCS (Rowe & Orsini, 2003).

(*d*) the geosynthetic component of the GCL is not critical to the long-term performance of the bentonite component of the GCL (otherwise the service life of the GCL is controlled by that of the geosynthetic component).

(*e*) the seams between GCL sheets are installed to ensure intimate contact and adequate overlap. The design and the construction procedures should be such that the seams do not open up prior to, during, or following waste placement (e.g. due to drying, shear induced by construction equipment, or differential settlement). Some GCL products with an initial moisture content greater than 20% have been found to experience opening up (by as much as 300 mm) of the seams between sheets of GCL on side slopes and hence a loss of composite action (Thiel & Richardson, 2005). This problem has been attributed, at least in part, to shrinkage of these GCLs with high initial moisture content after placement. There does not appear to have been any problem with products having initial moisture less than about 15%. However, even for these GCLs care is needed to ensure adequate overlap during construction, to ensure that there is appropriate moisture in the underlying subgrade, and to have the GM and GCL covered and protected from thermal gradients due to exposure to solar radiation.

(*f*) the design hydraulic conductivity is based on considerations of clay–leachate compatibility, considering

hydrating conditions, groundwater geochemistry, applied stress, and GCL and leachate characteristics (Rowe, 1998a; Rowe *et al.*, 2004).

(*g*) the GCL does not desiccate. This is the focus of the following discussion.

Desiccation can be related to a change in water content in the clay that could occur:

(*a*) after construction of the CCL and before placing the GM
(*b*) after placing the GM and before covering with waste
(*c*) after placement of waste.

These will be discussed below.

Desiccation before placement of waste

Unless a CCL is kept moist, desiccation can occur within hours of placement. Factors influencing this desiccation include the grain size distribution of the liner material, mineralogy, water content, the climatic conditions (especially temperature and wind), and the length of exposure to drying conditions. Special care is required when the CCL is covered with a GM, because the temperature of a GM exposed to the sun may reach 80°C (Felon *et al.*, 1992), and temperatures of 60–70°C are common. White-coated GMs have been used to reduce temperature, but even in this case temperatures close to 60°C have been reported on a hot (30°C ambient) day (Koerner & Koerner, 1995a).

When a GM is heated there is potential for:

(*a*) evaporation of water from the underlying CCL into any air space between the clay and the GM
(*b*) movement of evaporated moisture downslope upon cooling of the GM
(*c*) movement of moisture from the region of higher temperature to the region of lower temperature.

Mechanisms (*a*) and (*b*) are particularly problematic on side slopes, and have been found to result in desiccation cracking of the clay liner (e.g. Basnett & Bruner, 1993). Mechanism (*c*) is critical when there is a sustained temperature gradient (Döll, 1997), and will be discussed in more detail in the following subsection. Both mechanisms decrease the water content in the clay below the GM, which, in turn, can cause shrinkage and consequent desiccation. Corser *et al.* (1992) examined a test liner/cover left exposed for six months (April–October; temperature of GM reaching 43°C). Where the GM was in intimate contact with the clay there was no significant desiccation. However, in areas where there was an air space between the GM and clay (i.e. at wrinkles/waves) the clay had dried and cracked, with cracks up to 6 mm wide extending to a depth of about 75 mm.

The desiccation of CCLs prior to waste placement can be prevented by adopting appropriate construction procedures. In particular it is essential to cover the GM with a suitable thermal insulation layer (e.g. the protection layer, leachate collection layer and a layer of waste) as soon as possible after placement of the GM.

Desiccation after placement of the waste

The risk of desiccation of clay liners that have been covered, and are no longer subject to solar heating or freezing, depends on five key factors (Holzlöhner, 1995): the properties of the clay liner, the properties of the underlying subgrade, the overburden pressure, the temperature gradient across the liner, and the depth to the water table. There are limited data regarding the desiccation potential of CCLs and GCLs under thermal gradients. However, Southen and Rowe (2004, 2005b) have experimentally investigated the potential for moisture redistribution for geosynthetic clay liners forming part of a composite liner system when subjected to thermal gradients, based on both small (Southen & Rowe, 2004) and large-scale (Southen & Rowe, 2005b) experiments. In particular, the large-scale laboratory testing examined two different subsoils and two GCL materials. Both the spatial and temporal variation in temperature and water content within and beneath the GCLs were monitored. The effects of applied temperature gradient, initial GCL and subsoil water content, and the type of GCL were studied. The following sections describe the modelling of the thermo-hydro-mechanical behaviour of soils and some of the findings from both the experimental work and this modelling.

Numerical modelling of liner desiccation: theory

Of the numerical models that have been developed to describe the thermal behaviour and moisture movement in soils, two were directed at applications involving landfill liners, and will be discussed here. Döll (1997) developed the SUMMIT program using temperature and capillary pressure (suction) as the basic variables for the analysis of thermally driven moisture movement, subject to the assumptions of a rigid, heterogeneous, unsaturated medium. Southen & Rowe (2005a) used Döll's SUMMIT model to analyse their large-scale laboratory experiments, and found that the predicted variations in water content throughout the subsoil were in reasonable agreement with experimental results. The predictions of temperature in the subsoil were less accurate, but still in reasonable agreement with experimental results. However, the SUMMIT model underestimated the volumetric water content in the GCL by as much as a factor of two, and the temperature gradient through the GCL was consistently underpredicted. The poor predictions for the GCL were attributed primarily to the assumption of a rigid medium.

To address the shortcomings of the SUMMIT model, Zhou & Rowe (2003) developed a model that incorporates consideration of fully coupled heat–moisture–air flow, a non-linear constitutive relationship, the dependence of void ratio and volumetric water content on stress, capillary pressure and temperature, and the effect of mechanical deformation on all governing equations. They also proposed a mass conservative numerical scheme to improve the accuracy of the finite element solution to the governing equations.

Numerical modelling of liner desiccation: findings

Heibrock (1997) used Döll's (1997) SUMMIT model to numerically examine composite liners and from that to infer the potential for cracking of CCLs. In one example, cracking was predicted to a depth of 1 m in 20 years for a CCL on a silt loam where the temperature at the top of the liner was 40°C. However, in a second example there was no cracking predicted for a liner on loess with a much higher unsaturated hydraulic conductivity than the silt loam. In this case the calculated downward vapour flux of water was much smaller than the upward liquid flux from the water table induced by suction, and there was no drying.

Using the theoretical framework described in the previous section, Southen (2005) modelled the behaviour of the large-scale laboratory tests. To illustrate the results, consideration will be given here to a few aspects of one test involving a GM over a needle-punched and thermally treated GCL (4240 g/m^2 granular sodium bentonite between a 105 g/m^2 slit-film woven and a 200 g/m^2 needle-punched, nonwoven geotextile). The GCL rested on 1 m of silty sand (19% silt content, optimum water content 12%, and maximum dry

density 1·95 Mg/m^3). The sand and GCL were placed with volumetric water contents of 7·3% and 71% respectively, and a pressure of 50 kPa was applied. The test was left at room temperature (21°C) for 50 days to equilibrate. The temperature on the liner was then raised to, and maintained at, 56°C for 232 days, after which the test was terminated (at day 282).

Figure 24 shows the variation in volumetric water content with depth initially, after the 50-day pre-heat period, and after 232 days of heating (i.e. at test termination). During the isothermal pre-heating stage the GCL took up water from the underlying subsoil and approached saturation at the start of the heating phase. There was moisture redistribution within the subsoil under gravitational forces, such that the volumetric water content decreased by 0·7–2% in the upper portion of the subsoil and increased by 0·5–1·5% at the base. At the end of the test (day 282) the volumetric water content of the GCL had reduced to 9·5% (from 71%), while in the subsoil adjacent to the GCL the volumetric water content had reduced to the residual value of 0·5%. The volumetric water contents predicted by the numerical model fit the general trends observed in the experimental data, and agreement is especially good within the GCL and in the upper 5 cm of the subsoil.

The variation of capillary pressure is tied to the water content distribution, and hence large changes in capillary pressure were calculated, ranging from approximately 60 000 kPa at the GCL interface to approximately 50 kPa at a depth of 0·1 m. The downward migration of water vapour leads to a decrease in unsaturated hydraulic conductivity by several orders of magnitude, and this inhibits the upward transport of liquid water needed to offset the downward vapour transport. The temperature distribution was reasonably modelled. One of the key advantages of the Zhou & Rowe (2003) model over Döll's (1997) SUMMIT model is its ability to model deformable media and calculate stress changes arising from the thermo-hydro-mechanical response. The observed GCL void ratio decreased from 2·62 to 1·76, and the calculated final void ratio (1·78) was in very good agreement with that observed. The calculated variation of net total horizontal stress with depth is shown in Fig. 25. The capillary pressure had very little effect on predicted horizontal stress within the subsoil, because the compressibility of the silty sand with respect to changes in capillary pressure was very low. However, for the highly compressible GCL, the high capillary pressures caused the development of predicted tensile horizontal stresses within the GCL. Air pressure p_a was atmospheric at the beginning and end of the tests, such that the net total stresses were equal to the total stresses at these times. There was some transient variation in air pressure, but the effects were minor. The predicted desiccation cracking of the GCL was confirmed by physical observations.

Southen (2005) conducted a parametric study to evaluate the effect of applied temperature, overburden stress, depth to the aquifer, foundation layer and, for a CCL, liner thickness on the potential for desiccation cracking. This, combined with the experimental data (Southen & Rowe, 2004, 2005b), led to a number of tentative conclusions, although it should be emphasised that more work needs to be done on this challenging topic, especially on the determination of relevant soil parameters.

For both types of composite liner system (GM/GCL and GM/CCL), liner temperature was a key factor affecting the potential desiccation. For single composite liners involving a GCL, it was found that:

(*a*) the properties of the foundation layer underlying the GCL had a critical influence on the potential for desiccation. The unsaturated soil characteristics were important as well as the initial water content. Other things being equal, the higher the initial water content of the foundation soils (up to optimum water content) the better.
(*b*) the higher the overburden stress at the time of GCL hydration, the less the risk of desiccation. This implies that the waste should be placed over the composite liner as quickly as possible after the liner is placed to minimise the potential for both short-term (e.g. solar induced) and long-term (waste temperature induced) desiccation cracking.
(*c*) the risk of desiccation increases with increasing distance to the underlying water table. However, for the cases examined, the offsetting effects of reduced water content and temperature gradient limited the effect of aquifer depth, and there was no significant increase in risk of desiccation for aquifer depths greater than about 5 m below the GCL.

For single composite liners involving a CCL, it was found that:

(*a*) the properties of the liner had a significant effect on the distribution of moisture and stress. The properties of the underlying materials were of relatively less importance, although they still had some impact.
(*b*) although an increased overburden stress reduced the

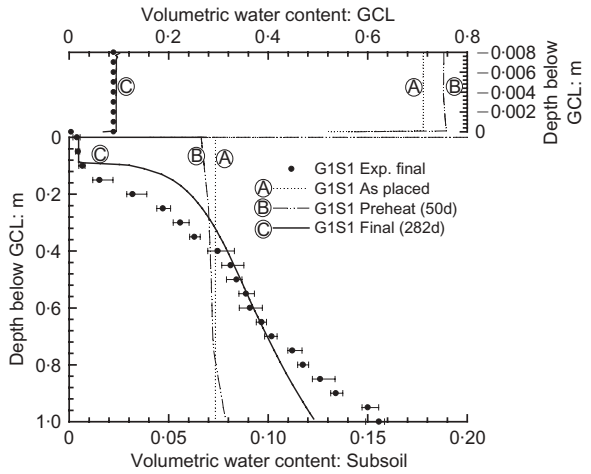

Fig. 24. Calculated and observed volumetric water content (–) profiles

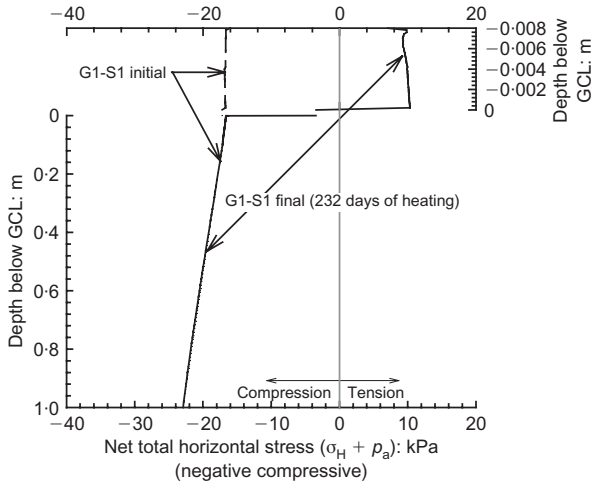

Fig. 25. Net total horizontal stress profiles. σ_H is total stress (tension positive), p_a is air pressure

risk of desiccation, it was not as significant as for a GCL.

(*c*) the depth to the underlying aquifer did not significantly affect the final (equilibrium) distribution of moisture within the CCL, but did increase the potential to develop transient peak net horizontal tensile stresses.

(*d*) the thickness of the CCL had a minor effect on predicted water content and stress distributions at equilibrium, but thicker liners were found to have significantly higher peak net horizontal tensile stresses.

To date, the potential for long-term desiccation of clay liners making up part of a composite liner has received relatively little attention in the design of landfills. The work discussed above shows that there is real potential for desiccation, but also suggests that this can be mitigated by appropriate design and construction. This is an area where more research is needed.

LONG-TERM CONTAMINANT IMPACT

Field examples for composite liners

Rowe *et al.* (2003) examined the performance of a composite liner involving a 1·5 mm HDPE GM over a 3 m thick CCL after 14 years of use as a leachate lagoon liner. The GM had no overlying protection layer. The OIT values obtained for the GM were all very low (typically less than 7 min). For the part of the GM exposed to the sun over the 14-year period, the OIT was only about 1 min, implying that the antioxidants originally in the GM (the initial OIT value is unknown) were almost completely depleted. The low measured tensile break properties and stress cracking resistance suggest that some oxidation had already occurred. When inspected at decommissioning, the GM had 82 cracks, holes and patches over an area of 1552 m^2, corresponding to 528 defects per hectare that had developed within 14 years of operation. Of these, 70% (348 defects/ha) were above the leachate level and 30% (180 defects/ha) were below the leachate level. Despite the fact that only 7% of the unrepaired holes were below the leachate level on the side slopes, this was sufficient to allow liquid to get between the GM and clay liner. No cracks or holes were found at the bottom of the lagoon at the time of decommissioning, although 6 of the 54 patches were on the bottom. Thus although there was external evidence that leachate had come into contact with the underlying clay liner, there remained the questions as to how long the GM had served as an effective barrier and to what extent contaminant had migrated through the CCL.

Soil samples taken from the liner at five different locations were analysed and contaminant concentration profiles were established, as shown for chloride in Fig. 26. The data from the five locations were quite consistent, suggesting that once leachate reached the clay liner it quickly spread over the entire base. The back-diffusion profile at the top was a result of water in the lagoon following removal of leachate but before decommissioning. Data show that chloride had migrated to a depth of 1·7 m (but did not have any adverse impact on the groundwater, as the CCL was 3 m thick). The clay hydraulic conductivity was about $2{\cdot}2 \times 10^{-10}$ m/s. Based on this and the possible gradient, the maximum advective transport was about 0·4 m assuming that the GM failed immediately after construction. Thus the fact that chloride had migrated 1·7 m implies that diffusion was the dominant transport mechanism. The chloride diffusion coefficient for the clay was about 7×10^{-10} m^2/s.

Figure 26 shows calculated chloride profiles assuming the leachate was in direct contact with the compacted clay (i.e. the GM was ineffective) at the end of construction (time = 0 years) and at various times after construction (4, 6, 8 and 10 years). Also shown is the profile expected with 2·5 holes/ha (GM in direct contact with the CCL). A comparison of the calculated and observed profiles shows a poor fit for 6, 8 and 10 years. However, assuming the GM functioned effectively for elapsed times of 0 and 4 years provides a reasonable fit to the majority of the data. Thus it appears that the GM ceased functioning effectively somewhere between 0 and 4 years after construction. This case highlights the need to have an adequate attenuation layer in the event of a failure of the GM, and the need to provide adequate protection to the GM. In this case the damage was attributed to a combination of inadequate design (no protection layer) and operating procedures that caused damage to the GM.

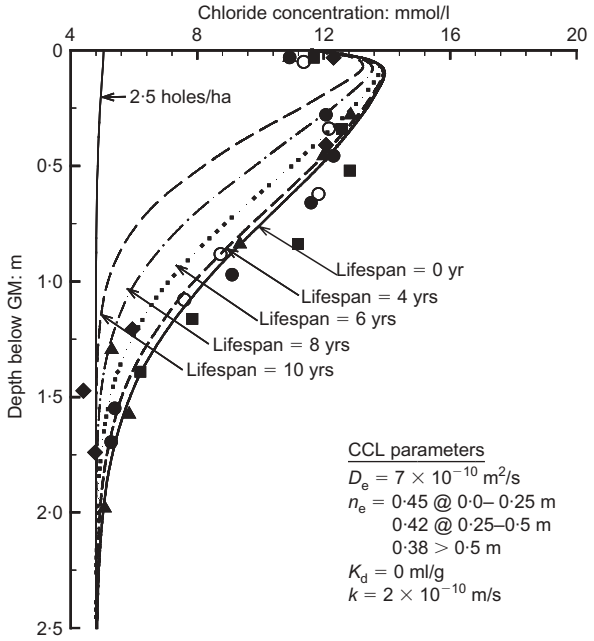

Fig. 26. Chloride concentration profile through compacted clay liner, based on samples from five boreholes, together with prediction of pore fluid concentration for different assumed geomembrane service lives (modified from Rowe *et al.*, 2003)

The foregoing example illustrates that the GM is only as good as the design and operations allow it to be. Although it also highlights the value of the clay component of a composite liner, it should not be concluded from the foregoing example that the GM plays a small to negligible role, if properly designed and protected. For example, a much more positive example of composite liner performance was first reported by Rowe *et al.* (1997) for two test sections at the KVL. For most of the KVL the liner is a CCL (minimum 1·2 m thick), and its performance was discussed earlier. At the locations discussed here the CCL is 2·4 m thick but otherwise as previously described. However, in addition to the normal CCL, a test section was prepared with a composite liner comprising a 2 mm GM over the 2·4 m CCL. In both the normal section (CCL only) and composite section (GM/CCL) the liner was covered with 0·3 m of fine to medium sand and 0·3 m of 50 mm gravel. The migration of ionic leachate constituents was monitored using 12 electrical conductivity sensors installed in the clay liner to a depth of about 0·8 m at each of the two sections. The sensors measure the electrical resistivity of the clay liner, which is a function of soil mineralogy, density, temperature and the concentration of ions in the clay pore water. Details of the method of measurement and the relationship between conductivity and concentration are given by Rowe *et al.* (1997). The increment in pore water conductivity required to give a

clear response from the sensors is 200 μS/cm, which corresponds to an increment in chloride concentration of about 25 mg/l. Rowe *et al.* (1997) reported that after about 5 years salt had migrated to detectable levels through the 0·3 m sand blanket and about 0·7 m into the clay liner where there was no GM. At the GM section there was no detectable migration below the GM.

At the time of writing, there are now 12 years of data (Fig. 27). A clear diffusion profile is evident for the section with compacted clay only, and this extends below the maximum depth of monitoring (0·8 m). Thus over the 12-year period ionic species have migrated more than 1·1 m (through 0·3 m of sand and more than 0·8 m of clay). Advective transport during this 12-year period is calculated to be less than 0·15 m. In contrast, at the composite lined section, even after 12 years, there is no evidence of a concentration profile for ionic species, and the measured conductivity is still representative of background values. This suggests that (a) there is negligible advective flow (leakage) through the GM near the conductivity sensors, and (b) there has been negligible diffusion of ionic species through the GM in 12 years. The lack of holes can be partly attributed to the 0·3 m sand protection layer between the GM and the coarse gravel (note that the same protection layer is used above the clay alone to minimise potential desiccation prior to waste placement). The lack of a diffusion profile after 12 years is entirely consistent with the findings from the laboratory tests (initiated at about the same time) discussed previously (Fig. 20).

Thus the direct comparison of the performance of a single CCL and composite liner at KVL for otherwise identical conditions clearly demonstrates the substantial better performance of the composite lined section in terms of minimising the migration of ionic contaminants and hence minimising long-term contaminant impact.

Factors influencing prediction of long-term contaminant impact

The evaluation of the suitability of a barrier system for a landfill should, in principle, be case dependent and should consider the potential impact on water quality (especially groundwater) due to the proposed landfill. To provide adequate environmental protection the combined engineered system and natural attenuation capacity of the site should be such that there will be negligible impact on groundwater quality for the entire contaminating lifespan of the landfill. As the contaminating lifespan depends on the nature the of waste, the mass of waste per unit area, the waste moisture content, and infiltration through the waste (Rowe *et al.*, 2004) a barrier system that may be perfectly suitable for one landfill will not necessarily be suitable for another (e.g. larger) landfill. In order to make a reasoned, quantitative assessment of potential impact (and hence the suitability of a proposed barrier system) it is usually necessary to solve the advection–dispersion equation subject to appropriate boundary conditions (see Rowe *et al.*, 2004 for a detailed discussion). Factors that influence the potential impact include:

(*a*) the landfill source concentration and its decay characteristics
(*b*) the advective flux (leakage) across the barrier system
(*c*) the thickness of any 'attenuation' layer between the base of the low-permeability liner(s) and the receptor aquifer (or distance to the water table if the liner is constructed in the unsaturated portion of the aquifer)
(*d*) diffusion (especially for VOCs) across the barrier system
(*e*) sorption/retardation in the liner and underlying soil
(*f*) biodegradation
(*g*) dilution in the aquifer
(*h*) the service life of the engineered components of the landfill (e.g. covers/caps, LCSs, liners)
(*i*) the mode of operation of the landfill
(*j*) consolidation of the liner and any underlying compressible soils.

Items (*a*)–(*i*) can be modelled using existing contaminant transport theory (Rowe & Booker, 1998; Rowe *et al.*, 2004) and codes (e.g. Rowe & Booker, 2005). However, item (*j*), the effect of liner consolidation, has received relatively little attention. Questions have been raised regarding the significance of the contribution of consolidation water to flows in leak detection systems (Bonaparte & Gross, 1993; Moo-Young *et al.*, 2004) and the effect of consolidation-induced advection on the rapid migration of VOC into leak detections systems, as reported by Workman (1993) and Othman *et al.* (1996). The issue of consolidation contributing to flows in LDS was discussed earlier. With respect to contaminant transport, Peters & Smith (2002) developed equations that account for the effects of consolidation on the transport of chemicals through clay liners. Results presented for a quasi-steady-state problem (with time-dependent porosity due to consolidation) suggested that consideration of consolidation has only a small effect on the concentration distribution and mass flux. These findings are consistent with those of Rowe & Nadarajah (1995), who found that, for typical liner properties, the change in flow due to consolidation was within the typical range of uncertainty concerning the hydraulic conductivity, and that the effect on contaminant transport and hence impact on a receptor aquifer was not significant for the cases examined. Rowe & Nadarajah (1995) also demonstrated that, to sufficient accuracy, the effect of the build-up of a leachate mound can be modelled as a sequence of steady-state flows without the need for a full consolidation analysis. Thus the effects of consolidation appear to be small for typical low-compressibility CCLs (e.g. Rowe *et al.*, 2000c), and hence conventional advective-diffusive contaminant transport modelling appears suitable for a wide range of practical cases. However, there may be situations involving highly compressible liners where consolidation-induced transport may be potentially significant, and a sophisticated one-dimensional, large-deformation model of coupled mechanical consolidation and solute transport has been developed to model these situations (Lewis, pers. comm).

Although there may be a clearly defined long-term trend

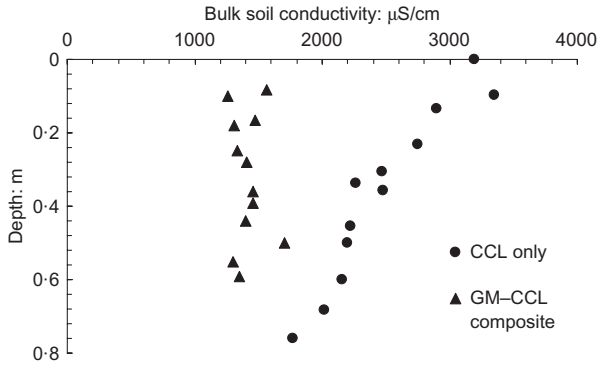

Fig. 27. Bulk soil conductivity profile through compacted clay liner at the Keele Valley Landfill after 12 years. Based on conductivity sensors in the compacted clay: ●, in a section of the landfill with a 2·4 m thick CCL; ▲, in an adjacent section with a trial composite liner comprising a 2 mm HDPE geomembrane over a 2·4 m thick CCL

in leachate characteristics, there is considerable variability in leachate characteristics around this long-term trend (Fig. 2). This raises the question of how important it may be to explicitly model the variability as opposed to the general trend. This issue was addressed by Rowe & Nadarajah (1996), who examined the effects of both cyclical (e.g. seasonal) and random variability about a mean concentration on contaminant transport through a clay liner. For example, Fig. 28 shows the calculated variation in chloride concentration with time at various depths in a clay liner for a leachate source that varies randomly about a mean of 2330 mg/l (standard deviation 620 mg/l; values based on KVL data for 1993). The solid lines represent the variation in concentration calculated using the mean concentration, and the dashed lines show those in response to the randomly varying source (Fig. 28(a)). The significant variability at the source is rapidly damped out by diffusion as the contaminant plume migrates through the clay (Figs 28(b) to 28(e)). The effect is already small by 0·25 m, minimal by 1 m, and negligible at 2 m.

The factors discussed in previous sections of this paper come together when one is faced with predicting the long-term impact of a landfill for a given barrier system. The service life of an LCS can be estimated and used as part of the input to a contaminant transport model. The temperature

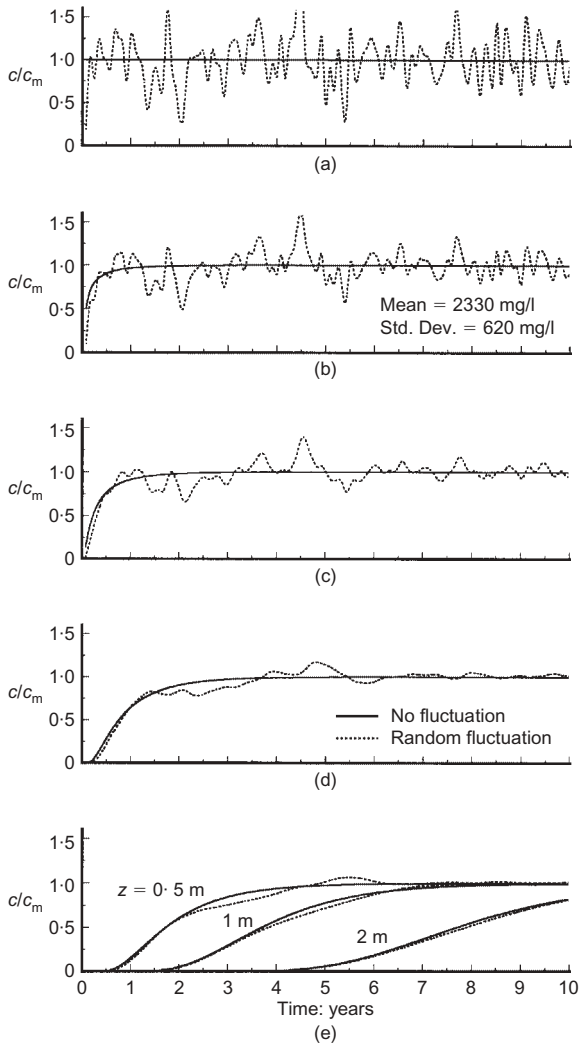

Fig. 28. Effect of random temporal fluctuations of the contaminant source on chloride concentrations c, relative to the mean source concentration c_m, at various depths in a clay liner (modified from Rowe & Nadarajah, 1996): (a) $z = 0$ m; (b) $z = 0{\cdot}05$ m; (c) $z = 0{\cdot}1$ m; (d) $z = 0{\cdot}25$ m; (e) $z = 0{\cdot}5$, 1 and 2 m

of the liner also needs to be considered in assessing suitable transport parameters, and in assessing the service life of the GM and any underlying clay liner. The leakage through the liner needs to be calculated, and the diffusion/sorption/permeation coefficients need to be appropriately selected, as discussed earlier. Finally one needs to evaluate the relative performance of different design options. In the following subsection the long-term impact is examined for both a single and a double composite-lined landfill system. Particular attention is focused on the question of equivalence of systems involving both a CCL and a GCL. The results to be presented were obtained using the program POLLUTE (Rowe & Booker, 2005). The theory upon which the modelling is based (Rowe *et al.*, 2004) allows consideration of the GM, clay liners and any natural aquitards and aquifers, changes in advective velocity, and diffusion properties at different times (e.g. the effects of leachate mounding, failure of a GM, or an increase in temperature can be modelled).

Equivalence of liner systems

There is growing interest in the use of GCLs as a replacement for conventional CCLs. Because, in many jurisdictions, regulations prescribe acceptable barrier system configurations in term of CCLs, this raises the question as to whether a liner involving a GCL is equivalent to one involving a CCL. Several people have attempted to address this question. For example, both Giroud *et al.* (1997a) and Richardson (1997) discussed this in the context of leakage through GCLs and CCLs and the steady-state advective travel time (i.e. neglecting the effect of diffusion on the first arrival time). Richardson also discussed chemical absorption capacity and dilution potential. However, to really assess equivalence from an environmental perspective it is necessary to assess the equivalence in terms of contaminant impact on a receptor aquifer beneath a landfill by solving the advection–dispersion equation. Rowe (1998a) provided a framework to model the contaminant transport through GM/CCL and GM/GCL composite liners considering items (*a*)–(*i*) of the previous subsection, and showed that the peak chloride and dichloromethane concentrations in an underlying aquifer were smaller for a GM/GCL composite liner than for a GM/CCL composite liner provided that the total distance between the GM and the aquifer was the same (i.e. the GCL was used with a more permeable soil that acted as an attenuation layer but not a low-permeability liner).

In selecting parameters for use in conjunction with a contaminant transport analysis, consideration should be given to:

(*a*) the potential for clay–leachate interaction and its effect on hydraulic conductivity (Rowe, 1998a)
(*b*) the interaction with the adjacent GM and the effect on leakage (as discussed earlier)
(*c*) diffusion and sorption (as discussed earlier)
(*d*) the leachate head and corresponding gradient (which will be affected by clogging of the LCS, as discussed earlier)
(*e*) the provision of appropriate protection to the GM and GCL to minimise potential squeezing and local thinning of the GCL (Stark, 1998; Dickinson & Brachman, 2003)
(*f*) the potential for desiccation and shrinkage of the GCL (as discussed earlier).

To illustrate the effect of both diffusion and the finite service lives of different components of the barrier system, consideration will now be given to contaminant transport through composite liner systems consisting of a GM on top of a CCL or GCL. The properties of the HDPE GM, soil

and landfill are as described by Rowe *et al.* (2004). The modelling was based on the following assumptions. The landfill operated for 20 years prior to closure, and all time is expressed relative to the middle of this period. Between times 0 and t_1, a low-permeability cover limited infiltration to 3×10^{-4} m^3/(m^2 yr), and the leachate head on the liner was 0·3 m. Operation of the LCS was terminated at time $t_1 = 40$ years, and the leachate head increased to a maximum of 12 m at time $t_2 = 60$ years. Between times 40 and 60 years an average 6 m head acts on the liner. After 40 years (t_1) the cover was no longer maintained, and the infiltration increased to 0·15 m /yr. The primary GM failed at time $t_3 = 160$ years (the median value at 35°C discussed earlier). For the double-lined system, the secondary GM failed at time t_4 and two values were considered: 300 and 400 years.

Single composite liners

The base case for the single composite liner system, shown schematically in Fig. 29, involved a GM, a 0·6 m CCL and a 0·5 m attenuation layer (GM/CCL/AL) above an aquifer. The second system involved a GM, GCL and 1·1 m attenuation layer (so that the distance from the GM to the receptor aquifer was identical for the two cases, as was discussed in the section on diffusion) (GM/GCL/AL). Fig. 29 shows the calculated dichloromethane (DCM) impacts on the underlying aquifer for these two liner systems. Also shown are the calculated impacts for two other similar systems, where the thickness of the clay liner and attenuation layers has been increased so that the distance from the GM to the aquifer is 3·75 m. In this diffusion-controlled system the peak impact decreases as the total thickness of the soil barrier increases. The impact for the 1·1 m thick system is less than the 50 μg/l limit imposed by some jurisdictions but well above the maximum acceptable concentration of 5 μg/l imposed in other jurisdictions. For the 3·75 m thick system the impact is below 5 μg/l. In both cases the GM/CCL/AL liner system gave a greater impact than that for GM/GCL/AL and similar total thickness, although the difference was of no practical significance, and the two systems may be regarded as equivalent from a contaminant impact perspective.

In all cases the peak impact occurred well before the GM failed ($t_3 = 160$ years), and is controlled by diffusion through the GM and underlying soil. In this particular case, the service life of the primary GM does not have any effect on DCM impact provided it exceeds 100 years. As the concentration of DCM in the landfill is decreasing faster than in the soil (because of the greater biodegradation in the landfill), when the GM does fail the concentration reaching the aquifer decreases (because of dilution of the DCM in the pore fluid by leachate now advecting from the landfill).

For chloride there is a very different response. While the GM is intact there is negligible chloride reaching the aquifer. However, as the decrease in chloride concentration in the landfill is only by dilution (there is no biodegradation or sorption), for this size of landfill there is still significant chloride in the leachate at the time the GM fails, and the peak impact in the aquifer (at about 180 years) is about 700 mg/l. This greatly exceeds a common drinking water objective of 250 mg/l. Thus, for this landfill, none of the single composite liner designs considered could be judged to provide adequate environmental protection unless the service life of the primary GM were very substantially greater than 160 years. At present there is a paucity of evidence to support such a long life for a primary GM in a MSW landfill, and a double-lined system would be required to provide adequate environmental protection.

Double composite liners

The impact of chloride and other conservative contaminants whose concentration decreases only by dilution can be controlled by a suitable double-lined system. Fig. 30 shows a schematic of a double-lined system with a GM/GCL/AL forming both the primary and secondary liner system above an aquifer. A system involving a GM and 0·75 m thick CCL primary liner, and a GM/0·75 m thick CCL and 1 m thick attenuation layer for a secondary liner system, was also modelled. In both cases the head acting above the secondary GM was taken to be 0·03 m for the service life of the secondary LCS (1000 years). The results for both cases are shown in Fig. 30 for two different times of secondary GM failure. Failure of the primary GM at 160 years had negligible impact on the aquifer until failure of the secondary GM at time t_4. If the service life of the secondary GM were 300 years the impact on the aquifer would exceed 420 mg/l (i.e. well in excess of 250 mg/l). However, for a service life of 400 years the impact is less than 250 mg/l and hence below the typical drinking water objective. Both these service lives are below the estimated service life of a secondary GM of 600 years, as discussed earlier (for $T < 20$°C). As in the case of a single liner, there was only a small difference between the results for the liner system with a CCL and that with a GCL, suggesting that again the two systems are practically equivalent for the case examined.

CONCLUSIONS

This lecture has focused on the long-term performance of barrier systems, with particular emphasis on data collected

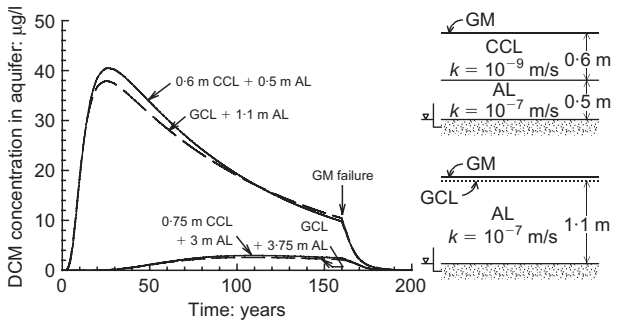

Fig. 29. Calculated variation in dichloromethane (DCM) concentration in an underlying aquifer with time for different single liner configurations for $t_1 = 40$ years, $t_2 = 60$ years and $t_3 = 160$ years (modified from Rowe *et al.*, 2004)

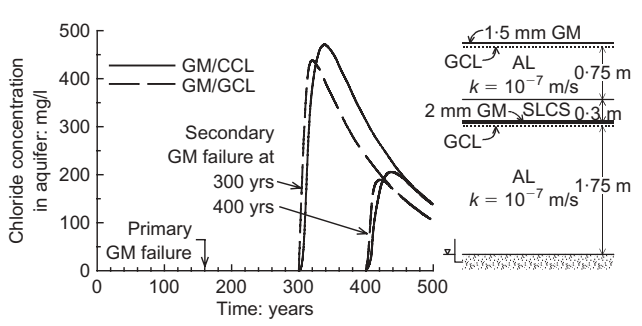

Fig. 30. Calculated variation in chloride concentration in an underlying aquifer with time for different double composite liner configurations for $t_1 = 40$ years, $t_2 = 60$ years and $t_3 = 160$ years (modified from Rowe *et al.*, 2004)

over the past 25 years. Many of the studies cited in this lecture are ongoing, and will provide considerably more information in coming years, which may well cause us to revise the present findings (particularly on issues such as the service life of HDPE GMs). As a considerable amount of research is required to make meaningful comments about long-term performance, in this lecture attention is restricted to those materials and systems for which there has been adequate study. There are many other materials and systems that have been proposed, but their use in landfill base liners should be questioned until data have been gathered that will allow a meaningful assessment of how they are likely to behave in the long term relative to the materials currently in use.

Based on the results and discussion presented herein, a number of practical conclusions can be drawn regarding the seven issues that have been discussed. An overarching conclusion is that, even with the best designs and products, the components of a barrier system will fail to provide adequate long-term (or even short-term) performance if there is poor installation, and/or subsequent operations do not comply with good practice. Thus all of the following conclusions assume that there has been appropriate design and construction (taking account of the current state of knowledge and with appropriate CQC/CQA programmes), and that the operating procedures are such as to maintain the integrity of the design. The available laboratory and field evidence, combined with modelling, indicates that primary LCSs in MSW landfills have a finite service life, which could range from less than a decade to more than a century depending on the design details, waste characteristics and mode of operation. The service life of LCSs can be extended by:

(*a*) the use of uniform coarse gravel in the drainage blanket
(*b*) minimising the flow in critical regions (e.g. by selection of pipe spacing and prudent location of sumps)
(*c*) increasing the thickness of gravel in critical areas and having alternative drainage paths
(*d*) using a suitable filter between the waste and the coarse gravel
(*e*) appropriate sequencing of waste placement
(*f*) regularly cleaning the leachate collection pipes.

There are also activities that may reduce the service life, including:

(*a*) disposal of sewage sludge near the LCS
(*b*) disposal of fines near the collection system.

When a collection system does clog it will result in an increased head on the primary liner, causing greater advection through the liner system. It may also increase the liner temperature.

It has been well known that high temperatures (up to 40–60°C) may be anticipated at the base of landfills where there is a significant leachate mound. Recent data now indicate that even with an effective LCS and negligible leachate mound the liner temperature can be expected to reach 30–40°C for normal landfill operations. With recirculation of leachate the liner temperature increases faster than under normal operating conditions, and may be expected to be greater than 40°C to 45°C.

Both monitoring of leakage through different primary liner systems and theoretical calculations have demonstrated that composite liners are substantially better than single liners in terms of controlling leakage from landfills, and that although there will typically be some leakage, the leakage rates with a composite liner are very small. Composite liners involving a GCL have resulted in substantially less reported leakage than those involving a CCL. This has been attributed, at least in part, to better contact between the GM and GCL and a consequent small interface transmissivity. It has also been shown that considerable care is needed in the design of double-lined systems where the primary and secondary GM are separated only by a GCL and geonet. Problems may include swelling of clay into the geonet, which substantially reduces flow in the geonet, and high temperatures on the geonet and secondary liner (reducing flow in the geonet and potentially causing a very substantial reduction in the service life of the secondary GM).

The observed leakage through composite liners (both with a CCL and with a GCL) is considerably greater than would be expected for the typical number of holes in GMs if the GM were in intimate contact with the underlying clay liner. However, the observed leakage can be explained by the holes being in, or closely adjacent to, wrinkles/waves in the GM, and a simple equation (Rowe, 1998a) can be used to estimate leakage through composite liners for this situation. Even with holes in wrinkles, the leakage rates are small and diffusion will dominate as a transport mechanism for contaminants that can readily diffuse through a GM.

HDPE GMs provide an excellent diffusive barrier to ions, and both laboratory and field tests conducted over a 12-year period (and still ongoing) show negligible (i.e. at the limit of the quantification techniques being used) diffusion of salts through HDPE GMs. On the other hand, both laboratory and field observations suggest relatively rapid diffusion of volatile organic compounds through HDPE GMs. They also diffuse through clay. However, migration of these volatile organic compounds is slowed by the GM, and can be controlled to acceptable levels by a combination of GM and an adequate thickness of liner and attenuation layer below the GM.

The long-term performance of HDPE GMs depends on:

(*a*) the selection of suitable material (e.g. meeting the requirements of GRI GM13)
(*b*) appropriate protection of the GM from both damage and stress concentrations
(*c*) the chemistry of the contacting fluid (e.g. contact with leachate decreases service life far more than contact with water)
(*d*) temperature.

There are three stages to the ageing of an HDPE GM. At present there are some good data for antioxidant depletion (Stage 1) of GMs in simulated liner situations. However, projections for Stages 2 (induction) and 3 (degradation) are based on very limited data relating to pressure pipes. More data are required for conditions more relevant to landfill situations to provide truly confident estimates of GM service life (and these tests are presently in progress but results will not be available for several more years). Given this caveat, based on the currently available data it would appear that the service life for HDPE GM in MSW landfill is likely about 160 years for a primary liner at 35°C and greater than 600 years for a secondary GM provided it is at a temperature of less than 20°C (this will be achieved only if there is an adequate thickness of soil between the primary and secondary systems to provide an adequate thermal barrier).

Clay liners are susceptible to both shrinkage and cracking during construction (because of heating by solar radiation or freezing) and after placement of the waste (because of temperature gradients generated by the waste). The former is critical for CCLs and some GCLs (those manufactured at greater than 15% initial water content) but can be controlled by appropriate placement of a suitable thermal protection layer (e.g. sand that is kept watered, or by quick placement of waste). The latter requires more sophisticated consideration. Based on laboratory tests and modelling it appears that the potential for thermally induced desiccation can be miti-

gated by controlling the applied temperature gradient (the lower the better), the initial water content of the subsoil (higher is better, within reason), and the initial water content of the GCL prior to the application of stress. Based on the studies reported herein, it appears that although there are certainly situations where desiccation can occur, it can be avoided by appropriate design and construction.

Numerical models can be effective in predicting the service lives of engineered systems and are essential to predicting long-term contaminant transport and assessing the equivalence and suitability of different barrier systems.

This lecture has sought to demonstrate that the assessment of the long-term performance of landfill barrier systems requires an understanding of both soil mechanics and geosynthetics. It has also sought to demonstrate that components of the barrier system (LCS, GM and CCL or GCL) should not be considered in isolation, but rather as part of a system where the characteristics and performance of one component impact on that of another. Finally, it has highlighted the importance of modelling coupled phenomena for assessing the long-term performance of LCSs, the desiccation of CCLs and GCLs, and contaminant transport through barrier systems.

ACKNOWLEDGEMENTS

The author is extremely grateful to the City of Toronto for providing extensive monitoring data, access for research purposes, and their willingness to allow data to be freely published. In doing so they have allowed identification of issues, advancement in design and greater environmental protection both for the KVL and for future landfills. In this regard special thanks are due to L. Ciardullo. F. Barone of Golder Associates and L. Josic and D. Bleiker of AMEC Earth and Environmental gave considerable assistance in providing both data and many useful insights with respect to the KVL. Many people offered information and assistance in the preparation of this lecture. The following people are thanked for their assistance in the preparation of figures: R. Brachman (Figs 1, 6, 16, 18, 20, 21, 29, 30), J. VanGulck (Figs 2, 3, 8, 9), S. Rimal (Figs 4, 23), Z. Islam (Figs 11–15, 28), K. AbdelAtty (Fig. 17), J. Southen (Figs 24, 25), C. Lake (Fig. 26) and F. Barone (Fig. 27). The careful review of sections of the written text by F. Barone, A. Bouazza, R. Brachman, P. Davies, Z. Islam, R. Krushelnitzky, C. Lake, K. Legge, R. McWatters, T. Mukunoki, S. Sheridan, N. Touze-Foltz, G. Hsuan and J. VanGulck is very much appreciated. The author is indebted to the many students and collaborators who have contributed to this research over the past 25 years, and in particular to the late Professors J. R. Booker and R. M. Quigley. The Natural Science and Engineering Research Council of Canada funded the majority of the research reported herein. Additional funding was provided by the Province of Ontario through CRESTech and by Terrafix Geosynthetic Inc. and NAUE GmbH & Co.

NOTATION

A constant (often called collision factor)
a distance in drainage layer where porosity reduction is maximum (m)
B thickness of a drainage layer (m)
B' portion of the thickness of drainage layer (m)
b half-width of a wrinkle (m)
c contaminant concentration (mg/l, μg/l)
$c(t)$ contaminant concentration at time t (mg/l; μg/l)
c_f contaminant concentration in solution (mg/l; μg/l)
c_g contaminant concentration in geomembrane (mg/l; μg/l)
c_0 initial concentration (mg/l; μg/l)
c_L contaminant concentration in leachate (mg/l; μg/l)
D diffusion coefficient in soil (m^2/s; m^2/yr)
D thickness of clay liner (m)
D_e effective diffusion coefficient in soil (m^2/s; m^2/yr)
D_g diffusion coefficient in geomembrane (m^2/s; m^2/yr)
E_a activation energy (J/mol)
f mass flux of contaminant ($g/(m^2\,yr)$)
f_{Ca} proportion of calcium in total clog material (–)
g gravitational acceleration (m/s^2)
h hydraulic head (m)
h_d head loss across composite liner (m)
h_w leachate head acting on top of geomembrane (m)
i hydraulic gradient
i_c concentration gradient
K_d partitioning or distribution coefficient (ml/g)
k hydraulic conductivity of liner (m/s)
k_{ave} average hydraulic conductivity of liner (m/s)
k_f hydraulic conductivity of foundation/attenuation layer (m/s)
k_n geotextile normal hydraulic conductivity (m/s)
k_{om} hydraulic conductivity of leachate collection layer (m/s)
L drainage length (m) in equations (18–21) and length of a wrinkle (m) in equation (22)
M_A mass per unit area (g/m^2)
n porosity (–)
n_e effective porosity (–)
n_0 initial porosity (–)
P geotextile permittivity (s^{-1})
P_g 'permeability' of polymer to given contaminant ($P_g = S_{gf}D_g$) (m^2/s; m^2/yr)
p_a pore air pressure (kPa)
Q flow through a hole in a geomembrane (m^3/s)
q_0 permeation through landfill cover reaching leachate collection system per unit area (m/s; m/yr)
q_T heat flux (W/m^2)
R universal gas constant (8·314 J/(mol K))
r_0 radius of a hole in a geomembrane (m)
S_{gf} partitioning (solubility, Henry) coefficient (–)
S antioxidant depletion rate ($month^{-1}$)
s_{av} average antioxidant depletion rate ($month^{-1}$)
T temperature (K)
T_{ave} average temperature (°C; °K)
t time (s; yr)
t_c time to clog (day, yr)
t_{GM} thickness of geomembrane (mm)
t_{GT} thickness of geotextile (mm)
t_{GCL} thickness of GCL (mm)
$V(t)$ volume of pore space filled with clog material at time t (m^3)
V_{tot} volume of mineral clog corresponding to permeability decrease (m^3)
v_a Darcy velocity (Darcy flux) through a layer (m/s; m/yr)
v_b Darcy velocity (Darcy flux) in an aquifer (m/yr)
v_f porosity reduction (–)
v_f^* maximum porosity reduction (–)
$Y(t)$ maximum possible volumetric yield
Δ density of a fluid (t/m^3; kg/m^3; g/cm^3)
Δ_c density of clog material (t/m^3; kg/m^3; g/cm^3)
Δ_d dry density of soil (t/m^3; kg/m^3; g/cm^3)
Δ_{GM} density of geomembrane (t/m^3; kg/m^3; g/cm^3)
θ transmissivity between geomembrane and clay liner (m^2/s)
λ' Fourier thermal conductivity
τ tortuosity (–)
σ_H applied horizontal stress (kPa)

ABBREVIATIONS

AOS apparent opening size (mm, μm)
AL attenuation layer
BOD_5 biochemical oxygen demand measured in a 5-day test.
BTEX benzene, toluene, ethyl benzene and xylenes
CCL compacted clay liner
COD chemical oxygen demand
CQA construction quality assurance
CQC construction quality control
DCA dichloroethane
DCM dichloromethane
EPS extracellular polysaccharides

FOS	filter opening size (mm, μm)
FSS	fixed (inorganic) suspended solid (mg/l)
GCL	geosynthetic clay liner
GM	geomembrane
GN	geonet
GT	geotextile
HBNW	heat-bonded nonwoven
HDPE	high-density polyethylene
HP-OIT	high-pressure oxidative induction time
ISS	industrial solids and sludge
KVL	Keele Valley Landfill
LCS	leachate collection system
LDS	leak detection system
LIW	light industrial waste
LR	leachate recirculation
lphd	litres per hectare per day
MSW	municipal solid waste
NPNW	needle-punched nonwoven
OIT	oxidative induction time (min)
PAC	powdered activated carbon
PB	powdered bentonite
PLCS	primary leachate collection system
POA	percentage open area (%)
PVC	polyvinyl chloride
SDR	standard dimension ratio for pipes (–)
SLCS	secondary leachate collection system (also called a leak detection system)
SP-NCLT	single-point notched constant-load test
STd-OIT	standard oxidative induction time
TCE	trichloroethylene
TSS	total suspended solids (mg/l)
VFA	volatile fatty acids
VOC	volatile organic compounds
VSS	volatile suspended solids (mg/l)
VVO	void volume occupancy (%)
W	woven

REFERENCES

Apse, J. L. (1989). Polyethylene resins for geomembrane applications. In *Durability and aging of geosynthetics* (ed. R. M. Koerner), pp. 159–176. Amsterdam: Elsevier Applied Science Publishers.

Armstrong, M. D. (1998). *Laboratory program to study clogging in a leachate collection system*. MESc thesis, University of Western Ontario, London, Ontario, Canada.

Armstrong, M. D. & Rowe, R. K. (1999) Effect of landfill operations on the quality of municipal solid waste leachate. *Proc. 3rd Int. Landfill Symp., Cagliari*, 81–88.

ASTM (2002). *Standard practice for air-oven aging of polyolefin geomembranes*, D5721-95. West Conshohocken, PA: American Society for Testing and Materials.

ASTM (2004a). *Standard test method for oxidative-induction time of polyolefins by differential scanning calorimetry*, D3895-04. West Conshohocken, PA: American Society for Testing and Materials.

ASTM (2004b). *Standard test method for oxidative-induction time of polyolefin geosynthetics by high-pressure differential scanning calorimetry*, D5885-04. West Conshohocken, PA: American Society for Testing and Materials.

ASTM (2005). *Standard test method for evaluation of stress crack resistance of polyolefin geomembranes using notched constant tensile load*, D5397-99. West Conshohocken, PA: American Society for Testing and Materials.

August, H. & Tatzky, R. (1984). Permeability of commercially available polymeric liners for hazardous landfill leachate organic constituents. *Proceedings of the international conference on geomembranes*, Denver, Vol. 1, pp. 163–168.

August, H., Tatzky-Gerth, R., Preuschmann, R. & Jakob, I. (1992). Permeations verhalten von Kombinationsdichtungen bei Deponien und Altlasten Gegenueber Wassergefaehrdenden Stoffen, Project 10203412 of the BMBF. Berlin: BAM.

Badu-Tweneboah, K., Giroud, J. P., Carlson, D. S. & Schmertmann, G. R. (1998). Evaluation of the effectiveness of HDPE geomembrane liner protection. *Proc. 6th Int. Conf. on Geosynthetics, Atlanta*, 279–284.

Barone, F. S., Costa, J. M. A. & Ciardullo, L. (2000). Temperatures at the base of a municipal solid waste landfill. *Proc. 6th Can Environ. Engng Conf., London, Ontario*, 41–48.

Barone, F. S., Costa, J. M. A., King, K. S., Edelenbos, M. & Quigley, R. M. (1993). Chemical and mineralogical assessment of in situ clay liner Keele Valley Landfill, Maple, Ontario. *Proceedings of the Joint CSCE–ASCE National Conference on Environmental Engineering, Montreal*, 1563–1572.

Basnett, C. R. & Bruner, R. J. (1993). Clay desiccation of a single-composite liner system. *Proc. Geosynthetics 93, Vancouver*, 1329–1340.

Bennett, P. J., Longstaffe, F. J. & Rowe, R. K. (2000). The stability of dolomite in landfill leachate collection systems. *Can. Geotech. J.* **37**, No. 2, 371–378.

Bishop, D. J. (1996). Discussion of 'A comparison of puncture behavior of smooth and textured HDPE geomembranes' and 'Three levels of geomembrane puncture protection' by Narejo, D.B. *Geosynthetics Int.* **3**, No. 3, 441–443.

Bonaparte, R. & Gross, B. A. (1993). *LDCRS flow from double lined landfills and surface impoundments*, EPA/600/R-93/070. Springfield, VA: NTIS Publication PB93-179885.

Bonaparte, R., Daniel, D. & Koerner, R. M. (2002). *Assessment and recommendations for improving the performance of waste containment systems*, EPA Report CR-821448-01-0. Washington, DC: US Environmental Protection Agency.

Bouchez, T., Munoz, M.-L., Vessigaud, S., Bordier, C., Aran, C., & Duquennoi, C. (2003). Clogging of MSW landfill leachate collection systems: prediction methods and in situ diagnosis. *Proc. 9th Int. Waste Management and Landfill Symp., Cagliari* (CD-ROM).

Brachman, R. W. I. & Gudina, S. (2002). A new laboratory apparatus for testing geomembranes under large earth pressures. *Proc. 55th Can. Geotech. Conf.*, Niagara Falls, ON, 993–1000.

Brady, K. C., McMahon, W. & Lamming, G. (1994). *Thirty year ageing of plastics*, Project Report 11, E472A/BG. Crowthorne: Transport Research Laboratory.

Brown, K. W., Thomas, J. C., Lytton, R. L., Jayawickrama, P. & Bahrt, S. (1987). *Quantification of leakage rates through holes in landfill liners*, USEPA Report CR810940. Cincinnati, OH: US Environmental Protection Agency.

Brune, M., Ramke, H. G., Collins, H. & Hanert, H. H. (1991). Incrustation process in drainage systems of sanitary landfills. *Proc. 3rd Int. Landfill Symp., Cagliari*, 999–1035.

Cartaud, F. & Touze-Foltz, N. (2004). Influence of geotextiles at the interface of landfill bottom liners. *Proc. 3rd Eur. Conf. on Geosynthetics, Munich*, 495–500.

Cartaud, F., Touze-Foltz, N. & Duval, Y. (2005a). Experimental investigation of the influence of a geotextile beneath the geomembrane in a composite liner on leakage through a hole in the geomembrane. *Geotextiles and Geomembranes* **23**, No. 2, 117–143.

Cartaud, F., Goblet, P. & Touze-Foltz, N. (2005b). Numerical simulation of the flow in the interface of a composite bottom liner. *Geotextiles and Geomembranes* **23**, No. 6, 513–533.

Collins, H. J. (1993). Impact of the temperature inside the landfill on the behaviour of barrier systems. *Proc. 4th Int. Landfill Symp., Cagliari* **1**, 417–432.

Colucci, P., & Lavagnolo, M.C. (1995). Three years field experience in electrical control of synthetic landfill liners. *Proc. 5th Int. Landfill Symp., Cagliari*, 437–452.

Cooke, A. J. & Rowe, R. K. (1999). Extension of porosity and surface area models for uniform porous media. *ASCE J. Environ. Engng* **125**, No. 2, 126–136.

Cooke, A. J., Rowe, R. K. & Rittmann, B. E. (2005a). Modelling species fate and porous media effects for landfill leachate flow. *Can. Geotech. J.* **42**, No. 4, 116–1132.

Cooke, A. J., Rowe, R. K., VanGulck, J. F. & Rittmann, B. E. (2005b). Application of the Bioclog model for landfill leachate clogging of gravel-packed columns. *Can. Geotech. J.* (in press).

Corser, P., Pellicer, J. & Cranston, M. (1992). Observations on long-term performance of composite clay liners and covers. *Geotech. Fabrics Report*, **10**, No. 8, 6–16.

Craven, W., Townsend, T. G., Vogel, K. & Laux, S. (1999). Field investigation of landfill leachate collection system clogging.

Practice Periodical of Hazardous, Toxic, and Radioactive Waste Management **3**, No. 1, 2–9.

Davies, P. L. & Legge, K. R. (2003). Geosynthetic clay liners: use and abuse in South Africa. *Proc. 9th Int. Waste Management and Landfill Symp., Cagliari* (CD-ROM).

Desaulniers, D. D., Cherry, J. A. & Fritz, P. (1981). Origin, age and movement of pore water in argillaceous quaternary deposits at four sites in Southwestern Ontario. *J. Hydrol.* **50**, 231–257.

Dickinson, S. & Brachman, R. W. I. (2003). Thickness of a GCL beneath a geomembrane wrinkle and coarse gravel backfill under large pressure. *Proc. 56th Can. Geotech. Conf., Winnipeg*, 465–472.

Döll, P. (1997). Desiccation of mineral liners below landfills with heat generation. *ASCE J. Geotech. Geoenviron. Engng* **123**, No. 11, 1001–1009.

Eloy-Giorni, C., Pelte, T., Pierson, P. & Margarita, R. (1996). Water diffusion through geomembranes under hydraulic pressure. *Geosynthetics Int.*, **3**, No. 6, 741–769.

Estornell, P. M. & Daniel, D. E. (1992). Hydraulic conductivity of three geosynthetic clay liners. *ASCE J. Geotech. Engng* **118**, No. 10, 1592–1606.

Felon, R., Wilson, P. E. & Janssens, J. (1992). Résistance mécanique des membranes d'étanchéité: membranes armées en théorie et en pratique. In *Vade mecum pour la realisation des systemes d'étancheite drainage artificiels pour les sites d'enfouissement technique en Wallonie*. Journées d'Études Ulg 92.

Fleming, I. R. & Rowe, R. K. (2004). Laboratory studies of clogging of landfill leachate collection and drainage systems. *Can. Geotech. J.* **41**, No. 1, 134–153.

Fleming, I. R., Rowe, R. K. & Cullimore, D. R. (1999). Field observations of clogging in a landfill leachate collection system. *Can. Geotech. J.* **36**, No. 4, 685–707.

Foose, G. J., Benson, C. H. & Edil, T. B. (2001). Prediction leakage through composite landfill liners. *ASCE J. Geotech. Geoenviron. Engng* **127**, No. 6, 510 – 520.

Gedde, U. W., Viebke, J., Leijstrom, H. & Ifwarson, M. (1994). Long-term properties of hot-water polyolefin pipes: a review. *Polymer Engng Sci.* **34**, No. 24, 1773–1787.

Giroud, J. P. (1996). Granular filters and geotextile filters. *Proc. Geofilters '96, Montreal*, 565–680.

Giroud, J. P. (1997). Equations for calculating the rate of liquid migration through composite liners due to geomembrane defects. *Geosynthetics Int.* **4**, No. 3–4, 335–348.

Giroud, J. P. & Bonaparte, R. (1989). Leakage through liners constructed with geomembranes. Part II: Composite liners. *Geotextiles and Geomembranes* **8**, No. 2, 71–111.

Giroud, J. P. & Bonaparte, R. (2001). Geosynthetics in liquid-containing structures. In *Geotechnical and Geoenvironmental Engineering Handbook* (ed. R. K. Rowe), pp. 789–824. Norwell: Kluwer Academic Publishing.

Giroud, J. P., Badu-Tweneboah, K. & Soderman, K. L. (1997a). Comparison of leachate flow through compacted clay and geosynthetic clay in landfill liner systems. *Geosynthetics Int.* **4**, No. 3–4, 391–431.

Giroud, J. P., Khire, M. V. & Soderman, K. L. (1997b). Liquid migration through defects in a geomembrane overlain and underlain by permeable media. *Geosynthetics Int.* **4**, Nos 3–4, 293–321.

GRI-GM13. (2003). *Specification high density polyethylene geomembranes*. Philadelphia, PA: Geosynthetics Research Institute.

Gross, B. A., Bonaparte, R. & Giroud, J. P. (1990). Evaluation of flow from landfill leakage detection layers. *Proc. 4th Int. Conf. on Geosynthetics, The Hague* **2**, 481–486.

Ham, R. K. & Bookter, T. J. (1982). Decomposition of solid waste in test lysimeters. *ASCE J. Environ. Engng* **108**, No. 6, 1147–1170.

Harpur, W. A., Wilson-Fahmy, R. F. & Koerner, R. M. (1993). Evaluation of the contact between geosynthetic clay liners and geomembranes in terms of transmissivity. *Proceedings of a GRI Seminar on Geosynthetic Liner Systems, Philadelphia, PA*, pp. 143–154.

Haxo, H. E. Jr & Lahey, T. (1988). Transport of dissolved organics from dilute aqueous solutions through flexible membrane liner. *Haz. Waste & Haz. Mater.* **5**, 275–294.

Heibrock, G. (1997). Desiccation cracking of mineral sealing liners. *Proc. 6th Int. Landfill Symp., Cagliari* **3**, 101–113.

Holzlöhner, U. (1995). Moisture balance, risk of desiccation in earthen liners. In *State of the art report: Landfill liner systems* (eds U. Holzlöhner, H. August, T. Meggyes and M. Brune), pp. H1–H22. Sunderland: Penshaw Press.

Hsuan, Y. G. & Guan, Z. (1998). Antioxidant depletion during thermal oxidation of high density polyethylene geomembranes *Proc. 6th Int. Conf. on Geosynthetics, Atlanta*, 375–380.

Hsuan, Y. G. & Koerner, R. M. (1998). Antioxidant depletion lifetime in high density polyethylene geomembranes. *ASCE J. Geotech. Geoenviron. Engng* **124**, No. 6, 532–541.

Hsuan, Y. G., Lord, A. E. Jr & Koerner, R. M. (1991). Effects of outdoor exposure on a high density polyethylene geomembrane. *Proc. Geosynthetics '91, Atlanta* **1**, 287–302.

Hwu, B., Koerner, R. M. & Sprague, C.J. (1990). Geotextile intrusion into geonets. *Proc. 4th Int. Conf. on Geotextiles, The Hague*, 351–356.

Jayawickrama, P., Brown, K. W., Thomas, J. C. & Lytton, R. L. (1988). Leakage rates through flaws in membrane liners. *ASCE J. Environ. Engng* **114**, No. 6, 1401–1419.

Jefferis, S. A. & Bath, A. (1999). Rationalising the debate on calcium carbonate clogging and dissolution in landfill drainage materials. *Proc. 7th Int. Landfill Symp., Cagliari*, 277–284.

Karlsson, K., Smith, G. D. & Gedde, U. W. (1992). Molecular structure, morphology and antioxidant consumption in medium density polyethylene pipes in hot-water applications. *Polymer Engng Sci.* **32**, No. 10, 649–657.

Klein, R., Baumann, T., Kahapka, E. & Niessner, R. (2001). Temperature development in a modern municipal solid waste incineration (MSWI) bottom ash landfill with regard to sustainable waste management. *J. Haz. Mater.* **B83**, 265–280.

Koerner, G. R. & Koerner, R. M. (1995a). Temperature behaviour of field deployed HDPE geomembranes. *Proc. Geosynthetics '95, Nashville*, 921–937.

Koerner, R. M. & Koerner, G. R. (1995b). *Leachate clogging assessment of geotextile (and soil) landfill filters*, Report CR-819371. Washington, DC: US Environmental Protection Agency.

Koerner, G. R. & Koerner, R. M. (2006). Long term temperature monitoring of geomembranes at dry and wet landfills. *Geotextiles and Geomembranes* **24** No. 1 (in press).

Koerner, G. R., Koerner, R. M. & Martin, J. P. (1994). Design of landfill leachate-collection filters. *ASCE J. Geotech. Engng* **120**, No. 10, 1792–1803.

Koerner, R. M., Knight, A. & Eith, A. (2003). Benefits of leachate recirculation: a case study. *Proceedings of the waste technology conference*, *New Orleans*, (CD-rom).

Kossendey, T. H., Gartung, E. & Schmidt, S. (1996). Microbiological influences on the long-term performance of geotextile filters. *Proc. Geofilters '96, Montreal*, 115–124.

Lake, C. B. & Rowe, R. K. (2000a). Diffusion of sodium and chloride through geosynthetic clay liners. *Geotextiles and Geomembranes* **18**, No. 2, 102–132.

Lake, C. B. & Rowe, R. K. (2000b). Swelling characteristics of needlepunched, thermally treated GCLs. *Geotextiles and Geomembranes* **18**, No. 2, 77–102.

Lake, C. B. & Rowe, R. K. (2004). Volatile organic compound (VOC) diffusion and sorption coefficients for a needlepunched GCL. *Geosynthetics Int.* **11**, No. 4, 257–272.

Lake, C. B. & Rowe, R. K. (2005). A comparative assessment of volatile organic compound (VOC) sorption to various types of potential GCL bentonites. *Geotextiles and Geomembranes* **23**, No. 4, 323–347.

Legge, K. R. & Davies, P. L. (2002). An appraisal of the performance of geosynthetic material used in waste disposal facilities in South Africa. *Proc. WasteCon 2002, Durban* (CD-ROM).

Maliva, R. G., Missimer, T. M., Leo, K. C., Statom, R. A., Dupraz, C., Lynn, M. & Dickson, J. A. D. (2000). Unusual calcite stromatolites and pisoids from a landfill leachate collection system. *Geology* **28**, No. 10, 931–934.

Manning, D. A. C. (2000). Carbonates and oxalates in sediments and landfill: monitors of death and decay in natural and artificial systems. *J. Geolog. Soc. London* **157**, 229–238.

Manning, D. A. C. & Robinson, N. (1999). Leachate-mineral reactions: implications for drainage system stability and clogging. *Proc. 7th Int. Landfill Symp., Cagliari*, 269–276.

McBean, E. A., Mosher, F. R. & Rovers, F. A. (1993). Reliability-based design for leachate collection systems. *Proc. 3rd Int. Landfill Symp., Cagliari*, 433–441.

McIsaac, R. S., Rowe, R. K., Fleming, I. R. & Armstrong, M. D. (2000). Leachate collection system design and clog development. *Proc. 6th Can. Environ. Engng Conf., London, ON*, 66–73.

Mitchell, J. K. (1991). Conduction phenomena: from theory to geotechnical practice. *Géotechnique* **41**, No. 3, 299–340.

Mitchell, J. K. & Soga, K. (2005). *Fundamentals of soil behavior*, 3rd edn. New York: Wiley.

Mlynarek, J. & Rollin, A. L. (1995). Bacterial clogging of geotextiles: overcoming engineering concerns. *Proc. Geosynthetics '95*, Nashville, TN, 177–188.

Moo-Young, H., Johnson, B., Johnson, A., Carson, D., Lew, C., Liu, S. & Hancock, K. (2004). Characterisation of infiltration rates from landfills: supporting groundwater modeling efforts. *Environmental Monitoring and Assessment* **96**, 283–311.

Mueller, W. & Jacob, I. (2003). Oxidative resistance of HDPE. *Polymer Degradation and Stability* **79**, 161–172.

Müller, W., Jakob, R., Tatzky-Gerth, R. & August, H. (1998). Solubilities, diffusion and partitioning coefficients of organic pollutants in HDPE geomembranes: experimental results and calculations. *Proc. 6th Int. Conf. on Geosynthetics, Atlanta*, 239–248.

Narejo, D., Koerner, R. M. & Wilson_Fahmy, R. F. (1996). Puncture protection of geomembranes. Part II: Experimental. *Geosynthetics Int.* **3**, No. 5, 629–653.

Nosko, V. & Touze-Foltz, N. (2000). Geomembrane liner failure: modeling of its influence on contaminant transfer. *Proc. 2nd Eur. Geosynthetics Conf., Bologna*, 557–560.

Osawa, Z. & Saito, T. (1978). The effects of transition metal compounds on the thermal oxidative degradation of polypropylene in solution. In *Stabilisation and degradation of polymers*, Advances in Chemistry, Series 169, pp. 2897–2907. American Chemical Society.

Othman, M. A., Bonaparte, R. & Cross, B. A. (1996). Preliminary results of study of composite liner field performance. *Proc. 10th GRI Conf.: Field performance of geosynthetics and geosynthetic related systems, Drexel University, Philidelphia*, pp. 110–137.

Owen, J. A. & Manning, D. A. C. (1997). Silica in landfill leachates: implications for clay mineral stabilities. *Appl. Geochem.* **12**, 267–280.

Paksy, A., Powrie, W., Robinson, J. P. & Peeling, L. (1998). A laboratory investigation of microbial clogging in granular landfill drainage media. *Géotechnique* **48**, No. 3, 389–401.

Parkin, G. F. & Owen, W. F. (1986). Fundamentals of anaerobic digestion of wastewater sludges. *ASCE J. Environ. Engng* **112**, No. 5, 867–920.

Pelte, T., Pierson, P. & Gourc, J. P. (1994). Thermal analysis of geomembranes exposed to solar radiation. *Geosynthetics Int.* **1**, No. 1, 21–44.

Petermann, J., Miles, M. & Gleiter, H. (1976). Growth of polymer crystals during annealing. *J. Macromol. Sci. Phys. B* **12**, No. 3, 393–404.

Peters, G. P. & Smith, D. W. (2002). Solute transport through a deforming porous medium. *Int. J. Numer. Anal. Methods Geomech.* **26**, 683–717.

Quigley, R. M. & Rowe, R. K. (1986). Leachate migration through clay below a domestic waste landfill, Sarnia, Ontario, Canada: Chemical interpretation and modelling philosophies. In *Hazardous and industrial solid waste testing and disposal*, ASTM STP 933, pp. 93–103. American Society for Testing and Materials.

Quigley, R. M., Gwyn, Q. H. J., White, O. L., Rowe, R. K., Haynes, J. E. & Bohdanowicz, A. (1983). Leda clay from deep boreholes at Hawkesbury, Ontario. Part I: Geology and geotechnique. *Can. Geotech. J*, **20**, No. 2, 288–298.

Reades, D. W., King, K. S., Benda, E., Quigley, R. M., LeSarge, K. & Heathwood, C. (1989). The results of on-going monitoring of the performance of a low permeability clay liner, Keele Valley landfill, Maple, Ontario. *Proceedings of a focus conference on eastern regional ground water issues*, National Water Well Assoc., Kitchener, ON, pp. 79–91.

Reddy, K. R., Bandi, S. R., Rohr, J. J., Finy, M. & Siebken, J. (1996). Field evaluation of protective covers for landfill geomembrane liners under construction loading. *Geosynthetics Int.* **3**, No. 6, 679–700.

Richardson, G. N. (1997). GCLs: alternative subtitle D liner systems. *Geotech. Fabrics Report*, **15**, No. 5, 36–42.

Rittmann, B. E., Fleming, I. R. & Rowe, R. K. (1996). Leachate chemistry: its implications for clogging. *Proc. ASCE North American Water and Environmentt Congress '96, Anaheim* (CD-ROM).

Rogers, C. E. (1985). Permeation of gases and vapors in polymers. In *Polymer permeability* (ed. J. Comyn), pp. 11–73. London: Elsevier Applied Science.

Rollin, A. L., Mlynarek, J., Lafleur, J. & Zanescu, A. (1994). Performance changes in aged in-situ HDPE geomembrane. In *Landfilling of wastes: Barriers* (eds T. Christensen, R. Cossu and R. Stegmann), pp. 431–443. London: E & FN Spon.

Rowe, R. K. (1998a). Geosynthetics and the minimization of contaminant migration through barrier systems beneath solid waste. *Proc. 6th Int. Conf. on Geosynthetics*, Atlanta **1**, 27–103.

Rowe, R. K. (1998b). From the past to the future of landfill engineering through case histories. *Proc. 4th Int. Conf. on Case Histories in Geotech. Engng, St Louis*, 145–166.

Rowe, R. K. & Booker, J. R. (1995). A finite layer technique for modelling complex landfill history. *Can. Geotech. J.* **32**, No. 4, 660–676.

Rowe, R. K. & Booker, J. R. (1998). Modelling impacts due to multiple landfill cells and clogging of leachate collection systems. *Can. Geotech. J.* **35**, No. 1, 1–14.

Rowe, R. K. & Booker, J. R. (2000). Theoretical solutions for calculating leakage through composite liner systems. *Developments in theoretical geomechanics: Proceedings of The John Booker Memorial Symposium*, Sydney, pp. 580–602.

Rowe, R. K. & Booker, J. R. (2005). *POLLUTEv7: Pollutant migration through a nonhomogeneous soil*. GAEA Environmental Engineering Ltd, Whitby, Canada.

Rowe, R. K. & Fleming, I. R. (1998). Estimating the time for clogging of leachate collection systems. *Proc. 3rd Int. Congress on Environ. Geotech., Lisbon* **1**, 23–28.

Rowe, R. K. & Iryo, T. (2005). Effect of geosynthetics on the hydraulic performance of leak detection systems. *Can. Geotech. J.* **42**, No. 5, 1359–1376.

Rowe, R. K. & McIsaac, R. (2005). Clogging of tire shreds and gravel permeated with landfill leachate. *ASCE J. Geotech. Geoenviron. Engng* **131**, No. 6, 682–693.

Rowe, R. & Nadarajah, P. (1995). Transport modelling under transient flow conditions. *Proc. 5th Int. Symp. on Numerical Models in Geomechanics, Davos*, 337–342.

Rowe, R. K. & Nadarajah, P. (1996). Effect of temporal fluctuation of leachate concentration in landfills. *Proc. 2nd Int. Cong. on Environ. Geotech., Osaka*, 305–310.

Rowe, R. K. & Orsini, C. (2003). Effect of GCL and subgrade type on internal erosion in GCLs. *Geotextiles and Geomembrane* **21**, No. 1, 1–24.

Rowe, R. K. & Sangam, H. P. (2002). Durability of HDPE geomembranes. *Geotextiles and Geomembranes* **20**, No. 2, 77–95.

Rowe, R. K. & Sawicki, D. W. (1992). The modelling of a natural diffusion profile and the implications for landfill design. *Proc. 4th Int. Symp. Numer. Methods in Geomech., Swansea*, 481–489.

Rowe, R. K. & VanGulck, J. F. (2004). Filtering and drainage of contaminated water. *Proc. 4th Int. Conf. on GeoFilters, Stellenbosch*, 1–63.

Rowe, R. K., Barone, F. S. & Hrapovic, L. (1997). Laboratory and field studies of salt diffusion through a composite liner. *Proc. 6th Int. Landfill Symp., Cagliari* **3**, 241–250.

Rowe, R. K., Hsuan, Y. G., Lake, C. B., Sangam, P. & Usher, S. (1998). Evaluation of a composite (geomembrane/clay) liner for a lagoon after 14 years of use. *Proc. 6th Int. Conf. on Geosynthetics, Atlanta*, 191–196.

Rowe, R. K., Armstrong, M. D. & Cullimore, D. R. (2000a). Mass loading and the rate of clogging due to municipal solid waste leachate. *Can. Geotech. J.* **37**, No. 2, 355–370.

Rowe, R. K., Armstrong, M. D. & Cullimore, D. R. (2000b). Particle size and clogging of granular media permeated with leachate. *ASCE J. Geotech. Geoenviron. Engng* **126**, No. 9, 775–786.

Rowe, R. K., Caers, C. J., Reynolds, G. & Chan, C. (2000c). Design and construction of barrier system for the Halton landfill. *Can. Geotech. J.* **37**, No. 3, 662–675.

Rowe, R. K., Goveas, L. & Dittrich, J. P. (2002). Excavations in gassy soils. *Geotech. Engng* **155**, No. 3, 159–161.

Rowe, R. K., Sangam, H. P. & Lake, C. B. (2003). Evaluation of an HDPE geomembrane after 14 years as a leachate lagoon liner. *Can. Geotech. J.* **40**, No. 3, 536–550.
Rowe, R. K., Quigley, R. M., Brachman, R. W. I. & Booker, J. R. (2004). *Barrier systems for waste disposal facilities*. London: Taylor & Francis (E & FN Spon).
Rowe, R. K., Mukunoki, T. & Sangam, P. H. (2005). BTEX diffusion and sorption for a geosynthetic clay liner at two temperatures. *ASCE J. Geotech. Geoenviron. Engng* **131**, No. 1, 1211–1221.
Sangam, H. P. & Rowe, R. K. (2001a). Migration of dilute aqueous organic pollutants through HDPE geomembranes. *Geotextiles and Geomembranes* **19**, No. 6, 329–357.
Sangam, H. P. and. Rowe, R. K (2001b). The role of HDPE geomembranes in retarding the diffusive migration of organic contaminants through composite liner systems. *Proc. 8th Int. Landfill Symp., Cagliari* **3**, 245–254.
Sangam, H. P. & Rowe, R. K. (2002). Effects of exposure conditions on the depletion of antioxidants from high-density polyethylene (HDPE) geomembranes. *Can. Geotech. J.* **39**, No. 6, 1221–1230.
Schnabel W. (1981). *Polymer degradation: principles and practical applications*. Toronto: Hanser.
Seeger, S. & Müller, W. (1996). Requirements and testing of protective layer systems for geomembranes. *Geotextiles and Geomembranes*, **14**, 365–376.
Shaner, K. R. & Menoff, S. D. (1992). Impacts of bentonite geocomposites on geonet drainage. *Geotextiles and Geomembranes* **11**, No. 4–6, 503–512.
Soong, T. Y. & Koerner, R. M. (1998). Laboratory study of high density polyethylene geomembrane waves. *Proc. 6th Int. Conf. on Geosynthetics, Atlanta*, 301–306.
Southen, J. M. (2005). *Thermally driven moisture movement within and beneath geosynthetic clay liner*. PhD thesis, University of Western Ontario.
Southen, J. M. & Rowe, R. K. (2004). Investigation of the behavior of geosynthetic clay liners subjected to thermal gradients in basal liner applications. *J. ASTM International* **1**, No. 2 ID JAI11470, www.astm.org. Also in *Advances in geosynthetic clay liner technology* (eds R. E. Mackey and K. von Maubeuge), pp. 121–133. West Conshohocken, PA: ASTM International.
Southen, J. M. & Rowe, R. K. (2005a). Modeling of thermally induced desiccation of geosynthetic clay liners. *Geotextiles and Geomembranes* **23**, No. 5, 425–442.
Southen, J. M. & Rowe, R. K. (2005b). Laboratory investigation of GCL desiccation in a composite liner subjected to thermal gradients. *ASCE J. Geotech. Geoenviron. Engng* **131**, No. 7, 925–935.
Stark, T. D. (1998). Bentonite migration in geosynthetic clay liners. *Proc. 6th Int. Conf. on Geosynthetics, Atlanta* **1**, 315–320.
Stone, J. L. (1984). Leakage monitoring of the geomembrane for proton decay experiment. *Proceedings of the international conference on geomembranes*, Denver, Vol. 2, pp. 475–480.
Thiel, R. & Richardson, G. N. (2005). Concern for GCL shrinkage when installed on slopes, *Proc. ASCE GeoFrontiers Conf.*, Austin, Paper GRI-18 (CD-ROM).
Tognon, A. R., Rowe, R. K. & Moore, I. D. (2000). Geomembrane strain observed in large-scale testing of protection layers. *ASCE J. Geotech. Geoenviron. Engng* **126**, No. 12, 1194–1208.
Touze-Foltz, N., Rowe, R. K. & Duquennoi, C. (1999). Liquid flow through composite liners due to geomembrane defects: analytical solutions for axi-symmetric and two-dimensional problems. *Geosynthetics Int.* **6**, No. 6, 455–479. Erratum: (2000) **7**, No. 1, 77.
Touze-Foltz, N., Schmittbuhl, J. & Memier, M. (2001a). Geometric and spatial parameters of geomembrane wrinkles on large scale model tests. *Proc. Geosynthetics 2001, Portland*, 715–728.
Touze-Foltz, N., Rowe, R. K. & Navarro, N. (2001b). Liquid flow through composite liners due to geomembrane defects: nonuniform hydraulic transmissivity at the liner interface. *Geosynthetics Int.* **8**, No. 1, 1–26.
VanGulck, J. F. (2003). *Biodegradation and clogging in gravel size material*. PhD thesis, Queen's University, Kingston, Ontario.
VanGulck, J. F. & Rowe, R. K. (2004a). Evolution of clog formation with time in columns permeated with synthetic landfill leachate. *J. Cont. Hydrol.* **75**, 115–135.
VanGulck, J. F. & Rowe, R. K. (2004b). Influence of landfill leachate suspended solids on clog (biorock) formation. *Int. J. Integrated Waste Management Sci. Tech* **24**, 723–738.
VanGulck, J. F., Rowe, R. K., Rittmann, B. E. & Cooke, A. J. (2003). Predicting biogeochemical calcium precipitation in landfill leachate collection systems. *Biodegradation* **14**, 331–346.
Viebke, J., Elble, E., Ifwarson, M. & Gedde, U. W. (1994). Degradation of unstabilized medium-density polyethylene pipes in hot-water applications. *Polymer Engng Sci.* **34**, No. 17, 1354–1361.
Wisse, J. D. M., Broos, C. J. M. & Boels, W.H. (1990). Evaluation of the life expectancy of polypropylene geotextiles used in bottom protection structures around the Ooster Schelde storm surge barrier: a case study. *Proc. 2nd Int. Conf. on Geotextiles, Las Vegas* **1**, 283–288.
Workman, J. P. (1993). Interpretation of leakage rates in double lined systems. *Proc. 7th GRI Conf.: Geosynthetic Liner Systems, Philadelphia*, 91–108.
Yanful, E. K., Quigley, R. M. & Nesbitt, W. (1988). Heavy metal migration at a landfill site. Part II: Metal partitioning and geotechnical implications. *Appl. Geochem.* **3**, 623–629.
Yoshida, H. & Rowe, R. K. (2003). Consideration of landfill liner temperature. *Proc. 8th Int. Waste Management and Landfill Symp., Cagliari* (CD-ROM).
Yoshida, H., Hozumi, H. & Tanaka, N. (1996). Theoretical study on temperature distribution in a sanitary landfill. *Proc. 2nd Int. Congress on Environ. Geotech., Osaka* **1**, 323–328.
Zhou, Y. & Rowe, R. K. (2003). Development of a technique for modelling clay liner desiccation. *Int. J. Numer. Anal. Methods Geomech.* **27**, 473–493.

VOTE OF THANKS

PROFESSOR W. POWRIE, Department of Civil and Environmental Engineering, University of Southampton

When the 45th Rankine lecturer was announced 12 months ago, the many people who know Professor Rowe expected this year's lecture to be educational, interesting and entertaining. This sense of expectation is evidenced by the many people in the hall who have travelled long distances to be here tonight. They will not have been disappointed: Professor Rowe has spoken eloquently and convincingly on the long-term performance of contaminant barriers—a subject he has in recent years made his own.

Professor Rowe's lecture has been an elegant fusion of chemistry, microbiology, materials science, conduction phenomena and soil mechanics. These are the key elements of modern geoenvironmental engineering. At a recent workshop on waste and landfill mechanics, the acceptance of pH as a geotechnical parameter was remarked upon. This evening's lecture has reminded us that there are several other parameters that must be added to this list.

In 1828, in the original charter for the Institution of Civil Engineers, Thomas Tredgold defined civil engineering in terms that included the phrase 'directing the great sources of Power in Nature for the use and convenience of man'.[1] While this is still relevant today—especially when we think of the potential for exploiting solar, wind and marine current energy—it is not the whole picture. We might define civil engineering as the application of science and other disciplines and skills to the solution of society's problems. Time moves on, and society's problems—and expectations—change. Among the problems that society now faces, the protection of the environment is paramount. Professor Rowe's lecture, which focused on exactly this, was therefore very timely. It was also highly relevant to Europe, particu-

[1] The full definition is reproduced in a paper by P. J. Jowitt in *Proceedings of the Institution of Civil Engineers, Engineering Sustainability*, **157**, No. 2, 79–88.

larly in view of impending legislation that will change fundamentally the nature of landfilled wastes: although the amount should reduce, its pollution potential will probably increase, and the design of effective contaminant barriers will be even more essential than it is now.

Professor Rowe's lecture has reminded us that Tredgold's 'great sources of Power in Nature' might include a mass of microorganisms. It contained a wealth of fundamental science presented with great clarity—the hallmark of an expert—and extensive reference to real data. The elegant and effective models for quantifying the complex processes and interactions involved will be of immense relevance and value to practice. The lecture represents a landmark in the development and maturity of environmental geotechnics as a subject, and will be remembered and referred to for a long time to come. It is with very great pleasure that I invite you all to join me in thanking Professor Rowe for what has been an excellent and memorable 45th Rankine Lecture.